

**OPTIMAL PLACEMENT, SIZING AND DISPATCH OF  
BATTERY ENERGY STORAGE SYSTEM  
INTEGRATED DISTRIBUTED GENERATION**

Kariyawasam Bovithanthri Jayaminda Anuradha

198026G

Degree of Master of Science by Research

Department of Electrical Engineering

University of Moratuwa

Sri Lanka

April 2020

**OPTIMAL PLACEMENT, SIZING AND DISPATCH OF  
BATTERY ENERGY STORAGE SYSTEM  
INTEGRATED DISTRIBUTED GENERATION**

Kariyawasam Bovithanthri Jayaminda Anuradha

198026G

Thesis submitted in fulfillment of the requirements for the degree of Master  
of Science by Research

Department of Electrical Engineering

University of Moratuwa

Sri Lanka

April 2020

## DECLARATION

I declare that this is my own work and this thesis does not incorporate without acknowledgement any material previously submitted for a Degree or Diploma in any other University or institute of higher learning and to the best of my knowledge and belief it does not contain any material previously published or written by another person except where the acknowledgement is made in the text.

Also, I hereby grant to University of Moratuwa the non-exclusive right to reproduce and distribute my thesis, in whole or in part in print, electronic or other medium. I retain the right to use this content in whole or part in future works (such as articles or books).

Signature: 

Date: 10/05/2020

The above candidate has carried out research for the Masters/~~MPhil/PhD~~ thesis/  
~~Dissertation~~ under my supervision.

1) Name of the supervisor: Dr. J.V.U.P. Jayatunga

Signature of the supervisor:



Date:10/05/2020

2) Name of the supervisor: Prof. H.Y.R. Perera

Signature of the supervisor: Ranjit Perera

Date:10/05/2020

## ABSTRACT

Distributed Generation (DG) has become a key component in modern power industry due its significant advantages over the traditional power generation methods. Nevertheless, it is required to integrate them for distribution networks in such a way that their best expected outcomes can be achieved as inappropriate allocation may impose power system stability, protection and quality issues. This thesis presents novel analytical approaches for optimizing the DG location, size and power dispatch. Analytical methodologies based on formulating objective functions using loss and voltage sensitivities are presented for optimizing the DG location and size. An alternative method for determining the optimal DG sizes which is solved by Lagrange Multiplier Method (LMM) is also presented for better comparison. Moreover, the values obtained for optimal DG sizes from the novel analytical methods are compared with the results obtained by Genetic Algorithm (GA). A novel approach for determining the Battery Energy Storage System (BESS) capacities is presented as a part of developing an optimal power dispatch schedule for BESS units. The time varying nature of loads and DG output are also taken into consideration in this approach. Raw data obtained from a Solar Photovoltaic (SPV) farm in Hambantota area and typical three load profile data (i.e. mix load, residential load and commercial load) obtained from Long Term Generation Expansion Plan (LTGEP) of Ceylon Electricity Board (CEB) are used for modelling the SPV generation and load patterns respectively. The BESS capacities are determined in terms of Load Proportionality Factor (LPF), State of Charge limits (SOC) of battery storages and proportion of off-peak solar period energy consumption expected to be served by each BESS unit. An optimal BESS dispatch algorithm is also presented in this thesis for minimizing the energy losses and voltage deviations. The applicability of the proposed methodologies are tested using standard IEEE-6 and IEEE-33 test bus systems. Simulation results obtained for active power loss variations, voltage profile variations, SOC variations of BESS units and charging/discharging rates of BESS units suggest the acceptability and the appropriateness of the proposed methodologies.

**Keywords-** *Distributed generation, optimal DG allocation, loss sensitivity index (LSI), voltage sensitivity index (VSI), loss-voltage sensitivity index (LVSI), load proportionality factor (LPF), loss minimization, voltage deviations,*

## **ACKNOWLEDGEMENT**

There were so many officials and non-officials who gave their full contribution and commitment towards the successful completion of my M.Sc. First of all, I would like to acknowledge my supervisors Dr. J.V.U.P. Jayatunga and Prof. H.Y.R. Perera of Department of Electrical Engineering, University of Moratuwa for their constant guidance, supervision and encouragement granted towards me from beginning to the end. Furthermore, I would like to grant my gratitude towards Prof. W.D.A.S. Wijayapala and Dr. Lidula N. Widanagama Arachchige for providing me with valuable advises and suggestions towards the successful completion of my M.Sc. I would also like to appreciate the valuable comments and assistance given by all the other academic staff members which were helpful in achieving the research objectives.

I express my sincere appreciation to the Senate Research Committee (SRC) of University of Moratuwa for providing me with financial support (SRC/LT/2018/23) towards the conduct of this research. Moreover, the support given by the non-academic staff of Department of Electrical Engineering is also commendable.

Finally, I would like to grant my heartfelt thanks to my beloved parents, my research mates and all the others who provided their support and dedication in numerous ways towards the successful completion of my M.Sc.

## TABLE OF CONTENTS

DECLARATION .....	i
ABSTRACT .....	ii
ACKNOWLEDGEMENT .....	iii
LIST OF FIGURES .....	viii
LIST OF TABLES .....	xi
LIST OF ABBREVIATIONS .....	xii
INTRODUCTION .....	1
1.1. Background of the Study.....	2
1.1.1. Problem Statement .....	2
1.1.2. Research Objectives .....	3
1.1.3. Scope of Work .....	3
1.2. Thesis Structure .....	3
1.3. Summary .....	4
LITERATURE REVIEW AND BACKGROUND STUDIES .....	5
2.1. Distributed Generation in Power Systems.....	5
2.1.1. Importance of Distributed Generation.....	5
2.1.2. Classification of DG.....	5
2.1.3. DG Allocation and its Impact on Network .....	6
Power Quality Issues .....	6
Protection Issues .....	7
Stability Issues .....	7
2.1.4. Significance of Optimizing DG Allocation .....	7
2.2. Taxonomy of Optimization Methods Used for DG Allocation .....	8
2.2.1. Problem Formulation.....	8
2.2.2. Constraints .....	8
2.2.3. DG Technology.....	9
2.2.4. Load Profile .....	9
2.2.5. Optimization Techniques Used in DG Allocation .....	9
Exact Optimization.....	10
Linear Programming .....	10
Non-Linear Programming .....	10
Sequential Quadratic Programming .....	11
Dynamic Programming .....	12
Ordinal Programming .....	12
Gradient Search Method .....	12

Heuristic Optimization.....	13
Genetic Algorithm .....	13
Particle Swarm Optimization .....	15
Ant-Colony Optimization.....	15
Artificial Bee Colony Optimization.....	16
Monte Carlo Simulation.....	16
Tabu Search.....	16
Simulated Annealing.....	17
Differential Evolution .....	17
Analytical Methods .....	17
Sensitivity Based Methods .....	18
2.3. Summary .....	20
OPTIMIZATION OF DG LOCATION .....	22
3.1. Mathematical Background .....	22
3.1.1. Jacobian Matrix.....	22
3.1.2. Exact Loss Formula.....	23
3.1.3. Loss Sensitivity Index .....	24
3.1.4. Voltage Sensitivity Index .....	25
3.2. Optimal DG Location Based on Loss & Voltage Sensitivity Analysis.....	25
3.2.1. Novel Objective Function.....	25
3.2.2. Constraints.....	26
3.2.3. Computational Procedure .....	27
3.3. Verification of the Proposed Methodology .....	27
3.3.1. Case I : Verification using IEEE-6 Bus System .....	28
Case I(A): Fixed DG Capacity-Active Power Loss.....	30
Case I(B): Fixed DG Capacity-Network Voltage Profile .....	30
Case II: Variable DG Capacity.....	31
3.3.2. Case II: Verification using IEEE-33 Bus System .....	34
3.4. Summary .....	38
NOVEL METHODOLOGIES FOR OPTIMIZING DG SIZES .....	39
4.1. Optimization of DG Sizes Using Loss and Voltage Sensitivity Analysis.....	39
4.1.1. Formulation of Objective function.....	39
4.1.2. Computational Procedure .....	41
4.1.3. Verification using IEEE-33 Bus System .....	41
4.2. Optimization of DG Sizes Using Lagrange Multiplier Method .....	44
4.2.1. Problem Formulation.....	44

Total Active Power Loss.....	44
Voltage Drop Between Two Busbars .....	45
Exact Loss Formula .....	45
4.2.2.    Formulation of Objective Function.....	45
4.2.3.    Constraints.....	46
4.2.4.    Solution Method.....	47
4.2.5.    Computational Procedure .....	48
4.2.6.    Verification using IEEE-6 & IEEE-33 Bus Systems .....	49
4.3.    Summary .....	53
BESS CAPACITY CALCULATION METHODOLOGY .....	54
5.1.    Modelling of Solar PV Output .....	55
5.1.1.    Calculation of PV Output .....	56
5.1.2.    Mapping Procedure of SPV Generation .....	60
5.2.    Modelling of Load Curves .....	61
5.2.1.    Mapping Procedure of Load Curves .....	61
5.3.    Analytical Method for PV & BESS Sizing .....	63
5.3.1.    Sample Calculation .....	67
5.4.    Verification of Results for PV Sizes (with BESS).....	71
5.5.    Summary .....	73
OPTIMAL POWER DISPATCH SCHEDULE .....	74
6.1.    Mathematical Background .....	74
6.2.    BESS Dispatch Algorithm .....	75
6.3.    Simulation Results .....	77
6.3.1.    Charge/Discharge Rate of BESS.....	77
6.3.2.    SOC Variation of BESS Units .....	79
6.3.3.    Active Power Loss Variation.....	81
6.3.4.    Voltage Profile Variation .....	85
Variation of Busbar Voltages for the Mix Daily Load Profile .....	85
Variation of Busbar Voltages for the Residential Daily Load Profile .....	87
Variation of Busbar Voltages for the Commercial Daily Load Profile .....	89
6.4.    Summary .....	90
CONCLUSIONS AND FUTURE WORK.....	92
7.1.    Conclusions .....	92
7.2.    Future Work .....	93
REFERENCES .....	95
APPENDIX – A – DERIVATION OF JACOBIAN MATRIX.....	102

APPENDIX – B – PARAMETERS OF IEEE-6 BUS SYSTEM .....	104
APPENDIX – C – PARAMETERS OF IEEE-33 BUS SYSTEM .....	105

## LIST OF FIGURES

Figure 3.1: IEEE-6 bus test system.....	28
Figure 3.2: LVSI for different DG locations for IEEE-6 bus network.....	29
Figure 3.3: Active power loss comparison for Case I & II.....	32
Figure 3.4: Busbar voltages for different locations of 4-MW DG unit.....	32
Figure 3.5: Combined active power loss reduction and bus voltage enhancement for different locations of 4-MW DG unit.....	34
Figure 3.6: IEEE-33 bus test system.....	34
Figure 3.7: Combined active power loss reduction and bus voltage enhancement for multiple DG locations of 0.2-MW DG units.....	38
Figure 4.1: Active power loss comparison (IEEE-33 bus system) .....	42
Figure 4.2: Voltage profile comparison (IEEE-33 bus system) .....	43
Figure 4.3: Typical configuration of a radial or meshed network.....	44
Figure 4.4: Active power loss comparison.....	51
Figure 4.5: Voltage profile comparison for IEEE-6 bus network.....	51
Figure 4.6: Voltage profile comparison for IEEE-33 bus network.....	52
Figure 4.7: Comparison of combined loss reduction and bus voltage enhancement for Case I and Case II.....	53
Figure 5.1(a): Expected PV output @ 7 a.m. (For Hambantota PV farm) .....	59
Figure 5.1(b): Expected PV output @ 9 a.m. (For Hambantota PV farm) .....	59
Figure 5.1(c): Expected PV output @ 12 noon (For Hambantota PV farm).....	59
Figure 5.1(d): Expected PV output @ 3 p.m. (For Hambantota PV farm) .....	59
Figure 5.1(e): Expected PV output @ 5 p.m. (For Hambantota PV farm) .....	59
Figure 5.1(f): Expected PV output @ 8 p.m. (For Hambantota PV farm) .....	59
Figure 5.2: Aggregated daily SPV output curve (For Hambantota PV farm).....	60
Figure 5.3: Total daily SPV output curves of the PV units (with No BESS) in the IEEE-33 network.....	61
Figure 5.4: Normalized mix daily load profile.....	62
Figure 5.5: Normalized residential load profile.....	62
Figure 5.6: Normalized commercial load profile.....	63

Figure 5.7: Illustration of the definitions of peak solar period and off-peak solar Period.....	64
Figure 5.8: Load areas of the IEEE-33 test bus system.....	65
Figure 6.1 BESS dispatch algorithm.....	76
Figure 6.2: Charge/Discharge rates of BESS units (For mix daily load profile).....	78
Figure 6.3: Charge/Discharge rates of BESS units (For residential daily load profile) .....	78
Figure 6.4: Charge/Discharge rates of BESS units (For commercial daily load profile) .....	79
Figure 6.5: SOC variation of BESS units (For mix daily load profile) .....	80
Figure 6.6: SOC variation of BESS units (For residential daily load profile) .....	80
Figure 6.7: SOC variation of BESS units (For commercial daily load profile) .....	81
Figure 6.8: Active power loss variation (For mix daily load profile) .....	82
Figure 6.9: Active power loss variation (For residential daily load profile) .....	82
Figure 6.10: Active power loss variation (For commercial daily load profile).....	83
Figure 6.11(a): Variation of busbar voltages @ 4 a.m. (For mix daily load profile) .....	85
Figure 6.11(b): Variation of busbar voltages @ 3 p.m. (For mix daily load profile) .....	85
Figure 6.11(c): Variation of busbar voltages @ 8 p.m. (For mix daily load profile) .....	86
Figure 6.12(a): Variation of busbar voltages @ 4 a.m. (For residential daily load profile).....	87
Figure 6.12(b): Variation of busbar voltages @ 3 p.m. (For residential daily load profile).....	87
Figure 6.12(c): Variation of busbar voltages @ 8 p.m. (For residential daily load profile).....	88
Figure 6.13(a): Variation of busbar voltages @ 4 a.m. (For commercial daily load profile).....	89
Figure 6.13(b): Variation of busbar voltages @ 3 p.m. (For commercial daily load	

profile).....	89
Figure 6.13(c): Variation of busbar voltages @ 8 p.m. (For commercial daily load profile).....	90

## LIST OF TABLES

Table 2.1: Comparison of DG technologies.....	5
Table 2.2: Optimization techniques used in DG allocation.....	9
Table 2.3: Summary of literature review and background studies.....	20
Table 3.1: VSI and LSI values at base case scenario (IEEE-6 network) .....	28
Table 3.2: Comparison of active power loss for Case I and Case II.....	31
Table 3.3: %TNVI values for different busbar locations.....	32
Table 3.4: Calculation of $\Delta P_{loss,i} \times TNVI$ values for Case I (IEEE-6 bus system) .....	33
Table 3.5: VSI and LSI values at base case scenario (IEEE-33 network) .....	35
Table 3.6: Calculation of $\Delta P_{loss,i} \times TNVI$ values (IEEE-33 bus system.....	37
Table 4.1: Comparison of DG sizes (IEEE-33 bus system) .....	42
Table 4.2: Summary of results for optimal DG sizes.....	50
Table 5.1: Summary of SPV parameters and calculations.....	58
Table 5.2: Case I ( $\eta=20\%$ , Mix daily load profile) .....	69
Table 5.3: Case II ( $\eta=25\%$ , Mix daily load profile) .....	69
Table 5.4: Case III ( $\eta=30\%$ , Mix daily load profile) .....	70
Table 5.5: Case IV ( $\eta=20\%$ , Residential load profile) .....	70
Table 5.6: Case IV ( $\eta=20\%$ , Commercial load profile) .....	71
Table 5.7: Comparison of PV sizes (with BESS).....	71
Table 6.1: Daily energy loss comparison for different load profiles.....	84

## LIST OF ABBREVIATIONS

ABCO	:	Artificial Bee Colony Optimization
ACO	:	Ant Colony Optimization
BESS	:	Battery Energy Storage System
BPDF	:	Beta Probability Density Function
CEB	:	Ceylon electricity Board
CSP	:	Concentrated Solar Power
DE	:	Differential Evolution
DER	:	Distributed Energy Resources
DG	:	Distributed Generation
DNO	:	Distribution Network Operator
DP	:	Dynamic Programming
DSO	:	Distribution System Operator
ELF	:	Exact Loss Formula
EV	:	Electric Vehicles
FF	:	Fill Factor
GA	:	Genetic Algorithm
GHG	:	Green House Gases
IA	:	Improved Analytical
IPP	:	Independent Power Producers
LMM	:	Lagrange Multiplier Method
LP	:	Linear Programming
LPF	:	Load Proportionality Factor
LSF	:	Loss Sensitivity Factor
LTGEP	:	Long Term Generation Expansion Plan
MCS	:	Monte Carlo Simulation
MINLP	:	Mixed Integer Non-Linear Programming
MIP	:	Mixed Integer Programming
MPPT	:	Maximum Power Point Tracking
NLP	:	Non-Linear Programming
OP	:	Ordinal Programming
OPF	:	Optimal Power Flow

PSO	:	Particle Swarm Optimization
RES	:	Renewable Energy Sources
SA	:	Simulated Annealing
SBM	:	Sensitivity Based Methods
SCL	:	Short Circuit Level
SOC	:	State of Charge
SPV	:	Solar Photo-Voltaic
SQP	:	Sequential Quadratic Programming
TS	:	Tabu Search
VI	:	Voltage Index
VPP	:	Virtual Power Plant

# CHAPTER 1

## INTRODUCTION

Due to the increase in the price of fossil fuels and natural gas, the electric power industry has undergone a significant change in terms of planning, operation and regulation. Moreover, the environmental pollution caused by the excessive emission of Green House Gases (GHG) by some of the conventional methods of power generation has also motivated the researchers in the power industry to shift towards more environmental friendly and economical methods of power generation. On the other hand, due to the ever-increasing power demand, the existing networks may not be able to supply the increasing demand as required. Hence, power industry researchers are more concerned about alternative options which can address these issues. Integration of Distributed Generation (DG) for distribution networks is one of the many ways that is used for addressing the above-mentioned problems.

Electric power generation by Distributed Energy Resources (DER) such as Solar Photovoltaic (SPV), Wind energy, Bio-mass energy, Diesel power generation within distribution networks or on the customer side of the meter is defined as Distributed Generation (DG) [1]. In the recent past, integration of DG units for distribution networks has taken a great interest in the modern power industry because of its wide variety of merits over the conventional methods of generation. Reduction of transmission costs, active and reactive power losses, contribution towards enhancing energy security and diversification of energy sources, minimizing system upgrades are some of the common advantages of DG over the conventional methods of power generation [2].

Due to the variety of merits gained by DGs, there has been a significant growth of interest in integrating DG units for power networks both globally and locally. Some of the developed countries such as Denmark and Belgium have invested a lot of money on researches on some of the DG technologies like solar and wind power generation. Countries such as India and Pakistan have increased their share of power generation by solar and wind. Even in Sri Lanka, government policies have been set up recently to enhance the share of green energy. The program “Soorya Bala Sangramaya” was also launched as a part of that policy so that the electricity consumers are motivated to have solar rooftops in their houses. Moreover, the governing bodies have taken

measures to give certain incentives for the investors to have solar rooftops with the intention of popularizing solar generation in the country.

## **1.1. Background of the Study**

### **1.1.1. Problem Statement**

DG allocation consists of mainly three pillars as DG location, DG size and power dispatch (which is optional if Battery Energy Storage Systems (BESS) are used for dispatching power). Usually the decision about the placement of DGs in distribution networks are taken by Independent Power Producers (IPPs), state owned utilities or just customers considering several practical aspects such as land and fuel availability, climatic variations and environmental factors. Apart from that, due to intermittency and non-dispatchable nature of some of the DG technologies such as Solar Photo-Voltaic (SPV) and wind power generation, electricity customers and investors may utilize BESS along with their DG in order to dispatch power at their will. Hence, the Distribution System Operators (DSO) have less control over the decision about DG placement problem [2]-[4]. Due to that there may be situations of inappropriate allocation of DG units for power networks which can have undesirable impacts on the network. Eventually, those undesirable impacts may increase system power losses, protection issues, violate stipulated voltage limits and diminish supply reliability. On the contrary, if the DG allocation problem is properly managed and optimized, it will further enhance the network performance in terms of power quality, protection and stability. Hence, proper allocation of DG units is essential in meeting the desired network performance.

Although certain research has been carried out with regard to the optimization of DG allocation as discussed in Chapter 2, certain issues need to be further addressed. Basically, DG allocation is investigated based on the impact of network performance and operating constraints such as violation of operating voltage limits, violation of line capacity limits, variations of network power losses and harmonic losses. In practical case, all these parameters come into play simultaneously. Hence, it is essential to study the behavior of these parameters collectively. However, the combined effect of few parameters has not been taken into consideration in the existing work. Thus, the work completed in the thesis has proposed a novel concept for DG allocation based on the voltage and network power loss sensitivity analysis.

The specialty and novelty of this research is further highlighted as all these approaches can be applied for multiple DG and BESS allocation. Moreover, since all these are analytical methods, the internal nature and behavior of each methodology can be easily understood whereas in existing work which are based on conventional optimization techniques [5]-[9], it is difficult to observe what is actually happening internally.

### **1.1.2. Research Objectives**

The research is based on mainly two objectives as listed below.

1. To develop separate criterion for optimizing the DG location and size based on network loss and voltage sensitivity analysis.
2. To develop an optimal power dispatch schedule for Battery Energy Storage System (BESS) integrated networks.

### **1.1.3. Scope of Work**

In this research, new systematic approaches have been developed for all the aspects of DG allocation (DG location, DG size and Power Dispatch). As mentioned earlier, in order to optimize the DG allocation and cope with the intermittency and non-dispatchable nature of DG technologies such as SPV and wind power generation, separate methodologies addressing each research objective are presented in this thesis. Furthermore, analytical methods are used as the optimization techniques.

A novel objective function based on network loss and voltage sensitivity analysis is used for presenting an analytical method for determining the optimal DG location. A similar kind of an approach is proposed for calculating the optimal DG size. A Lagrange Multiplier Method (LMM) based scheme is also presented as an alternative method for optimizing the DG size. An analytical method is presented to optimize the BESS capacities for serving a portion of demand during the off-peak solar generation period as a part of this research. Ultimately, an optimal power dispatch schedule based on all the previously proposed novel schemes is also given in this thesis.

## **1.2. Thesis Structure**

The thesis is organized as follows. Chapter 1 presents the research motivation for optimal DG allocation, scope of the study and the objectives achieved in this research. A comprehensive literature review including the classification of DG based on their technologies and different optimizing techniques for DG allocation is

presented in Chapter 2. Furthermore, a comprehensive summary of previous research work based on optimizing DG location, size, power dispatch and BESS sizing including the optimization techniques used in them is also discussed in this chapter. The third chapter is dedicated for presenting the novel optimization method developed for determining the optimal DG location. Moreover, the theoretical background used in this method including the mathematical definitions of loss and voltage sensitivities, bus admittance and bus impedance matrices, Exact Loss Formula (ELF) are also detailed in this chapter. The verifications done by using IEEE-6 and IEEE-33 standard test bus systems are presented in this chapter. The next chapter is about the two analytical methods proposed in this research for optimizing the DG size. The two methodologies are described in two subsections for the easiness of comparing the results. As a verification of the proposed methodologies, minimization of active power losses and voltage deviations with the calculated DG size integration for the IEEE-6 and IEEE-33 networks are also given in this chapter. Chapter 5 presents a new analytical method proposed for determining the BESS capacities used for serving a fraction of demand in the off-peak solar generation period. In this chapter, modelling of SPV power output and load profiles based on standard mathematical relationships are presented. The applicability of the proposed scheme is illustrated by simulating the IEEE-33 network under different scenarios. Furthermore, as an extension of verification, BESS capacities are determined for different load profiles of residential, commercial and industrial. In Chapter 6, the proposed algorithm for dispatching power from BESS is presented. Verified results for the IEEE-33 network is presented with appropriate sensitivity analysis. As the last chapter, an overall conclusion of this research and suggestions and recommendations for future work are detailed.

### **1.3. Summary**

This chapter presents an introduction about the research describing existing problems associated with DG allocation and how they are going to be addressed through acquiring the research objectives. In addition to that, the novelty of the proposed schemes for optimizing DG location, size, power dispatch and BESS sizing was also summarized in this section.

## CHAPTER 2

### LITERATURE REVIEW AND BACKGROUND STUDIES

This chapter presents a detailed overview about the previous research work done for optimizing the DG location, size, power dispatch and BESS capacity. Moreover, a detailed description about the optimization techniques used for optimizing the above-mentioned things is also presented in this chapter for better understanding.

#### 2.1. Distributed Generation in Power Systems

##### 2.1.1. Importance of Distributed Generation

The increasing trend for integrating DG units for power networks is due to some reasons. A few of those reasons are;

- Reduce the transmission costs and costs associated with active power and reactive power losses, voltage deviations.
- Diversification of energy resources and thereby improve the energy mix of a country.
- Enhance energy security.
- Can be located at any location if the resources are abundantly available.
- Can enhance the reliability of utility system with its ability to give supply for essential protective functions of the grid in case of a supply failure

##### 2.1.2. Classification of DG

Classification of DG is done based on the technology of DG used. Table 2.1 presents a summary of DG technologies with a comparison of their advantages and disadvantages.

Table 0.1: Comparison of DG technologies [10]

DG technology	Merits	Demerits
1. Solar Photo-Voltaic (SPV)	<ul style="list-style-type: none"><li>• Clean and silent form of electricity</li><li>• Less environmental impacts</li></ul>	<ul style="list-style-type: none"><li>• High initial cost</li><li>• Poor efficiency</li></ul>
2. Concentrated Solar Power (CSP)	<ul style="list-style-type: none"><li>• Low maintenance cost</li></ul>	<ul style="list-style-type: none"><li>• Occupy a large space</li><li>• High initial cost</li></ul>

3. Wind Energy	<ul style="list-style-type: none"> <li>• Free and unlimited</li> <li>• Enhance energy security</li> </ul>	<ul style="list-style-type: none"> <li>• Large structural area needed</li> <li>• Large noise of rotor blades</li> </ul>
4. Bio-mass Energy	<ul style="list-style-type: none"> <li>• Renewable and domestically available</li> <li>• Curtail GHG (Green House Gas) emissions</li> </ul>	<ul style="list-style-type: none"> <li>• Threat for food security</li> <li>• Environmental impacts like soil erosion</li> </ul>
5. Diesel power generation	<ul style="list-style-type: none"> <li>• Needs less space</li> <li>• Can be located at any place</li> </ul>	<ul style="list-style-type: none"> <li>• High emission</li> <li>• High unit cost</li> </ul>

### 2.1.3. DG Allocation and its Impact on Network

As described in Chapter 1, since DSOs have less control over the decision about DG allocation, there may be instances of inappropriate DG allocation which can disturb the smooth performance of a power network. The inappropriate allocation of DG units may affect the system mainly in three areas as [1],[11];

- 1) Power quality
- 2) Protection
- 3) Stability

#### Power Quality Issues

With inappropriate allocation of DG units power quality issues such as voltage violations and excessive injection of harmonics may occur. In case for a traditional distribution network having unidirectional power flow which shows a significant voltage drop towards the downstream of the network, it is desirable to have DG integrated for the network. Nevertheless, it will not be possible to have a desired voltage profile enhancement if insufficient capacity of DG is integrated for the network. On the contrary, if excessive capacity of DG is integrated, then there will be cases of overvoltage situations where both customers and the DG plant are badly affected. Since almost all the DG technologies need to have a power electronic interface to be integrated for the power system, the power electronic components may inject harmonics to the network which can cause significant power quality issues. Thus, it is essential to have the exact DG capacity integrated at the optimal locations in order to minimize the harmonic effects. Furthermore, if excessive harmonics are

injected over a lengthy period of time, the costs incurred by harmonic losses such as aging of distribution system components (cables, transformers) will also increase [12].

### **Protection Issues**

One of the issues with DG integration is that it tends to cause the fault current limits of a network to increase. Due to this, mis-coordination of protection schemes will occur with the mismatch of traditional overcurrent grading system. Thus, unwanted tripping of relays and blinding of protection may become more severe with inappropriate DG allocation. DG units with synchronous generation tend to produce unnecessary tripping of relays. On the other hand, blinding of protection which is one of the frequent problem arises with DG integration is a phenomenon that occurs due to the limitation of fault current levels caused by power electronic components used in DG units [11],[13]. This problem is frequently recorded with SPV and wind power generation.

### **Stability Issues**

Improper allocation of DG units can affect the network in terms of stability as well. For example, in case of a DG unit is tripped, there will be a sudden step reduction of voltage. However, in order to guarantee that the voltage limits are not violated even with this kind of a fault situation, the location and size of the DG unit should have been properly assessed before the fault occurs. Hence, it is required to have optimal DG capacities at optimal DG locations with an optimal power dispatch scheme (in case BESS are used) to maintain voltages and other relevant parameters within acceptable limits in a given network.

#### **2.1.4. Significance of Optimizing DG Allocation**

Optimization of DG allocation is vital for power system operation in many ways. One of the main advantage of optimizing DG allocation is that it helps in minimizing the demand outage due to mismatch of supply and demand. If the DGs can supply the deficit demand at required time (in case of a sudden large conventional generation trip), the mismatch of supply and demand will be minimized. Thereby the reliability of system operation is also enhanced. Moreover, at certain time periods in a day, it may be more economical to operate the system with the power generated by DG than operating with conventional thermal generations. Hence, if the DG allocation is optimized, then by utilizing the power generated by local DGs, utility will be able to operate the power system with minimum operation cost.

## **2.2. Taxonomy of Optimization Methods Used for DG Allocation**

In the last few decades, many researches have been done regarding optimizing DG allocation. The optimization is carried out using numerous optimization techniques. This section of the thesis presents a detailed analysis about the methodologies used for optimizing DG allocation.

### **2.2.1. Problem Formulation**

In optimizing DG allocation, the problem is formulated as optimizing DG location, DG size and power dispatch or as a combination of each of these aspects. The objective function can be formulated as single or multi-objective function. The commonly considered objective functions in the literature can be listed as below.

- Minimization of active power losses
- Minimization of voltage deviations
- Minimization of cost of operation
- Minimization of total energy losses
- Maximization of DG capacity
- Maximization of voltage limit loadability

### **2.2.2. Constraints**

The constraints used in optimizing DG allocation can be mainly classified as equality constraints and inequality constraints. The major constraints used in DG allocation are listed below.

- Power balance constraints (Active and Reactive power)
- Voltage magnitude limits
- Line capacity limits
- DG penetration limit
- Transformer capacity limits
- Short Circuit Level (SCL) limits
- Reliability constraints
- Power generation limits
- No. of DG units

### 2.2.3. DG Technology

Several DG technologies have been considered in previous work for optimizing the DG allocation. SPV, wind power generation and fuel cell technologies are the most commonly used ones among them.

### 2.2.4. Load Profile

The commonly used load profile patterns in DG allocation problem can be listed as follows.

- Constant load levels
- Multi load levels
- Time-varying loads
- Stochastic load patterns

### 2.2.5. Optimization Techniques Used in DG Allocation

A synopsis of the classification of optimization techniques used in DG allocation is presented in Table 2.2.

Table 2.2: Optimization techniques used in DG allocation [1],[10]

Optimization Techniques	Exact Optimization	• Linear programming (LP)
		• Non-Linear Programming (NLP)
		• Sequential Quadratic Programming (SQP)
		• Dynamic Programming (DP)
		• Ordinal Programming (OP)
		• Gradient Search Method
	Heuristic Optimization	• Genetic Algorithm (GA)
		• Particle Swarm Optimization (PSO)
		• Ant-Colony Optimization (ACO)
		• Artificial Bee Colony Optimization (ABCO)

		<ul style="list-style-type: none"> <li>• Monte Carlo Simulation (MCS)</li> </ul>
	Analytical Methods	<ul style="list-style-type: none"> <li>• Sensitivity Based Methods (SBM)</li> </ul>

### **Exact Optimization**

In Exact Optimization (EO), objective function and constraints are known parameters. Some of the examples for exact optimization techniques are Linear Programming (LP), Non-Linear Programming (NLP), Sequential Programming (SQ), Sequential Quadratic Programming (SQP), Ordinal Programming (OP) and Gradient Search Method (GSM).

### **Linear Programming**

Linear Programming (LP) method is applied for problems which consists of linear objective functions and linear constraints [10]. The main advantage of this kind of optimization is that always the solution is converging. On the contrary, the main disadvantage is that this method can be applied only for problems that consists of linear constraints and objective function [16].

In [14], LP is used for maximizing the DG capacity integrated for an Irish distribution network. In this work, multiple DG units are considered for integrating for the considered distribution network. The optimal DG locations and their respective DG capacities are calculated using the LP method. A similar kind of an approach is followed in [15] by the same authors for maximizing the profits by optimizing the energy harvested through distributed generation. In this research, the time varying nature of loads are taken into consideration whereas in [14], it considered only constant loads. Here also, the results are validated for the same distribution network considered in [14].

### **Non-Linear Programming**

Non-Linear Programming (NLP) is the contrary of LP and in this method objective function and constraints are non-linear in nature. Since most of the power system problems and constraints are non-linear in nature, this method is widely used in many research work. A research based on NLP method for optimally placing wind DG units is given in [17]. In this paper, a probabilistic generation and load model is used. Then they are reduced to deterministic models by taking into account their all

possible operating scenarios. The problem is solved as a multi-objective function using Optimal Power Flow (OPF).

In some cases, the value of constraints may be integers. For example, if the number of DG units to be integrated for a network is taken as a constraint, it should output its final value as an integer. In order to account for this, some objective functions will have to be solved as a combination of LP, NLP and Mixed-Integer Programming (MIP). Thus, these problems are solved using Mixed-Integer Non-Linear Programming (MINLP) method. This method can be applied for variables in non-linear functions that are either discrete or continuous in nature. Moreover, this method can be used for solving multi-objective functions as it gives accurate and reliable solutions efficiently. The DG units are optimally allocated by taking into account the fluctuation of electricity market prices in [18] using MINLP as the solution method. Here, the objective function is formulated as a multi-objective function with weights. A similar kind of an approach is used in [19] for a hybrid electricity market for optimizing the DG location and their sizes. In this work, the problem is solved for minimizing the cost of operation. Furthermore, the objective function subject to several constraints are solved by MINLP technique. A novel model based on MINLP for distribution network planning is presented in [20] such that the minimization of operation cost is achieved. A novel methodology for enhancing the voltage stability of a distribution network by optimally allocating the DGs is given in [21]. In this approach a novel parameter named as “Voltage Index (VI)” is defined and observed the variation of it by changing the DG location and their capacities. Eventually, the problem is solved by MINLP and optimized the DG allocation. Similar kind of methodologies for optimizing DG allocation using MINLP are presented in [3], [22]-[25].

### **Sequential Quadratic Programming**

This is an iterative optimization technique used for solving highly non-linear objective functions with inequality constraints. In [26], Sequential Quadratic Programming (SQP) is used for maximizing the profits by determining the optimal DG sizes. Here, the optimal DG locations are pre-decided and hence only the optimal DG sizes are calculated using SQP. The specialty of this work is that, switchgear fault ratings are also considered as an additional constraint. An improved SQP method is used in [27] for optimizing the DG location and size. Minimization of active power losses is taken as the objective function in this approach. The SQP method is modified

in this approach by combining a sensitivity analysis for optimizing the DG placement with pre-specified and unspecified power factors. A multi-objective function is formulated in [5] for optimizing the DG location and size. This is also solved as a SQP problem.

### **Dynamic Programming**

This is also another widely used optimization technique for optimizing the DG allocation. In this method, the problem is solved as a sequential optimization problem for handling real time variations. Therefore, this method is ideal for solving problems that consist of variable load and generation models. Moreover, the results can be obtained in an efficient and reliable manner with less computational time by this approach. A Dynamic Programming (DP) approach is used in [29] for maximizing the profits gained by Distribution Network Operators (DNOs). In this research, the loads are modelled as light, medium and peak loads and the results obtained for each scenario are compared for better understanding. The results show that DG locations and sizes vary according to the states of load.

### **Ordinal Programming**

This is an optimization technique that is considered as an improved version of LP. In Ordinal Programming (OP), the desired results can be obtained with less computational burden [10], [30]. Hence, this method is frequently used in researches based on DG allocation. The optimal DG locations and sizes are determined as a compromise of minimizing active power losses and maximizing DG capacities in [31]. Furthermore, OP is used in this paper for solving the problem as a multi-objective function. Similar kind of methodologies for optimizing DG allocation using OP are presented in [32],[33].

### **Gradient Search Method**

Gradient Search Method (GSM) is an iterative optimization technique used for finding the minimum of a differentiable function [34],[35]. GSM based optimization is used in [34] for maximizing the profits gained by integrating DGs. In this work, constraints due to fault levels are transformed into non-linear inequality constraints for simplifying the solution procedure. Optimal DG sizes are determined using GSM for minimizing the active power losses in [35]. The optimal DG locations are pre-decided and the DG sizes for minimizing the active power losses are calculated from GSM.

## **Heuristic Optimization**

Heuristic optimization techniques are the most widely used type of optimization technique in optimizing DG allocation. The reason for this is that, in heuristic methods, the objective function need not to be mathematically formulated by using the variables of interest. Nevertheless, heuristic methods are still capable for producing very accurate results with less computational burden [30]. Genetic Algorithm (GA), Particle Swarm Optimization (PSO), Ant-Colony Optimization (ACO), Artificial Bee Colony Optimization (ABCO) , Tabu Search (TS), Simulated Annealing (SA), Differential Evolution (DE) and Monte-Carlo Simulation (MCS) are some of the common examples for heuristic optimization methods.

### **Genetic Algorithm**

Genetic Algorithm (GA) is an optimization technique based on the theory of natural evolution [36]. As the first step, a population of chromosomes is produced randomly. Here a chromosome is a complete solution for the problem and its fitness is checked based on the objective function. The chromosomes which are fitting best are stored to create a new generation. This is iteratively followed to find a generation of chromosomes with a greater fitness value than the previous generation. The iteration of this process continues until it reaches a stopping criterion. The basic steps followed in GA can be listed as follows [10],[30],[37].

- 1) Initialization
- 2) Evolution
- 3) Crossover
- 4) Mutation

In the Initialization step, the population size needs to be specified. The passing of best fitting chromosomes to the next generation is the Evolution. Exchanging of gene information between two chromosomes is done randomly in the Crossover step. Mutation happens randomly to modify the value of a chromosome to avoid the possibility of losing complete genetic information through crossover. The variables used in implementing the GA algorithm are population size, mutation rate, crossover rate and maximum number of iterations.

GA is used in [38] for determining the optimal DG locations and sizes for minimizing the active power losses in the network. In this work, the loads are modelled

as power concentrated loads. A similar kind of an approach but for distributed loads in a radial network and constant loads for a meshed network is discussed in [39]. A novel method for maximizing the benefit/cost ratio by integrating DG units is presented in [40]. In this research, the reliability constraints are also considered apart from the conventional constraints used in most of the similar work. Another research for maximizing benefit/cost ratio is given in [41]. Nevertheless, in this work GA is implemented for computing the optimal number of DG units, optimal DG locations and their respective sizes including the optimal DG technology whereas in [40] it considered only optimizing the DG location and size. GA for solving a non-linear bi-level problem for maximizing the profits of the DG investor subject to the minimization of payments done by DSO is discussed in [42]. A combination of GA and Decision theory is used in [12] for determining the optimal DG locations and sizes by considering the uncertainties of DG units and the power quality issues imposed by them. A hybrid method of GA and OPF is used for optimally siting and sizing the DG units in [7]. A Fuzzy GA for minimizing the cost incurred by active power losses is presented in [43]. An improved GA method is used in [44] for maximizing the wind power generation DG capacity.

A novel power dispatch schedule for BESS with the objective of minimizing the power taken from the grid is presented in [45]. In this work, the real time scheduling of the usage of domestic appliances is optimized with GA method. The usage pattern of the domestic appliances is modelled using the past usage data. GA is used to optimize the power dispatch from BESS for three scenarios as 10%, 25% and 40% reduction of energy taken from the grid and match the household energy consumption with the availability of battery storage energy. A system with conventional generation, DG technologies such as SPV and wind energy and BESS units is studied in [46] for minimizing the fuel cost of generation. Fuzzy logic is used for accounting for the forecast errors of generation and load. Membership functions are defined for each of the constraints and those are eventually used for determining the solutions for fitness functions. Ultimately, GA is used for optimizing the power dispatch schedule of conventional generators and the BESS units. For minimizing the charging cost of Electric Vehicles (EVs) and battery degradation cost, a novel multi-objective function in terms of technical and economic aspects is defined in [47]. GA is used in this work for optimizing the charging schedule.

## **Particle Swarm Optimization**

Particle Swarm Optimization (PSO) is a heuristic optimization technique that is quite similar to GA [48]. In this method a population of particles is generated, and their positions are the candidate solutions. Each of these particles have their own velocities as they move in the search space. The new positions of the particles are the solution set in the next generation. Furthermore, the velocities of particles are dependent on the best solution gained so far for a particular generation (local best solution) and the best solution of all generations (global best solution) [30],[49].

PSO is applied in [50] for optimizing the DG placement of multiple DGs in a distribution network with loads that are time varying. Maximization of DG capacities for inverter type and synchronous type DG units is presented in [51]. In addition to the commonly considered constraints, the authors have taken into account the standard harmonic limits and protection constraints as well. Moreover, optimal DG locations are also determined by using PSO method. A modified version of PSO as a discrete optimization method for determining the optimal DG locations is given in [52]. A hybrid optimization based on PSO and GA is presented in [53] for optimizing the DG placement. An improved PSO method is discussed in [54] for optimizing the sizes of DG units which are capable of absorbing or injecting reactive power.

A novel work based on PSO algorithm is used in [55] for optimizing the reactive power dispatch with the objective of minimizing the active power losses. The proposed methodology is applied for two distribution networks and compared the results obtained in this method and GA method. Optimization of active and reactive power from SPV and BESS units as a day ahead scheduling is presented in [56]. In this approach, PSO is used as the optimization technique for obtaining the results. Another work based on PSO is applied for an off-grid hybrid system for optimizing the power dispatch from BESS such that the voltage levels are regulated within the acceptable limits [57].

## **Ant-Colony Optimization**

Ant-Colony Optimization (ACO) is based on the behavior of ants for determining the shortest path when searching for food. The decisions made by ants about the path they should follow to reach the food in the shortest length is dependent on pheromone [10]. This is the concept used in this optimization method. ACO

optimization is used in [58] for determining the optimal locations for DGs and Reclosers such that total active power losses are minimized.

### **Artificial Bee Colony Optimization**

In the Artificial Bee Colony Optimization (ABCO), three types of bees are considered namely Onlooker bees, Scout bees and Employee bees [10]. In this method, it is supposed that number of employee bees is equal to the number of sources of food available. As the first step of algorithm, initial food sources are designated for each employee bee. Then these employee bees go for their food sources and while keeping in memory the shortest path and the nectar amount. The onlooker bees watch the behavior of employee bees and choose one of the sources and calculate the nectar amount available there. The employee bees become scout bees when they abandon their food sources. These scout bees search for new food sources and then replace the abandoned ones with the newly found food sources. The best food found until a certain criterion is reached is taken as the best solution. ABCO method is utilized in [59] for determining the optimal number of DG units, their locations and sizes such that the active power losses are minimized.

### **Monte Carlo Simulation**

Monte Carlo Simulation (MCS) is an iterative optimization method which is capable of giving better results with less processing time. It is of two types as deterministic and probabilistic [10]. MCS method is used in [60] and [61] for optimizing the DG placement such that the network active power losses are minimized.

### **Tabu Search**

Tabu Search (TS) is another heuristic optimization technique extensively used in optimizing DG allocation. In this technique, a neighborhood search method is adopted such that the potential solution moves to an improved solution in the same neighborhood [62]. One of the key merits of this method over the other heuristic optimization techniques is that, getting trapped in a local minima is highly minimized when solving since this maintains a list named “tabu list”. This tabu list keeps in memory about all the past solutions that have been searched before and it avoids searching solutions that have been searched before. Thereby, the computational speed is also enhanced. However, the quality of the final solution is highly dependent on the initial solution which is one of the disadvantage of this method.

TS method is used in [63] for a network with uniformly distributed loads in order to determine the optimal DG locations and sizes to acquire minimum active power losses in the network. Optimizing the allocation of DG units and Reactive power components with the objective of minimizing the cost of operation is solved by using TS method in [64]. A hybrid GA and TS method is used by the authors in [65] for minimizing the cost of operation for a wind power generation integrated network considering the intermittency nature of wind energy and time varying nature of loads. An optimal power dispatch schedule for BESS integrated network in Japan is developed using TS method in [66]. The weather forecast data and load data from past are used for modelling the DG outputs and load curves. The results obtained from TS method is compared with GA method and it is observed that there is hardly any difference between the results obtained from the two methods.

### **Simulated Annealing**

Simulated Annealing (SA) is based on the principle of heating of a certain material and letting it to cool down slowly in order to decrease its defects. SA method has the ability to give optimum results in lesser time when compared with GA and PSO [10],[30]. SA is applied in [67] for optimizing the energy management of a smart grid such that the operating cost is minimized. In this work, a Virtual Power Plant (VPP) is used which consists of fuel cells, SPV, wind farms and EVs. The results obtained from SA method is compared with MILP method and almost the same results are obtained by both methods.

### **Differential Evolution**

Differential Evolution (DE) is an iterative optimization technique. One of the main advantage of DE is that, it does not need to have a differentiable function in order to carry out the optimization algorithm. DE is used in [68] for optimizing the DG sizes such that the total active power losses are minimized. Furthermore, the optimal DG locations are determined in this approach by using a bus voltage sensitivity analysis.

### **Analytical Methods**

The optimization methods that cannot be categorized under either exact optimization or heuristic optimization are considered as analytical optimization methods. These optimization methods are usually based on theoretical and mathematical relationships used in power system analysis. An analytical method

known as "2/3 rule" is applied in [69] such a way that a DG unit of the size of 2/3 capacity of the incoming generation is located at 2/3 distance of the line for radial distribution systems. However, this method may not be able to provide acceptable system performance for nonuniformly distributed loads. Novel approaches for determining the most suitable locations for placing DG units that minimizes the total active power loss in a network are presented in [4], [6]. An objective function for minimizing the real power loss is developed as a function of bus impedance matrix and complex load power in [4]. Several case studies are presented for time variant and time invariant load systems. The validity of the objective function is verified using the standard IEEE-6 bus system and IEEE-33 bus system. A method based on load concentration busbars is presented in [6]. Busbars with the highest loads are categorized according to zones, and then they are selected as the candidate locations for placing DGs in this method. An Improved Analytical (IA) method is given in [70] for determining the best locations in a network for integrating multiple DG units. The effectiveness of the methodology presented is checked by the Loss Sensitivity Factor (LSF) method and Exhaustive Load Flow (ELF) method. The optimal locations for multiple DG units are determined such that the total power loss in the network is minimized. Other than minimizing system losses and improving the voltage profile of a network, the optimal allocation of DG units can enhance some other network aspects as well. A methodology for minimizing the reactive losses and excessive loadings in lines of networks with the optimal allocation of DGs is presented in [71]. A solution procedure based on Lagrange multipliers is used in [71] determining the optimal locations for placing DG units.

### **Sensitivity Based Methods**

There are also Sensitivity Based Methods (SBM) which are used for optimizing the DG allocation. Since most of the existing work have considered minimizing active power losses and voltage deviations by integrating DG units, loss and voltage sensitivity analyses are extensively used. However, since they are two completely different analysis, the combined effect of those parameters has not been addressed in the previous work.

There are many appearances of voltage sensitivity analysis in the literature. voltage sensitivity values computed at different busbars of a network are utilized to determine the weighting factors for pricing the voltage control services at

corresponding busbars in [72]. Furthermore, a novel method of cost minimization of real and reactive power injections associated with a network with Renewable Energy Sources (RES) has been developed in this work using approximated voltage sensitivity values of radial distribution network. Reactive power allocation for a given network could be optimized with the proposed method in [73]. The voltage sensitivity values are used as the decision parameter in this work, since reactive power has a strong association with the voltages in a network.

Many research work have used loss sensitivity as a parameter for determining the optimum locations for allocating DG units for networks [11], [70], [74]. Loss sensitivity values are used as parameters for checking the applicability and accuracy of the novel method presented for minimizing the losses in a distribution network in [70]. A method for allocating DG units with energy storages is presented in [74]. In here the difference between the highest loss sensitivity value and the lowest loss sensitivity value of a bus system is used for determining the optimum locations for placing the DG units with energy storages. A combined analysis of loss and voltages sensitivities is considered in [11]. The loss and voltage sensitivity values before connecting DGs are calculated first, and then a selected number of buses with the highest loss and voltage sensitivity values are decided as the optimal locations for placing DG units.

### 2.3. Summary

In this chapter, the literature and background studies related to this research were presented. A synopsis of the literature discussed is given in Table 2.3.

Table 2.3: Summary of literature review and background studies

<b>Objective Function</b>	<b>Optimization Technique</b>	<b>Reference</b>
Minimizing active power loss	Analytical Method	[4],[6],[70],[74]
	Sequential Quadratic Programming	[5],[27]
	Genetic Algorithm and Optimal Power Flow	[7]
	Genetic Algorithm	[12],[38],[39]
	Non-linear Programming	[17]
	Gradient Search Method	[35]
	Particle Swarm Optimization	[50],[55]
	Particle Swarm Optimization and Genetic Algorithm	[53]
	Ant-Colony Optimization	[58]
	Artificial Bee Colony Optimization	[59]
	Monte Carlo Simulation	[60],[61]
	Tabu Search	[63]
	Differential Evolution	[68]
Maximizing DG capacity	Linear Programming	[14]
	Improved Genetic Algorithm	[44]
	Particle Swarm Optimization	[51]
	Improved Particle Swarm Optimization	[54]
	Analytical Method	[69]
Maximizing profits	Linear Programming	[15]
	Sequential Quadratic Programming	[26]
	Dynamic Programming	[29]
	Gradient Search Method	[34]
	Genetic Algorithm	[42]

Minimizing active power loss and voltage deviations	Mixed-Integer Non-linear Programming	[18]
	Improved Particle Swarm Optimization	[52]
Minimizing cost of operation	Mixed-Integer Non-linear Programming	[19],[20]
	Tabu Search	[64],[65]
	Simulated Annealing	[67]
Minimizing voltage deviations	Mixed-Integer Non-linear Programming	[21]
	Particle Swarm Optimization	[57]
	Analytical Method	[73]
Minimizing active power losses and maximizing DG capacity	Ordinal Programming	[31]
Maximizing benefit/cost ratio	Genetic Algorithm	[41],[42]
Minimizing cost of active power losses	Fuzzy logic and Genetic Algorithm	[43]
Minimizing power taken from grid	Genetic Algorithm	[45]
	Particle Swarm Optimization	[56]
	Tabu Search	[66]
Minimizing fuel cost	Genetic Algorithm	[46]
Minimizing the charging cost of (EVs) and battery degradation cost	Genetic Algorithm	[47]
Minimizing reactive power losses	Analytical Method	[71]
Minimizing the price of voltage control services	Analytical Method	[72]

## CHAPTER 3

### OPTIMIZATION OF DG LOCATION

In this chapter, the analytical method used for optimizing the DG location is presented. At first, the mathematical relationships used in developing the novel analytical method for optimizing the DG location are presented as follows.

#### 3.1. Mathematical Background

The general relationship between bus injection currents and voltages can be expressed as (3.1).

$$[I] = [Y_{Bus}][V] \quad (3.1)$$

The bus admittance matrix can be represented as  $Y_{Bus}$  as given in (3.1). The bus impedance matrix is defined as the inverse of bus admittance matrix

$$Z_{Bus} = [Y_{Bus}]^{-1} \quad (3.2)$$

##### 3.1.1. Jacobian Matrix

For a  $N$  Busbar system, the Jacobian matrix is given by (3.3). The detailed derivation of the Jacobian matrix is given in Appendix I.

$$\begin{bmatrix} \Delta P_2^k \\ \vdots \\ \vdots \\ \vdots \\ \Delta P_n^k \\ \vdots \\ \Delta Q_2^k \\ \vdots \\ \vdots \\ \vdots \\ \Delta Q_n^k \end{bmatrix} = \begin{bmatrix} \frac{\partial P_2^k}{\partial \delta_2} & \cdots & \frac{\partial P_2^k}{\partial \delta_n} & \frac{\partial P_2^k}{\partial |V_2|} & \cdots & \frac{\partial P_2^k}{\partial |V_n|} \\ \vdots & & \vdots & \vdots & & \vdots \\ \vdots & & \vdots & \vdots & & \vdots \\ \frac{\partial P_n^k}{\partial \delta_2} & \cdots & \frac{\partial P_n^k}{\partial \delta_n} & \frac{\partial P_n^k}{\partial |V_2|} & \cdots & \frac{\partial P_n^k}{\partial |V_n|} \\ \vdots & & \vdots & \vdots & & \vdots \\ \frac{\partial Q_2^k}{\partial \delta_2} & \cdots & \frac{\partial Q_2^k}{\partial \delta_n} & \frac{\partial Q_2^k}{\partial |V_2|} & \cdots & \frac{\partial Q_2^k}{\partial |V_n|} \\ \vdots & & \vdots & \vdots & & \vdots \\ \vdots & & \vdots & \vdots & & \vdots \\ \frac{\partial Q_n^k}{\partial \delta_2} & \cdots & \frac{\partial Q_n^k}{\partial \delta_n} & \frac{\partial Q_n^k}{\partial |V_2|} & \cdots & \frac{\partial Q_n^k}{\partial |V_n|} \end{bmatrix} \begin{bmatrix} \Delta \delta_2^k \\ \vdots \\ \vdots \\ \vdots \\ \Delta \delta_n^k \\ \vdots \\ \Delta |V_2^k| \\ \vdots \\ \vdots \\ \vdots \\ \Delta |V_n^k| \end{bmatrix} \quad (3.3)$$

Jacobian matrix

The matrix given in (3.3) can be expressed in a more general manner as given in (3.4). Since the Jacobian matrix is of order  $(2n - 2) \times (2n - 2)$ , the matrices  $J_{p\delta}, J_{PV}, J_{Q\delta}$  and  $J_{QV}$  are of order  $(n - 1) \times (n - 1)$ .

$$\begin{bmatrix} \Delta P \\ \Delta Q \end{bmatrix} = \begin{bmatrix} J_{P\delta} & J_{PV} \\ J_{Q\delta} & J_{QV} \end{bmatrix} \begin{bmatrix} \Delta \delta \\ \Delta |V| \end{bmatrix} \quad (3.4)$$

### 3.1.2. Exact Loss Formula

Total active power loss (say " $P_{Loss}$ ") and total reactive power loss (say " $Q_{Loss}$ ") are functions of all the bus voltage magnitudes, bus phase angles and their respective bus active power & reactive power [11].

$$P_{Loss} = P_{Loss}(|V|, \delta, P, Q) \quad (3.5)$$

$$Q_{Loss} = Q_{Loss}(|V|, \delta, P, Q) \quad (3.6)$$

Hence, by partially differentiating  $P_{Loss}$  with respect to its four variables, a relationship between those partially differentiated terms and Jacobian matrix can be obtained.

$$\begin{bmatrix} \frac{\partial P_{Loss}}{\partial P} \\ \frac{\partial P_{Loss}}{\partial Q} \end{bmatrix} = [J^T]^{-1} \begin{bmatrix} \frac{\partial P_{Loss}}{\partial \delta} \\ \frac{\partial P_{Loss}}{\partial |V|} \end{bmatrix} \quad (3.7)$$

Moreover, the Exact Loss Formula (ELF) for a bus system can be expressed as (3.8) [11],[74].

$$P_{Loss} = \sum_{i=1}^N \sum_{j=1}^N [\alpha_{ij} (P_i P_j + Q_i Q_j) + \beta_{ij} (Q_i P_j - P_i Q_j)] \quad (3.8)$$

Where;

$$\alpha_{ij} = \frac{R_{ij}}{V_i V_j} \cos(\delta_i - \delta_j) \quad , \quad \beta_{ij} = \frac{R_{ij}}{V_i V_j} \sin(\delta_i - \delta_j)$$

$$Z_{ij} = R_{ij} + jX_{ij}; \quad ij^{th} \text{ element of bus impedance matrix}$$

$$\alpha_{ij} = \alpha_{ji} \quad , \quad \beta_{ij} = -\beta_{ji} \quad , \quad R_{ij} = R_{ji}$$

Loss Sensitivity Index (LSI) and Voltage Sensitivity Index (VSI) are two widely used sensitivity parameters in power system analysis. As the proposed novel objective function for determining the optimal DG location is based on these two parameters, it is essential to have an understanding about their theoretical explanations.

### 3.1.3. Loss Sensitivity Index

Loss Sensitivity Index (LSI) is a parameter used in power system analysis for identifying the most loss sensitive busbar in network [11],[74]. In other words, LSI can be used for identifying the busbar that is most responsible for producing active power losses in a network. Loss Sensitivity Index is derived by linearizing the exact loss formula given in (3.8) [74]. The LSI values can be used to predict the behavior of power loss variations in different busbars for power flow changes. In general, a common practice is to integrate DG units at the busbars with the highest LSI values [11], [74] such that the active power losses are minimized.

By partially differentiating (3.8) with respect to active power and reactive power of busbar "i", (3.9) and (3.10) can be derived.

$$\frac{\partial P_{Loss}}{\partial P_i} = 2 \sum_{j=1}^N (\alpha_{ij} P_j) - 2 \sum_{j=1, j \neq i}^N (\beta_{ij} Q_j) \quad (3.9)$$

$$\frac{\partial P_{Loss}}{\partial Q_i} = 2 \sum_{j=1}^N (\alpha_{ij} Q_j) + 2 \sum_{j=1, j \neq i}^N (\beta_{ij} P_j) \quad (3.10)$$

By definition, LSI for  $i^{th}$  busbar can be expressed as given in (3.11)

$$LSI_i = \frac{\partial P_{Loss}}{\partial P_i} + \frac{\partial P_{Loss}}{\partial Q_i} \quad (3.11)$$

However, since active power loss changes are more dominant for active power changes, the term  $\frac{\partial P_{Loss}}{\partial P_i}$  is the dominant factor when compared with  $\frac{\partial P_{Loss}}{\partial Q_i}$ .

### 3.1.4. Voltage Sensitivity Index

Voltage Sensitivity Index (VSI) is a parameter used in power system analysis for identifying the most voltage sensitive busbar in network [72],[73]. In other words, VSI can be used for identifying the busbar that is most responsible for producing voltage deviations in a network.

By definition, VSI for  $i^{th}$  busbar can be expressed as given in (3.12)

$$VSI_i = \frac{\partial V_i}{\partial Q_i} + \frac{\partial V_i}{\partial P_i} \quad (3.12)$$

However, since voltage changes are more dominant for reactive power changes, the term  $\frac{\partial V_i}{\partial Q_i}$  is the dominant factor when compared with  $\frac{\partial V_i}{\partial P_i}$ . Thus, an approximation for VSI can be made as given below.

Assuming that P-V decoupling exists and  $\Delta P = 0$ , the relationships given by (3.13) and (3.14) are obtained. The diagonal elements of  $J_R^{-1}$  gives the VSI values of all the busbars except that of the slack bus [72].

$$[\Delta Q] = [J_{QV} - J_{Q\delta} J_{P\delta}^{-1} J_{PV}] [\Delta |V|] \quad (3.13)$$

$$[\Delta |V|] = [J_{QV} - J_{Q\delta} J_{P\delta}^{-1} J_{PV}]^{-1} [\Delta Q] = [J_R]^{-1} [\Delta Q] \quad (3.14)$$

## 3.2. Optimal DG Location Based on Loss & Voltage Sensitivity Analysis

### 3.2.1. Novel Objective Function

This section presents the novel methodology of optimal DG location. Since active power loss minimization and voltage profile improvement are key aspects to be addressed in integrating DGs, a novel objective function is defined in terms of LSI and VSI as Loss-Voltage Sensitivity Index (LVSI) for evaluating the most suitable locations to allocate DGs. Those two parameters are used as representatives of voltage profile and the real power loss in a distribution network. The understanding about a particular network gained by computing the combination of both VSI and LSI parameters will be vital in developing a strategy for minimizing active power losses and maintaining optimal busbar voltage levels. Since, the computed values for LSI and

VSI at base case (i.e. before integrating DG units) are used, it is reasonable to consider their multiplied index as those values are fixed for a given network. Thus, for a N busbar system, a new sensitivity parameter as Loss-Voltage Sensitivity Index (LVSI) is defined by (3.15).

$$f_k = LVSI_k = \frac{1}{LSI_k \times VSI_k} \quad , \quad k = 2, 3, \dots, N \quad (3.15)$$

The objective is to determine the busbar which gives the minimum value for  $LVSI_k$

$$f_{obj} = \min(f_2, f_3, \dots, f_N) \quad , \quad k = 2, 3, \dots, N \quad (3.16)$$

### 3.2.2. Constraints

The objective function is solved under certain network constraints. The equality and inequality constraints considered when solving this problem are listed from (3.17) to (3.20).

- Power balance constraint of the system;

$$\sum_{k=1}^N P_{k,Gen} = \sum_{k=1}^N P_{k,Load} + \sum_{k=1}^N P_{k,Loss} \quad (3.17)$$

- Voltage limit constraint of busbars;

$$V_{k,min} \leq V_k \leq V_{k,max} \quad (3.18)$$

- Line capacity limits;

$$MVA_{ij} \leq MVA_{ij,max} \quad (3.19)$$

Power loss limit constraints are defined in this approach in such a way that the line losses with DGs should be less than the line losses before connecting DG units.

- Line active power loss limits;

$$\sum P_{Loss,ij,DG} \leq \sum P_{Loss,ij} \quad (3.20)$$

### **3.2.3. Computational Procedure**

The computational method of determining the optimal location for placing a DG can be described as follows.

- 1) Calculate all the busbar voltages, magnitudes and phase angles, bus admittance and impedance matrices from the initial load flow.
- 2) Determine all the intermediate parameters such as elements of the Jacobian matrix and coefficients of exact loss formula to find VSI and LSI. Then find LSI and VSI values for all the busbars at the base case scenario.
- 3) Using (3.15) and (3.16), calculate LVSI for all the busbars and identify the busbar with minimum value.
- 4) For simplicity assume a single DG unit is to be connected to the system and decide on the capacity of the DG unit based on the system requirement.
- 5) Allocate the DG unit for the busbar that gives the minimum value for LVSI.
- 6) Sensitivities can be evaluated to check whether the constraints are satisfied after allocating the DG unit

### **3.3. Verification of the Proposed Methodology**

In order to verify the acceptability and the accuracy of the proposed methodology, IEEE-6 test bus system and IEEE-33 test bus system are used. The network arrangements of those two systems are shown by Figure 3.1 and Figure 3.6 respectively. IEEE-6 and IEEE-33 bus systems can be considered as sub-transmission or distribution type of networks. The parameters of both IEEE-6 and IEEE-33 test bus systems [4],[41], [71],[76] are given in Appendix II and III respectively.

IEEE-6 bus system has a total load of 21.25 MW and 5.75 MVar which is assumed to be the peak load of the network [4], [71], while IEEE-33 bus system has a total load of 3.715 MW and 2.30 MVar [41],[76]. For the IEEE-6 bus system, the active power loss and reactive power loss during the base case scenario are 455 kW and 110 kVar respectively. For the IEEE-33bus system, the active power loss and reactive power loss during the base case scenario are 211 kW and 130 kVar respectively. MATLAB integrated optimization with Newton Raphson method was used for doing the optimization and power flow studies.

### 3.3.1. Case I : Verification using IEEE-6 Bus System

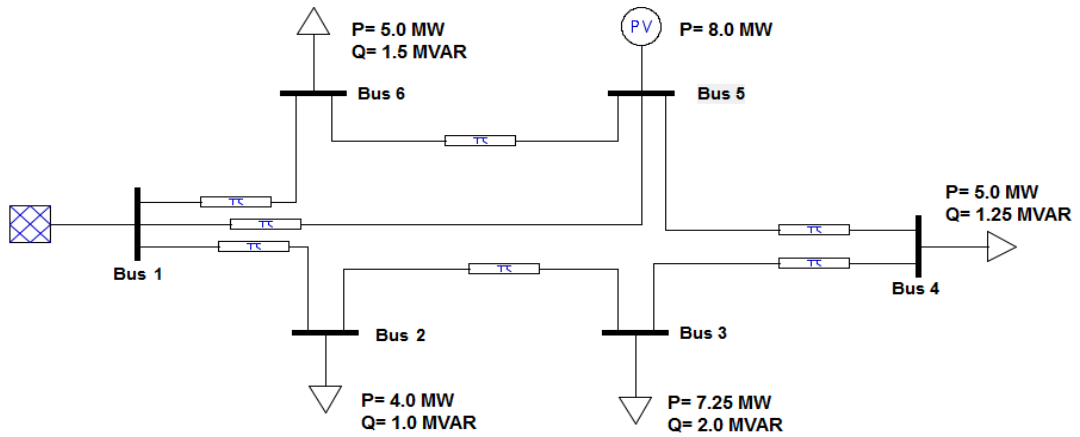


Figure 3.1: IEEE-6 bus test system

As described in the previous section, with the load flow studies for the base case scenario (no DGs connected to the network), VSI and LSI parameters are calculated for all the busbars except the slack bus (busbar no.1) as shown in Table 3.1. (Load parameters and line parameters of the network are given in Annex II).

Table 3.1: VSI and LSI values at base case scenario (IEEE-6 network)

Bus No.	LSI	VSI	LVSI
2	0.0231	0.0887	488.05
3	0.0481	0.0932	223.07
4	0.0273	0.0910	402.53
5	0.0206	0.0669	725.62
6	0.0222	0.0681	661.45

From the values obtained it can be seen that busbar 3 has the highest value for both VSI and LSI whilst busbar 5 has the lowest value for both VSI and LSI. That means, busbar 3 is the most voltage sensitive and loss sensitive busbar for the selected network. The sensitivity parameter (as defined in (3.15)) is calculated for all the busbars except the slack bus is shown in Figure 3.2. Accordingly, busbar 3 is selected as the candidate busbar for allocating the DG unit as the minimum value for LVSI was obtained for busbar 3.

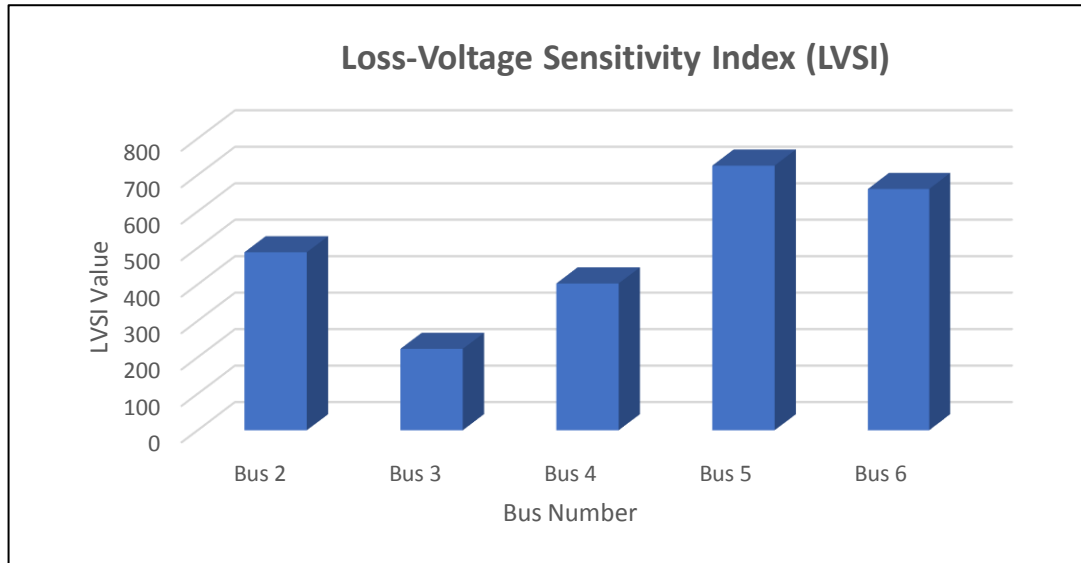


Figure 3.2: LVSI for different DG locations for IEEE-6 bus network

Moreover, similar results have been recorded in previous work that have used IEEE-6 bus test system for validating their criteria of determining the optimum DG location. In research work [4], [71] minimum active power losses and best voltage profile were obtained when the DG was placed at busbar 3. For this particular network, busbar 3 is the most voltage sensitive as well as the most loss sensitive busbar. Thus, it is obvious that busbar 3 should make the best location for the DG connection. However, the applicability of the proposed approach is significant in complex networks where voltage sensitivity and loss sensitivity may not occur at the same busbar but with several busbars. Further argument can be made with a blind prediction that busbar 3 is the optimum location for allocating the DG unit as it is the busbar with the highest load and its location is somewhat distant from the reference busbar when compared with the loads and location of other remaining busbars.

In order to verify the acceptability of LVSI defined in (3.15), two cases are considered. The Case I is understood in terms of active power loss and network voltage

profile improvement when a DG unit of a fixed capacity is connected to busbars 2 to 6, one at a time (one scenario is considered as a DG unit connected at a given busbar). In Case I(A) the active power losses are observed while in Case I(B) the network voltage profile was observed by defining a new parameter as given in (3.21). In Case II, each busbar is connected with a DG unit with the capacity which gives the minimum network loss. Again, a single DG at a given busbar is considered at a given time except for the slack bus.

### Case I(A): Fixed DG Capacity-Active Power Loss

In this case a 4-MW DG was considered as the DG capacity to be added for each busbar. For simplicity it is assumed that DG unit is generating power at the unity power factor. As described earlier, the 4-MW DG unit is connected to all the buses changing the DG location, one at a time. The total network loss obtained for different scenarios when DG is connected for different busbars is tabulated in Table 3.2 and shown in Figure 3.3.

### Case I(B): Fixed DG Capacity-Network Voltage Profile

In order to check the voltage profile improvement in the network after placing a DG unit one at a time for each busbar, a parameter for monitoring network voltage profile is defined as Total Network Voltage Improvement (TNVI) as given in (3.21). This is evaluated by connecting a 4-MW DG unit at each busbar as discussed in Case I(A). The voltages observed in busbars in all the scenarios are given in Figure 3.4. The calculated values for %TNVI are tabulated in Table 3.3. From the values in Table 3.3, it can be observed that the highest network voltage improvement was attained when the DG unit was placed at busbar 3. Thus, these values also validate the acceptability of LVSI defined for determining the optimal place for allocating DGs.

$$\begin{array}{l} \text{Total Network} \\ \text{Voltage} \\ \text{Improvement} \end{array} \quad \rightarrow \quad \%TNVI_j = \sqrt{\sum_{i=1}^N \left\{ \frac{|V_{i,j}| - |V_{i,base}|}{|V_{i,base}|} \right\}^2} \times 100\% \quad (3.21)$$

$\%TNVI_j$  : TNVI value when DG at  $j^{th}$  busbar

$V_{i,j}$  : Voltage of  $i^{th}$  busbar when DG at  $j^{th}$  busbar

$V_{i,base}$  : Voltage of  $i^{th}$  busbar without DG

### Case II: Variable DG Capacity

In this case, the DG capacity connected at a particular busbar is varied until minimum active power loss is observed, and the corresponding DG capacity and the total network loss were monitored. The minimum active power loss along with their corresponding busbar location is also given in Table 3.2. Moreover, it was seen that the minimum real power loss attainable at a particular busbar by varying the DG capacity was also given by the busbar 3.

Comparing the Figure 3.2 and 3.3, it is clear that the minimum network loss is observed when the DG is connected at busbar 3 further to the similar pattern followed by LVSI values and actual power losses. Hence, the proposed LVSI based approach evaluates the optimum location for DG placement in terms of loss minimization and best voltage profile.

Table 3.2: Comparison of active power loss for Case I and Case II

DG Location	Case I: Active Power Loss (DG Size=4 MW)	Case II: Minimum Active Power Loss Attainable
Bus 2	0.321 MW	0.245 MW
Bus 3	0.247 MW	0.114 MW
Bus 4	0.303 MW	0.233 MW
Bus 5	0.439 MW	0.438 MW
Bus 6	0.411 MW	0.411 MW

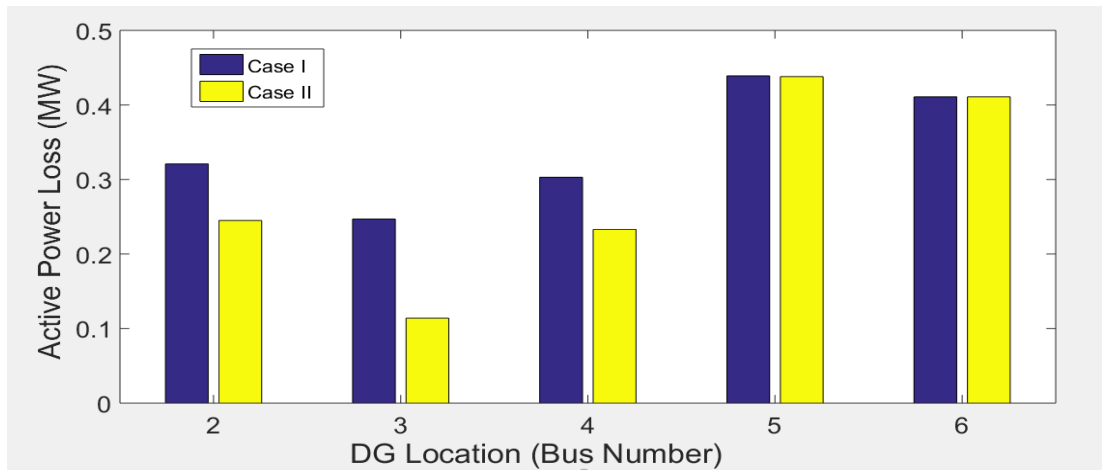


Figure 3.3: Active power loss comparison for Case I & II

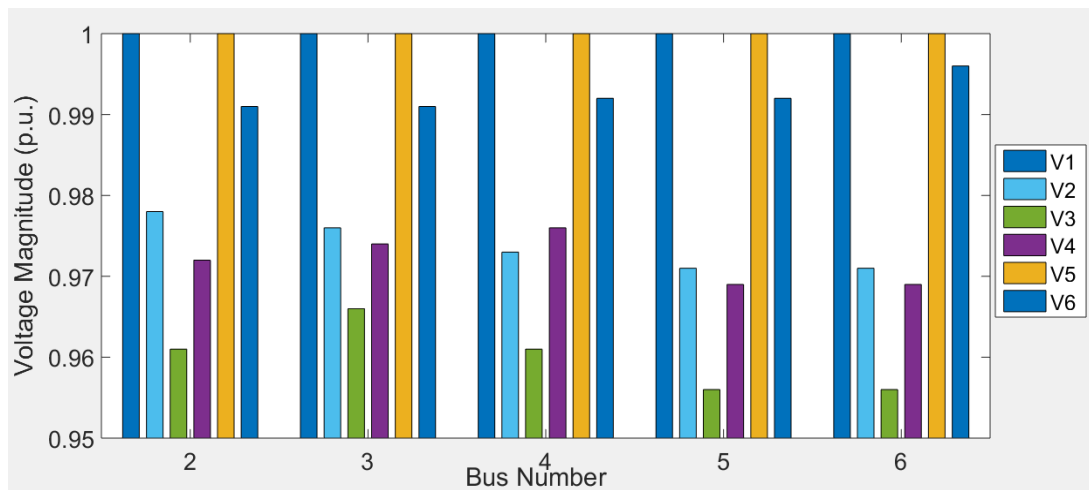


Figure 3.4: Busbar voltages for different locations of 4-MW DG unit

Table 3.3: %TNVI values for different busbar locations

Bus No.	(%TNVI)
2	0.943
3	1.275
4	0.921
5	0.101
6	0.505

In order to further verify the results, consider the case of 4 MW DG unit connected to all the busbars one at a time. The behavior of active power loss reduction and voltage profile enhancement can be further analyzed by plotting their combined behavior as shown in Figure 3.5.

In order to do the analysis, another parameter named  $\Delta P_{Loss,i}$  is defined.

Here;

$$\Delta P_{Loss,i} = P_{Loss,base} - P_{Loss,DG,i} \quad (3.22)$$

Where;

$\Delta P_{Loss,i}$  : Total active power loss reduction when a DG is integrated for busbar "i"

$P_{Loss,base}$  : Total active power loss at base case

$P_{Loss,DG,i}$  : Total active power loss when a DG is integrated for busbar "i"

For the case of 4 MW DG unit integrated for all busbars, the results obtained can be tabulated as given in Table 3.4.

Table 3.4: Calculation of  $\Delta P_{Loss,i} \times TNVI$  values for Case I (IEEE-6 bus system)

Bus No.	$\Delta P_{Loss,i}(MW)$	(%TNVI)	$\Delta P_{Loss,i} \times TNVI$
2	0.134	0.943	0.1264
3	0.208	1.275	0.2652
4	0.152	0.921	0.1400
5	0.016	0.101	0.0162
6	0.044	0.505	0.0222

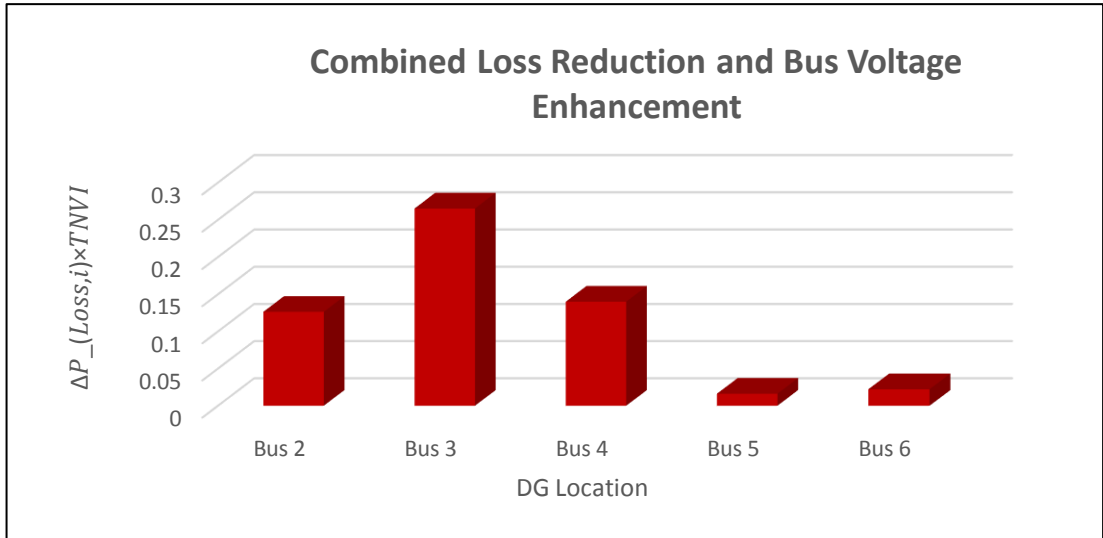


Figure 3.5: Combined active power loss reduction and bus voltage enhancement for different locations of 4-MW DG unit.

### 3.3.2. Case II: Verification using IEEE-33 Bus System

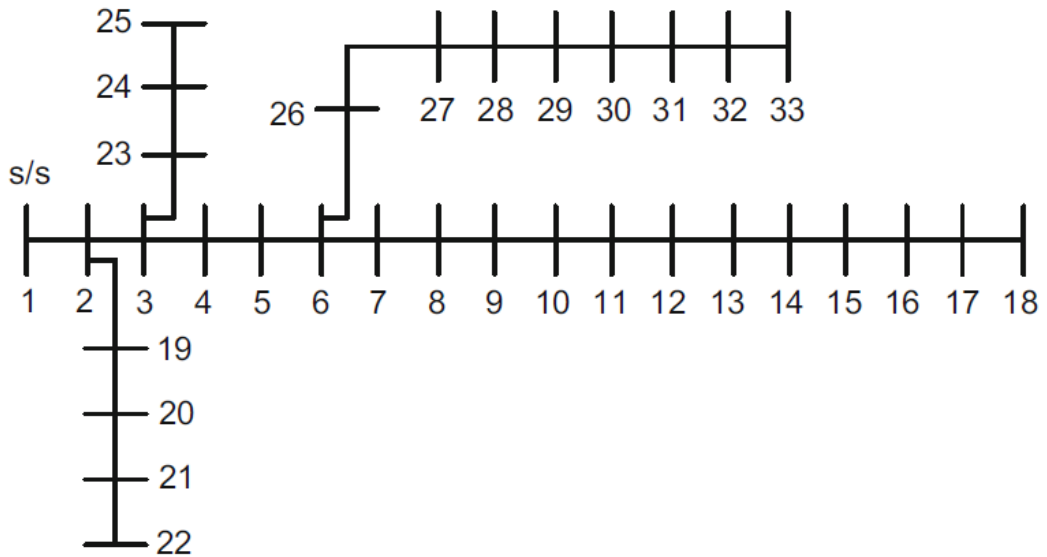


Figure 3.6: IEEE-33 bus test system

In order to further verify the proposed methodology, IEEE-33 standard test bus system was used. (Load parameters and line parameters of the network are given in Annex III). Same as in Case I, the base case power flow was run and obtained the

values for LSI and VSI. By substituting those values in (3.15), all the 32 LVSI values were calculated. A summary of the results is given in Table 3.5.

Table 3.5: VSI and LSI values at base case scenario (IEEE-33 network)

<b>Bus No.</b>	<b>Normalized LSI</b>	<b>Normalized VSI</b>	<b>LVSI</b>
2	0.009311544	0.00026468	405749.2229
3	0.031222254	0.003147678	10175.2588
4	0.031318651	0.005327935	5992.914188
5	0.031415893	0.007638856	4166.988061
6	0.031622214	0.013550594	2333.723431
7	0.03166703	0.015976266	1976.593586
8	0.031668721	0.019995879	1579.170307
9	0.031718611	0.026784578	1177.066614
10	0.031766809	0.033698078	934.1600365
11	0.031778647	0.034822966	903.6470516
12	0.03179725	0.036964694	850.7918647
13	0.031842066	0.038582088	813.9787071
14	0.031847985	0.042966054	730.7899628
15	0.031851367	0.047041786	667.4029505
16	0.031859823	0.051889779	604.8877915
17	0.031860668	0.059498482	527.5203636
18	0.031864051	0.060359529	519.9399328
19	0.01775975	0.009461461	5951.205759
20	0.01770817	0.016620376	3397.703632
21	0.017695486	0.01915326	2950.494544
22	0.017686184	0.024110978	2345.044173
23	0.049881703	0.021573068	929.2804643
24	0.05005843	0.025475418	784.1541668

25	0.050145525	0.029331701	679.8773578
26	0.032500774	0.030948257	994.1916432
27	0.032548126	0.03186626	964.1462501
28	0.032741764	0.046104518	662.4520236
29	0.032890587	0.042312731	718.5505456
30	0.032964998	0.04411272	687.6747982
31	0.03299713	0.049909707	607.2098492
32	0.033002204	0.053726623	563.9849555
33	0.033005586	0.056783003	533.5734329

Compared to IEEE-6 bus system, where busbar 3 was the one which recorded the highest value for both LSI and VSI, two different busbars have recorded the highest value for LSI and VSI in IEEE-33 test bus system. In this case, the highest value for LSI has been recorded by busbar 25 while the highest value for VSI has been recorded by busbar 18. Overall, the minimum value for LVSI has been recorded by busbar 18. Hence, according to the proposed methodology, the optimal location for integrating DG units is busbar 18 for achieving minimum active power losses and voltage deviations. Nevertheless, if multiple DG units are to be integrated for the network, then a priority order of LVSI in ascending order needs to be arranged. For example, if we assume three DG units are expected to be integrated for the network, based on the priority order of calculated values for LVSI, busbars 18, 17 and 33 are selected as the optimal DG locations respectively.

In order to verify the obtained results for optimal DG locations, the same strategy of observing the behavior of parameter  $\Delta P_{Loss,i} \times TNVI$  can be performed for this network as well.

3 DG units of each 0.2 MW are assumed to be allocated for three selected busbars. As there are many combinations available, for simplicity we will randomly take five different busbar combinations including the combination suggested by this novel approach. A summary of the results obtained for this case is given in Table 3.6

Furthermore, since the voltage profile enhancement index given in (3.21) is defined only for single DG placement, the format of the equation needs to be altered

slightly without harming the meaning of it as given in (3.23), so that it could be used for multiple DG allocation as well. Here  $N$  is the number of busbars in the network.

$$\%TNVI = \frac{\sqrt{\sum_{i=1}^N \left\{ \frac{|V_{i,DG}| - |V_{i,init}|}{|V_{i,init}|} \right\}^2}}{N} \times 100\% \quad (3.23)$$

Table 3.6: Calculation of  $\Delta P_{Loss,i} \times TNVI$  values (IEEE-33 bus system)

Case	DG Combination	$\Delta P_{Loss,i}(MW)$	(%TNVI)	$\Delta P_{Loss,i} \times TNVI$
Case I	Bus 9,15,21	0.052	0.642	0.033384
Case II	Bus 18,25,23	0.084	0.773	0.064932
Case III	Bus 18,33,12	0.072	0.878	0.063216
Case IV	Bus 2,10,30	0.030	0.295	0.00885
Case V	Bus 18,17,33	0.072	0.921	0.066312

Based on the values obtained for  $\Delta P_{Loss,i} \times TNVI$  for each case, it can be concluded that Case V, which is the DG combination that consists of the DG locations suggested by this novel methodology, gives the best combined result for minimization of active power losses and enhancement of voltage profile of network. This is graphically shown in Figure 3.7.

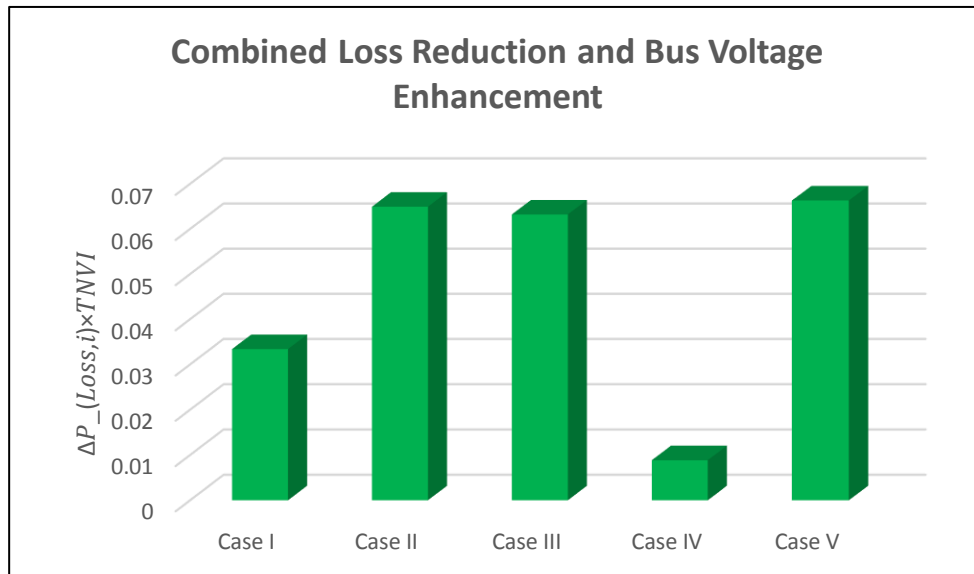


Figure 3.7: Combined active power loss reduction and bus voltage enhancement for multiple DG locations of 0.2-MW DG units

### 3.4. Summary

This chapter presented the novel analytical method developed by using LSI and VSI for determining the optimal DG location in order to minimize the total network active power loss and voltage deviations. The proposed methodology was verified using the standard IEEE-6 and IEEE-33 test bus systems by evaluating the optimal DG locations. Several scenarios studied by analyzing the results obtained for  $\Delta P_{Loss,i} \times TNVI$  parameter, active power loss variation and voltage profile behavior justify the acceptability of the proposed methodology.

## CHAPTER 4

### NOVEL METHODOLOGIES FOR OPTIMIZING DG SIZES

In this chapter, two analytical methods are developed for optimizing the DG size are presented. The first method is based on the analysis of LSI and VSI parameters whilst the other method is based on Lagrange Multiplier Method (LMM). At the end, a comparison of the results obtained for each method is also given for better understanding.

#### 4.1. Optimization of DG Sizes Using Loss and Voltage Sensitivity Analysis

##### 4.1.1. Formulation of Objective function

The inverse function of LVSI defined in Chapter 3 is used for determining the optimal DG sizes such that the total network active power losses and voltage deviations are minimized. The idea behind the formulation of this objective function is to take the combined effect of active power losses and voltage deviations together rather than considering their individual effects separately. Since the variation of VSI parameter for different generation and load configurations is significantly less when compared with LSI, it is reasonable to assume VSI as a constant in relation to LSI. Moreover, since  $\frac{\partial P_{Loss}}{\partial P_i} \gg \frac{\partial P_{Loss}}{\partial Q_i}$ , LSI parameter may be considered as the gradient of  $P_{Loss}$  vs  $P_i$  curve. Based on the properties mentioned above, the behavior of  $LSI \times VSI$  function may be approximated to the behavior of offset gradient of  $P_{Loss}$  vs  $P_i$  curve. Thus, a novel objective function in terms of LSI and VSI is defined as given in (4.1).

$$\text{Objective function} = f_{obj} = LSI \times VSI \quad (4.1)$$

By using the definitions of LSI and VSI given in (3.11) and (3.12);

$$f_{obj} = \left( \frac{\partial P_{Loss}}{\partial P_i} + \frac{\partial P_{Loss}}{\partial Q_i} \right) \times \left( \frac{\partial V_i}{\partial Q_i} + \frac{\partial V_i}{\partial P_i} \right) \quad (4.2)$$

By expanding (4.2), (4.3) can be obtained as;

$$f_{obj} = \frac{\partial P_{Loss}}{\partial P_i} \frac{\partial V_i}{\partial Q_i} + \frac{\partial P_{Loss}}{\partial P_i} \frac{\partial V_i}{\partial P_i} + \frac{\partial P_{Loss}}{\partial Q_i} \frac{\partial V_i}{\partial Q_i} + \frac{\partial P_{Loss}}{\partial Q_i} \frac{\partial V_i}{\partial P_i} \quad (4.3)$$

As mentioned earlier, since  $\frac{\partial P_{Loss}}{\partial P_i} \gg \frac{\partial P_{Loss}}{\partial Q_i}$  and  $\frac{\partial V_i}{\partial Q_i} \gg \frac{\partial V_i}{\partial P_i}$ , the term  $\frac{\partial P_{Loss}}{\partial Q_i} \frac{\partial V_i}{\partial P_i}$  is assumed to be much smaller than the other three terms. Hence, the objective function can be approximated as given in (4.4).

$$f_{obj} \approx \frac{\partial P_{Loss}}{\partial P_i} \frac{\partial V_i}{\partial Q_i} + \frac{\partial P_{Loss}}{\partial P_i} \frac{\partial V_i}{\partial P_i} + \frac{\partial P_{Loss}}{\partial Q_i} \frac{\partial V_i}{\partial Q_i} \quad (4.4)$$

Here, it is assumed that VSI parameter is almost a constant for a given busbar at different generation and load configurations. Moreover, by substituting (3.9) at zero gradient for (4.4), (4.5) can be obtained.

$$\left(\frac{\partial V_i}{\partial P_i} + \frac{\partial V_i}{\partial Q_i}\right) \times (2\{\alpha_{ii}P_i - \beta_{ii}Q_i\} + 2\{\sum_{j=1, j \neq i}^N \alpha_{ij}P_j - \beta_{ij}Q_j\}) + \frac{\partial P_{loss}}{\partial Q_i} \frac{\partial V_i}{\partial Q_i} = 0 \quad (4.5)$$

But bus power can be expressed in terms of bus generation and bus load as given in (4.6)

$$P_i = P_{G,i} - P_{L,i} \quad (4.6)$$

Thus, by substituting (4.6) in (4.5), an expression for optimal DG size can be obtained.

$$P_{DGi} = P_{Li} + \frac{1}{\alpha_{ii}} \{ \beta_{ii}Q_i - \sum_{j=1, j \neq i}^N \alpha_{ij}P_j - \beta_{ij}Q_j - \frac{1}{2\left(\frac{\partial V_i}{\partial P_i} + \frac{\partial V_i}{\partial Q_i}\right)} \left\{ \frac{\partial P_{loss}}{\partial Q_i} \frac{\partial V_i}{\partial Q_i} \right\} \} \quad (4.7)$$

For each term in (4.7), their base case values are substituted [77].

The objective function is solved under certain network constraints. The equality and inequality constraints considered when solving this problem are listed from (4.8) to (4.11).

- Power balance constraint of the system;

$$\sum_{k=1}^N P_{k,Gen} = \sum_{k=1}^N P_{k,Load} + \sum_{k=1}^N P_{k,Loss} \quad (4.8)$$

- Voltage limit constraint of busbars;

$$V_{k,min} \leq V_k \leq V_{k,max} \quad (4.9)$$

- Line capacity limits;

$$MVA_{ij} \leq MVA_{ij,max} \quad (4.10)$$

Power loss limit constraints are defined in this approach in such a way that the line losses with DGs should be less than the line losses before connecting DG units.

- Line active power loss limits;

$$\sum P_{Loss,ij,DG} \leq \sum P_{Loss,ij} \quad (4.11)$$

#### 4.1.2. Computational Procedure

The computational method of determining the optimal DG capacities can be described as follows.

- 1) Calculate all the busbar voltages, magnitudes and phase angles, bus admittance and impedance matrices from the initial load flow.
- 2) Determine all the intermediate parameters such as elements of the Jacobian matrix and coefficients of exact loss formula.
- 3) Determine the optimal DG locations by using the methodology presented in the previous chapter.
- 4) Decide the number of DG units to be integrated for the network.
- 5) For each DG location, apply (4.7) to calculate their optimal DG sizes.

#### 4.1.3. Verification using IEEE-33 Bus System

In order to verify the proposed methodology, it was assumed that only three DG units are integrated for the IEEE-33 bus network. At first, the base case power flow is run to calculate the required parameters listed in the first two steps of computational procedure. Then, the novel method proposed in Chapter 3 was used for identifying the optimal DG locations as busbar 18,17 and 33. Finally, the optimal DG sizes at each bus were calculated using (4.7).

Genetic Algorithm (GA) was also used as an optimization method for comparing the results obtained from the proposed methodology. The results for GA method are obtained by programming the objective function and constraints with suitable network parameters and run the programme in the inbuilt GA platform in MATLAB software.

The DG sizes obtained from the novel loss-voltage sensitivity-based method and GA method are tabulated in Table 4.1. It can be seen that the results obtained from both cases are nearly same and thereby the acceptability of the proposed technique is justified.

The active power loss and voltage profile obtained after allocating the DG sizes suggested by the two methods are given as a comparison in Figure 4.1 and 4.2. respectively.

Table 4.1: Comparison of DG sizes (IEEE-33 bus system)

<b>Optimal DG Locations</b>	<b>Sensitivity Based Method</b>	<b>Genetic Algorithm (GA)</b>
Bus 18	652 kW	660 kW
Bus 17	500 kW	468 kW
Bus 33	474 kW	455 kW

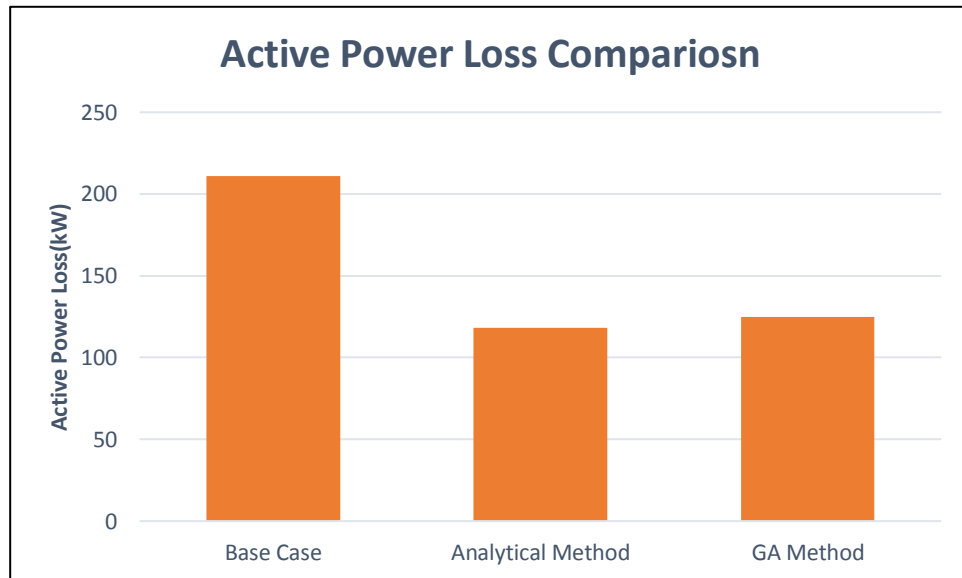


Figure 4.1: Active power loss comparison (IEEE-33 bus system)

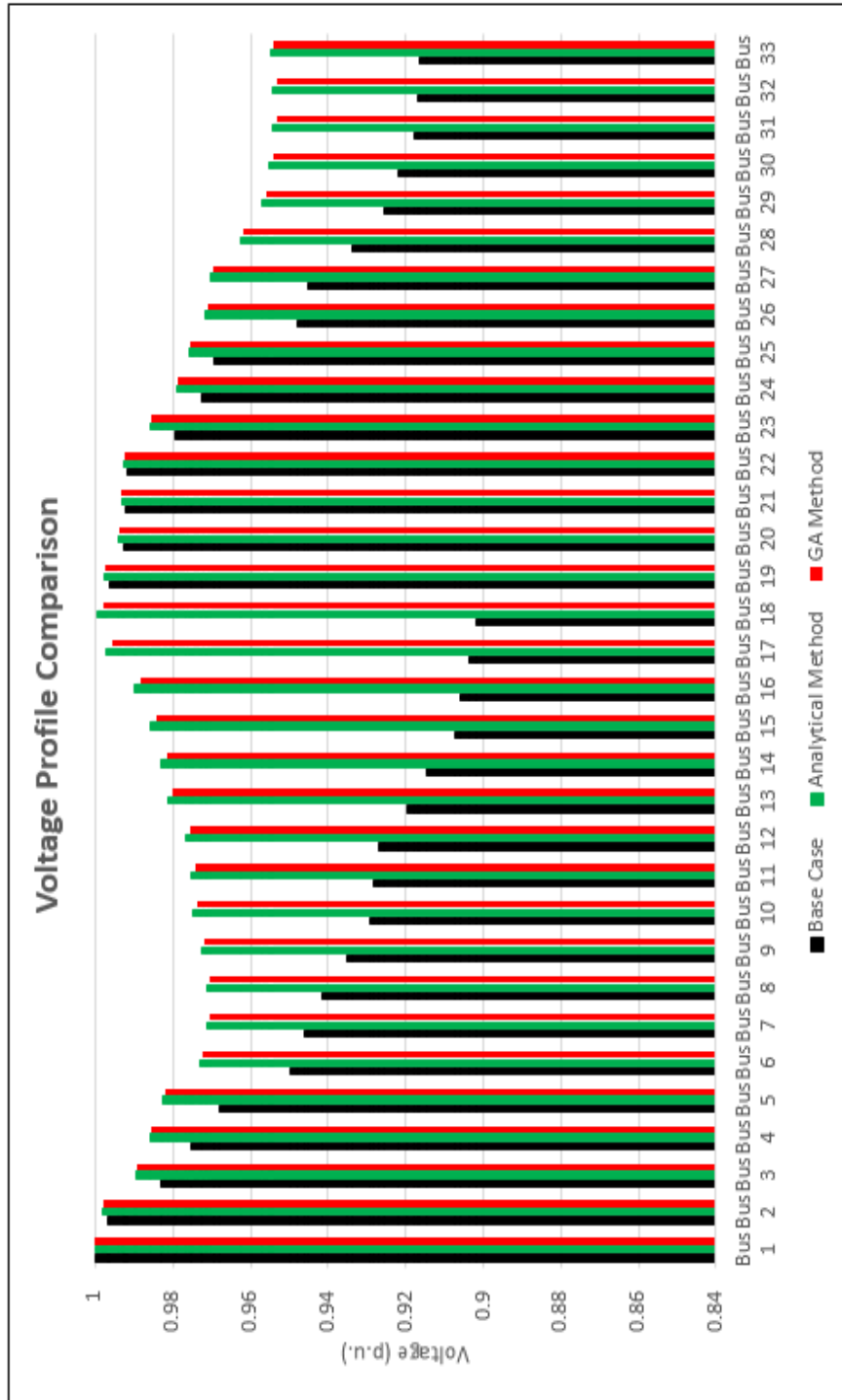


Figure 4.2: Voltage profile comparison (IEEE-33 bus system)

In this section, a novel analytical method for sizing DG units based on loss and voltage sensitivity indices was presented. The close relationship between the obtained results from the proposed methodology and GA method justify the acceptability of the novel approach. The next section is dedicated for presenting another novel method for DG sizing which is solved by using Lagrange Multiplier Method (LMM).

## 4.2. Optimization of DG Sizes Using Lagrange Multiplier Method

### 4.2.1. Problem Formulation

The mathematical basis for solving the novel multi-objective function in determining the optimal DG sizes for minimizing total active power loss and voltage deviations is detailed in the following subsections.

#### Total Active Power Loss

Consider a N busbar radial or meshed network as shown in Figure 4.3. For two consecutive nodes (say "i" and "j"), the active power loss between those two busbars can be expressed by (4.12), [75].

$$P_{loss(ij)} = P_{(ij)} + P_{(ji)} \quad (4.12)$$

Active bus power for  $i^{th}$  busbar can be expressed as a function of the real power flows from the busbar  $i$  to the all connected nodes as given in (4.13). Assume that  $i^{th}$  busbar is connected up to the  $n^{th}$  busbar.

$$P_i = P_{ij} + P_{ik} + P_{il} \dots + P_{in} \quad (4.13)$$

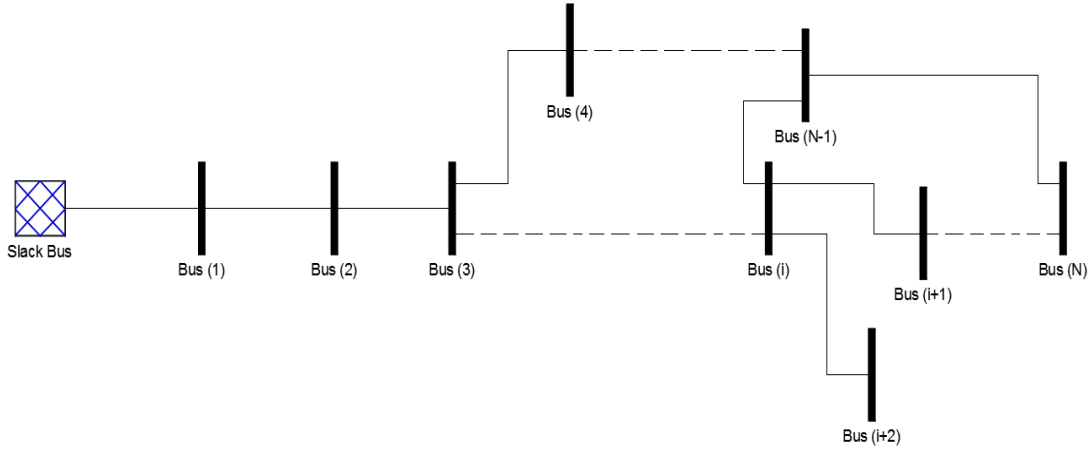


Figure 4.3: Typical configuration of a radial or meshed network

Bus power could also be expressed as a function of its respective generation " $P_{G,i}$ " and load " $P_{L,i}$ " as given in (4.14) and (4.15).

$$P_i = P_{G,i} - P_{L,i} \quad (4.14)$$

$$\sum_{i=1}^N P_i = \sum_{i=1}^N P_{G,i} - \sum_{i=1}^N P_{L,i} \quad (4.15)$$

Hence, the total active bus power can be expressed as given in (4.16), (4.17) and (4.18).

$$\sum P_i = P_1 + P_2 + P_3 \dots \dots + P_N \quad (4.16)$$

$$\begin{aligned} \sum P_i = & (P_{ij} + P_{ji}) + (P_{ik} + P_{ki}) + \dots \\ & + (P_{in} + P_{ni}) + (P_{kn} + P_{nk}) + \dots \\ & + P_{(N-1)N} + P_{N(N-1)} \end{aligned} \quad (4.17)$$

$$\sum P_i = P_{Loss,Total} \quad (4.18)$$

### Voltage Drop Between Two Busbars

Consider two consecutive busbars (say “  $i$  ” and “  $i+1$  ”), connected together as shown in Figure 4.3. The voltage drop across these two nodes can be approximated as given in (4.19), [78].

$$|\Delta V_{i,(i+1)}| = |V_i| - |V_{i+1}| \approx \frac{R_{i,(i+1)}P_{i,(i+1)} + X_{i,(i+1)}Q_{i,(i+1)}}{|V_{i+1}|} \quad (4.19)$$

Here  $|V_i|$  and  $|V_{i+1}|$  are the voltage magnitudes of  $i^{th}$  and  $(i+1)^{th}$  busbar respectively.  $R_{i,(i+1)}$  and  $X_{i,(i+1)}$  are the resistance and reactance of lines connecting nodes  $i$  and  $(i+1)$ . The active and reactive power flow from  $i^{th}$  node to  $(i+1)^{th}$  node are given by  $P_{i,(i+1)}$  and  $Q_{i,(i+1)}$  respectively.

### Exact Loss Formula

The theories presented about ELF in 3.1.2. and 3.1.3. sub sections are also used in this approach.

#### 4.2.2. Formulation of Objective Function

Since it is expected to minimize the total active power losses and voltage deviations by optimizing the DG sizes, an objective function in terms of those two parameters is defined as given in (4.20).

$$f = P_{loss,Total} + \sum y_{kj} |\Delta V_{kj}|^2 \quad (4.20)$$

Here  $y_{kj}$  is the magnitude of the  $kj^{th}$  element of the bus admittance matrix. Furthermore, the  $kj^{th}$  element of the bus admittance matrix is a function of resistance and reactance of the line connected between those two busbars. Since active power loss and voltage deviations are two different parameters, they are combined together by considering the effect of  $y_{kj}$  for voltage deviations.

#### 4.2.3. Constraints

The objective function is solved in a way that constraints given by (4.21) to (4.25) are satisfied.

Active power balance constraint of the network;

$$\sum_{k=1}^N P_{G,k} = \sum_{k=1}^N P_{L,k} + P_{loss,Total} \quad (4.21)$$

Reactive power balance constraint of the network;

$$\sum_{k=1}^N Q_{G,k} = \sum_{k=1}^N Q_{L,k} + Q_{loss,Total} \quad (4.22)$$

DG penetration of the network;

$$\sum_{k=1}^N P_{DG,k} = \eta \sum_{k=1}^N P_{L,k} \quad (4.23)$$

- Here  $\eta$  is a fraction expressed in terms of total load in the network.

Voltage magnitude constraint of all busbars;

$$|V_{k,min}| \leq |V_k| \leq |V_{k,max}| \quad (4.24)$$

MVA capacity of lines;

$$MVA_{kj} \leq MVA_{kj,max} \quad (4.25)$$

#### 4.2.4. Solution Method

The objective function given in (4.20) can be expressed in a more comprehensive manner by using (4.18) and (4.19).

$$f = \sum P_k + \sum y_{kj} \left( \frac{R_{kj}P_{kj} + X_{kj}Q_{kj}}{|V_j|} \right)^2 \quad (4.26)$$

Since the proposed methodology is an analytical method, the computational burden is increased if all the constraints are incorporated in the Lagrange function. Hence, for simplicity, only the active power balance constraint is incorporated for the LMM as given in (4.27). Nevertheless, as the other constraints are monitored throughout the solution procedure, optimal DG sizes are determined such that the constraints are not violated whilst minimizing the active power losses and voltage deviations.

Lagrange expression for the objective function;

$$\begin{aligned} \Omega = \sum P_k + \sum y_{kj} \left( \frac{R_{kj}P_{kj} + X_{kj}Q_{kj}}{|V_j|} \right)^2 \\ + \lambda \left( \sum_{k=1}^N P_{L,k} + P_{loss,Total} - \sum_{k=1}^N P_{G,k} \right) \end{aligned} \quad (4.27)$$

Assuming that the DG is placed at the  $k^{th}$  busbar, and using the equations given in (4.13), (4.16), (4.18) and (4.21), the expression given by (4.28) is obtained.

$$\begin{aligned} \Omega_k = \sum_{k=1}^N P_k + \sum y_{kj} \left( \frac{R_{kj} \left( P_k - \sum_{i \neq j} P_{ki} \right) + X_{kj}Q_{kj}}{|V_j|} \right)^2 \\ + \lambda_k \left( P_{loss,Total} - \sum_{k=1}^N P_k \right) \end{aligned} \quad (4.28)$$

According to (4.14) as mentioned before, bus active power is a function of its own generation and connected load. Furthermore, since voltage magnitude change for active power change for a particular busbar is comparatively negligible when compared with the voltage magnitude change for reactive power change, it is

reasonable to assume that  $\frac{\partial|V_i|}{\partial P_i}$  and  $\frac{\partial|V_i|}{\partial P_j}$  are also negligible. Hence, by partial differentiating the previous equation with respect to active bus power of busbar ‘k’ (which is  $P_k$ ), (4.29) can be obtained.

$$\frac{\partial\Omega_k}{\partial P_k} = 1 + \sum y_{kj} \left( \frac{2R_{kj}}{|V_j|} \left\{ \frac{R_{kj} \left( P_k - \sum_{i \neq j} P_{ki} \right) + X_{kj} Q_{kj}}{|V_j|} \right\} \right) + \lambda_k \left( \frac{\partial P_{loss, Total}}{\partial P_k} - 1 \right) \quad (4.29)$$

At minima  $\frac{\partial\Omega_k}{\partial P_k} = 0$ . Moreover, by using the relationship given in (4.14), an expression in terms of bus generation can be derived as given in (4.30). Here,  $\lambda_k$  is the ‘Incremental Loss’ of  $k^{th}$  busbar.

$$\lambda_k = \frac{1 + 2 \sum \frac{y_{kj} R_{kj}}{|V_j|^2} \left\{ R_{kj} \left( P_{G,k} - P_{L,k} - \sum_{i \neq j} P_{ki} \right) + X_{kj} Q_{kj} \right\}}{1 - \frac{\partial P_{loss, Total}}{\partial P_k}} \quad (4.30)$$

Hence, this expression can be applied for any candidate DG busbar, such that the optimal DG sizes for those respective multiple DG locations can be determined, assuming that the maximum DG penetration level ( $\eta$ ) is known, as given in Equation (4.23).

#### 4.2.5. Computational Procedure

The computational procedure for determining the optimal DG sizes is presented in the following steps.

- 1) Decide the candidate busbar locations for placing the DGs, No. of DG units and the DG penetration level as a fraction of the total load in the network.
- 2) Determine all the elements of the bus admittance matrix and bus impedance matrix.
- 3) Run the initial load flow and determine the voltage magnitudes, bus voltage angles and line flows. Hence, by using the necessary values obtained in Steps 2 and 3, calculate the coefficients of the exact loss formula and the value of the partial derivatives of  $P_{loss}$  for DG busbars.
- 4) Substitute the values obtained in previous steps in (4.30) for different pre-decided DG locations and obtain expressions for  $P_{G,k}$ . Then, obtain the

relationship (as a summation of DG sizes for each busbar), considering the equality condition in (4.23).

5) Solve the simultaneous equations obtained and determine the optimal values for DG sizes at each busbar.

6) Finally, check whether other constraints in (4.21) to (4.25) are also satisfied. If not, change the DG penetration level and repeat the Steps 4 and 5.

#### 4.2.6. Verification using IEEE-6 & IEEE-33 Bus Systems

IEEE-6 and IEEE- 33 test bus systems were used to validate the proposed methodology. At first, initial load flow for base case scenario is obtained. The real power loss and TNVI values of the two networks for the base case are given in Table 4.2. In order to assess the behavior of network voltage profiles, TNVI parameter defined in (3.23) is utilized. For the base case, it is trivial that the value for TNVI is zero. For both networks, calculation of optimal DG sizes are done for two cases. That is, in Case I, 2 DG units are allocated for two buses and in Case II, it is assumed that 3 DG units are integrated for each network. Determination of the optimal locations for allocating DG units such that the total active power loss and voltage deviations are minimized, is based on the methodology presented in Chapter 3. For the IEEE-6 bus test system, busbar 3 and 4 are selected as the optimal locations for Case I. In Case II, busbar 3,4 and 2 are the optimal locations for allocating DG units for minimizing active power loss and voltage deviations. Likewise, for the IEEE-33 test bus system, it was determined that for Case I, busbar 18 and 17 are the optimal DG locations. Busbar 33 is selected as the next optimal location for placing the DG unit for Case II.

A comparison of the results obtained for the two networks are tabulated in Table 4.2. By analyzing the results obtained, it can be concluded that by allocating DG units with optimal sizes will result in minimizing active power losses and voltage deviations. Nevertheless, better results can be obtained when the DG units are allocated in a decentralized manner as in Case II.

When comparing the results obtained, it can be observed that both active power loss and voltage deviations are minimized after allocating the DG units with optimal DG sizes as in Case I and II. It can be further observed that in Case II, which has more DG units than Case I but with the same DG penetration gives better results for  $P_{loss}$  and TNVI. A comparison of the active power loss reduction for the two networks is

shown in Figure 4.4. The minimum active power losses are given in Case II when compared with the base case scenario and Case I. The same trend is followed by the voltage profile in the two networks as well. The best voltage profile and the highest value for TNVI is from Case II. This is graphically shown in Figure 4.5 and Figure 4.6 for the two networks.

Table 4.2: Summary of results for optimal DG sizes

	<b>IEEE-6 Bus Network</b>	<b>IEEE-33 Bus Network</b>
<b>Initial Load Flow</b>		
$P_{loss}$	0.455 MW	0.211 MW
TNVI	0 %	0 %
<b>Case I</b>		
<b>No. of DG busbars</b>	2 (3,4)	2 (18,17)
<b>DG Penetration (<math>\eta</math>)</b>	30%	30%
<b>DG sizes</b>	Busbar 3 (2.37 MW) Busbar 4 (4.01 MW)	Busbar 18 (0.71 MW) Busbar 17 (0.4045 MW)
$P_{loss}$	0.206 MW	0.146 MW
TNVI	0.285%	0.499%
<b>Case II</b>		
<b>No. of DG busbars</b>	3 (3,4,2)	3 (18,17,33)
<b>DG Penetration (<math>\eta</math>)</b>	30%	30%
<b>DG sizes</b>	Busbar 3 (0.95 MW) Busbar 4 (2.49 MW) Busbar 2 (2.94 MW)	Busbar 18 (0.284 MW) Busbar 17 (0.377 MW) Busbar 33 (0.4535 MW)
$P_{loss}$	0.194 MW	0.124 MW
TNVI	0.303%	0.609%

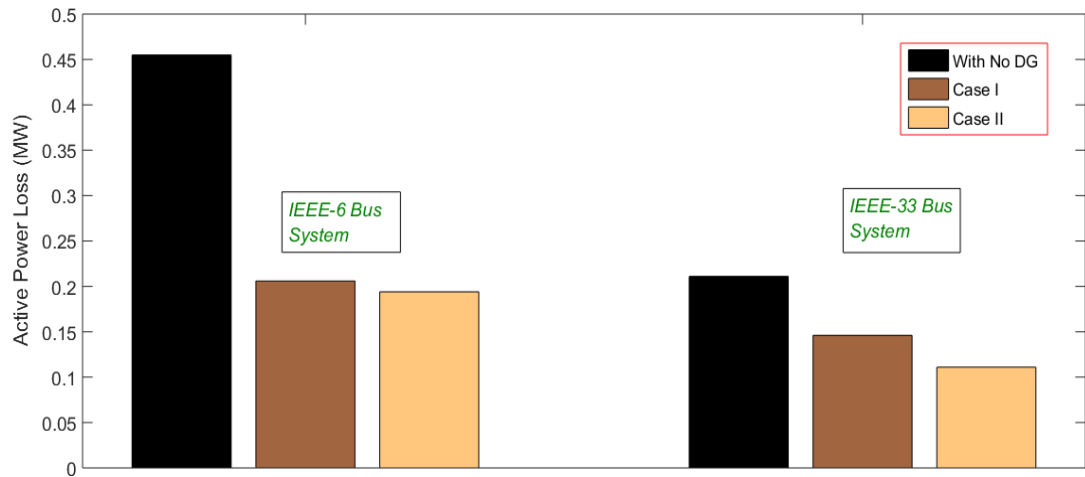


Figure 4.4: Active power loss comparison

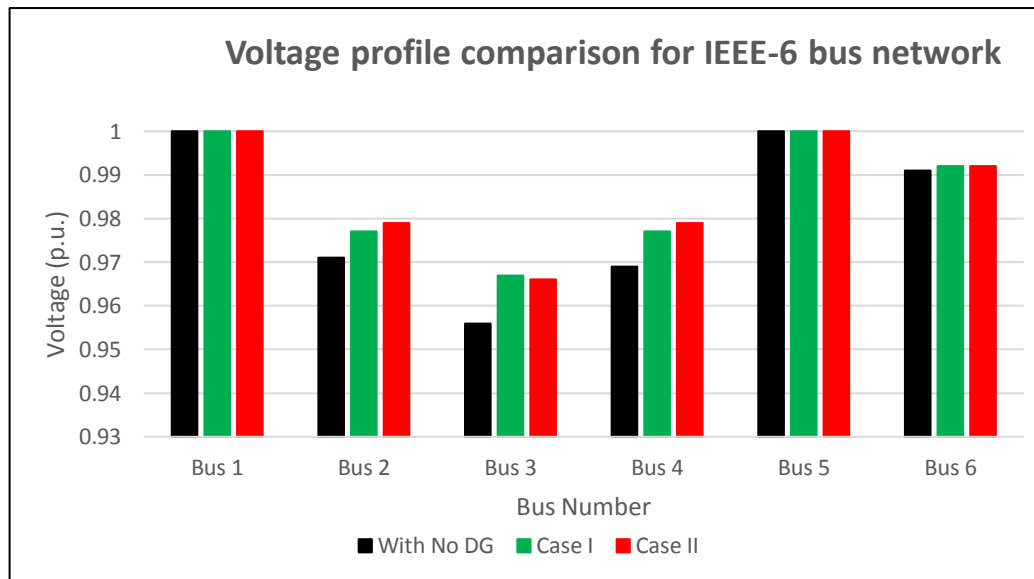


Figure 4.5: Voltage profile comparison for IEEE-6 bus network

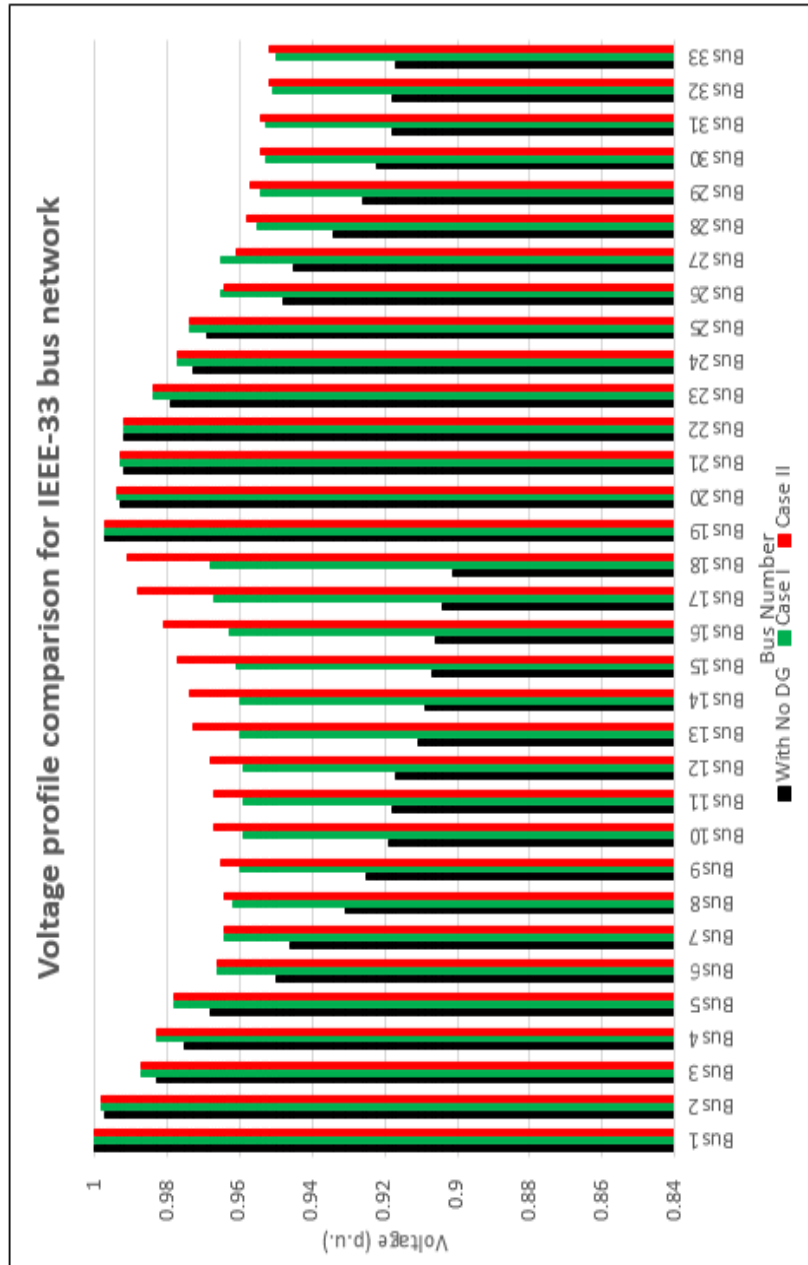


Figure 4.6: Voltage profile comparison for IEEE-33 bus network

For better understanding about the results obtained for the two cases for IEEE-6 and IEEE-33 bus networks, the analysis based on  $\Delta P_{Loss,i} \times TNVI$  is performed. A comparison of the results obtained is shown in Figure 4.7. From this diagram also, it is conclusive that better results are given in Case II, which has used more DG units with decentralized generation.

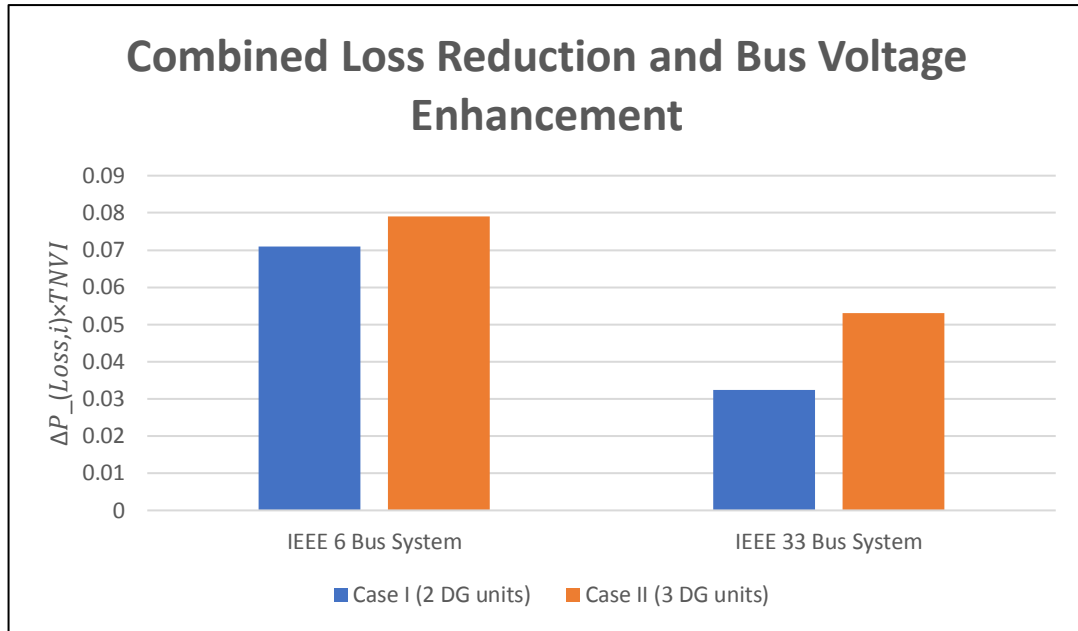


Figure 4.7: Comparison of combined loss reduction and bus voltage enhancement for Case I and Case II

### 4.3. Summary

In this chapter, two different approaches in determining optimal DG sizes for minimizing active power losses and voltage deviations were presented. The first method is based on loss and voltage analysis (which is formulated as the inverse function of LVSI defined in Chapter 3) while the second approach is solved using LMM. In the first method, the optimal values obtained at zero gradient as given in (4.7) were used for calculating the DG sizes. In the second approach, A mathematical relationship is obtained for Incremental Loss term ( $\lambda$ ) for each DG busbar when  $\frac{\partial \Omega}{\partial P_k} = 0$ . Furthermore, when the desired DG penetration level ( $\eta$ ) is known, optimal DG sizes for multiple DGs are determined for all DG allocations.

The validity of the proposed methodologies were tested using standard IEEE-6 and IEEE-33 test bus systems. The results confirmed that, with optimal DG sizes determined by these methods, contribute in minimizing real power losses and improving the network voltage profiles significantly. Moreover, this method could be utilized even for a network with large number of busbars for finding the optimal DG sizes. It involves less computational burden since only the parameters associated with the particular DG busbar are needed for calculating the optimal DG size of that specific busbar whereas in other existing heuristic methods, parameters of all the busbars are also taken into calculation.

## CHAPTER 5

### BESS CAPACITY CALCULATION METHODOLOGY

In Chapters 3 and 4, DG allocation methodologies for determining optimal DG locations and sizes were presented. Chapter 5 and 6 explain the novel approaches used in achieving the other remaining part of DG allocation (i.e. power dispatch). Due to the intermittency and non-dispatchable nature of some of the DG technologies like SPV and wind power generation, it is required to have BESS so that power can be dispatched based on the network requirement. Therefore, it is clear that BESS need to be integrated for a network to harness the best results expected from integrating DGs.

If BESS units are undersized, then expected results from them such as dispatching power during peak load hours, providing the deficit of power required in case of a lack of grid generation may not be able to achieve as desired. On the contrary, if BESS units are oversized, then it will directly affect the cost aspect which is incurred by customer or DSO. Hence, there should be a proper mechanism in sizing the BESS units to optimal capacities.

Although there are many researches done regarding developing BESS sizing strategies, most of them are based on heuristic optimization techniques [25],[55],[79]-[84]. Nevertheless, with that kind of approaches, it becomes difficult to understand the mathematical formulations behind the BESS sizing strategies. Hence, an analytical method based on mathematical relationships for sizing BESS units will facilitate better understanding of internal behavior. Thereby, changing of BESS sizes according to the requirement of the network can be done easily.

When determining the sizes of BESS units several aspects need to be taken into consideration. For example, as the BESS capacities are dependent on the behavior of DG technology, their power output should be modelled accordingly. In case of SPV, the PV output should be modelled using the Beta Probability Density Function (BPDF) and in case of wind power generation, the wind power output should be modelled using the Weibull Probability Density Function. On the other hand, since power consumption as load also affects the BESS capacities, the time varying nature of loads should also be considered by modelling them accordingly.

Before moving on to discuss about the BESS sizing strategy, it is required to be familiar with some of norms that are going to be used in the rest of the thesis. Some of those important facts are listed below.

- In the previous methodologies suggested for optimizing DG location and size, the calculations were done considering peak loads and peak DG output for an instant of time. However, in BESS sizing approach, the actual behavior of loads and DG units need to be considered according to the time of the day. Therefore, the time varying nature of loads and generation from DG units are taken into account.
- It is assumed that each DG unit consists of a BESS unit and the location of DG unit and BESS unit is same. In other words, both DG unit and BESS unit are placed at the optimal DG location suggested by the novel method presented in Chapter 3.
- Although it is possible to charge the BESS units with grid power, it is assumed that each BESS unit is charged only through their respective DG units so that no power from the grid is taken to charge the batteries. That is done with the intention of reducing the additional burden on grid to charge the batteries.
- The proposed methodologies for optimal DG location and size can be applied for any DG technology irrespective of their type. Nevertheless, for simplicity from here onwards it is assumed that DG technology is strictly specified to SPV generation.
- All the validations are done for the IEEE-33 test bus system.

### **5.1. Modelling of Solar PV Output**

This section describes about the methodology used in modelling the Solar PV output by taking into account the intermittency nature of it. For doing this, Solar PV raw data collected from a PV farm in Hambantota district for a period of one year (01/05/2017 to 30/04/2018) are used [85]. During this time period, SPV data have been recorded for every 30-minute intervals.

### 5.1.1. Calculation of PV Output

The intermittency nature of SPV generation is taken into account by using the Beta Probability Density Function (BPDF) for modelling the solar irradiance level [23],[37],[86]. The mathematical definition of BPDF is given by (5.1).

$$f_b(s) = \begin{cases} \frac{\Gamma(\alpha+\beta)}{\Gamma(\alpha)\Gamma(\beta)} s^{\alpha-1} (1-s)^{\beta-1} & 0 \leq s \leq 1, \alpha, \beta \geq 0 \\ 0 & \text{otherwise} \end{cases} \quad (5.1)$$

Where;

$$\beta = (1 - \mu) \left( \frac{\mu(1 - \mu)}{\sigma^2} - 1 \right)$$

$$\alpha = \frac{\mu\beta}{1 - \mu}$$

- $f_b(s)$  : Beta Probability Density Function
- $\Gamma(\bullet)$  : Gamma function
- $\alpha, \beta$  : Parameters of Beta function (Calculated using solar irradiance)
- $s$  : Solar irradiance level ( $kW/m^2$ )
- $\mu$  : Mean of solar irradiance
- $\sigma$  : Standard deviation of solar irradiance

The SPV output at a particular solar irradiance level " $P_0(s)$ " is dependent on PV module parameters, solar irradiance level and some other factors. The equations used in calculating " $P_0(s)$ " can be listed as follows.

$$T_{cy} = T_A + s \left( \frac{N_{OT} - 20}{0.8} \right) \quad (5.2)$$

$$I_y = s[I_{sc} + K_i(T_{cy} - 25)] \quad (5.3)$$

$$V_y = V_{oc} - K_v^* T_{cy} \quad (5.4)$$

$$FF = \frac{V_{MPPT} * I_{MPPT}}{V_{oc} * I_{sc}} \quad (5.5)$$

$$P_o(s) = N * FF * V_y * I_y \quad (5.6)$$

Hence, the expected power output from SPV at solar irradiance level “s” can be calculated by (5.7)

$$EP(s) = P_o(s) * f_b(s) \quad (5.7)$$

Thereby, the total expected power output for a particular time period can also be calculated as follows.

$$ETP = \int_0^1 P_o(s) * f_b(s) ds. \quad (5.8)$$

Where;

$T_{cy}$  : Module temperature

$T_A$  : Ambient temperature

$I_{sc}$  : Short circuit current of PV module

$V_{oc}$  : Open circuit voltage of PV module

$I_{MPPT}$  : Maximum Power Point Tracking (MPPT) current of PV module

$V_{MPPT}$  : Maximum Power Point Tracking (MPPT) voltage of PV module

$K_v$  : Voltage temperature coefficient of PV module

$K_i$  : Current temperature coefficient of PV module

$FF$  : Fill Factor

$EP(s)$  : Expected power output at solar irradiance “s”

$ETP(s)$  : Expected total power output at solar irradiance “s”

In order to model the SPV output, the mean and standard deviations of solar irradiance are calculated for different irradiance levels. Furthermore, it is assumed that

SPV modules in Hambantota PV farm have the same parameters specified in [37]. A synopsis of the PV parameters is given in Table 5.1.

Table 5.1: Summary of SPV parameters and calculations

$T_{cy}$	PV module temperature	Calculated
$T_A$	Ambient temperature	30.76°C
$I_{SC}$	Short circuit current	8.38 A
$V_{OC}$	Open circuit voltage	36.96 V
$K_i$	Current temperature coefficient	0.00545 A/°C
$K_v$	Voltage temperature coefficient	0.1278 V/°C
$V_{MPPT}$	MPPT voltage	28.36 V
$I_{MPPT}$	MPPT current	7.76 A
$FF$	Fill Factor	Calculated
$P_0(s)$	PV output at solar irradiance 's'	Calculated

By using the parameter values given in Table 5.1 and raw data available for solar irradiance & module temperature, expected power output and total expected power outputs for a certain time duration from SPV can be calculated. Since the raw data from SPV farm are extracted for every 30 minutes, 48 graphs for expected PV output can be plotted for 24h time. Some of the sample graphs obtained for different time stamps are plotted in Figure 5.1(a) - 5.1(f).

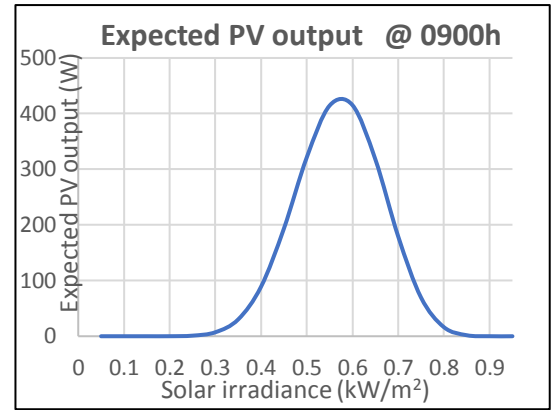
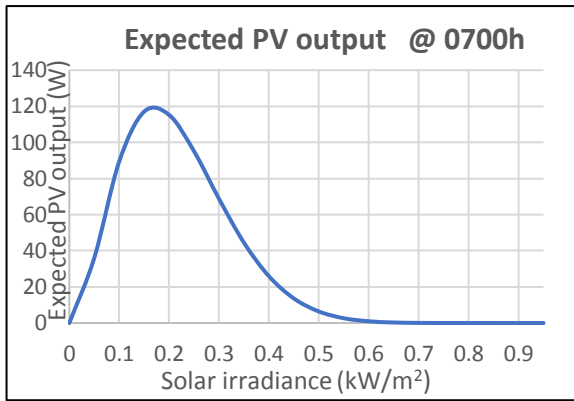


Figure 5.1 (a): Expected PV output @ 7 a.m. Figure 5.1 (b): Expected PV output @ 9 a.m.

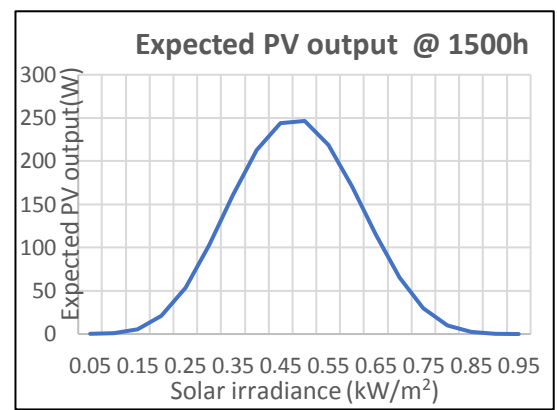
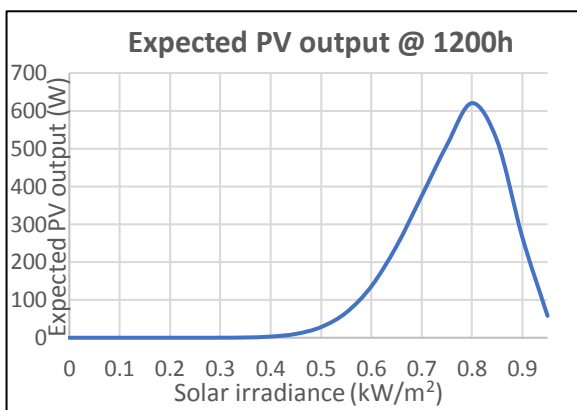


Figure 5.1 (c): Expected PV output @ 12 noon Figure 5.1 (d): Expected PV output @ 3 p.m.

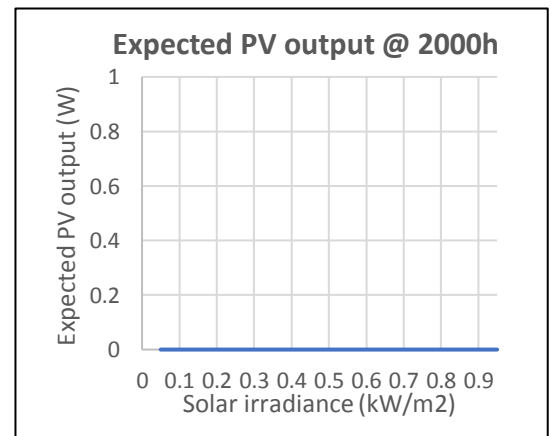
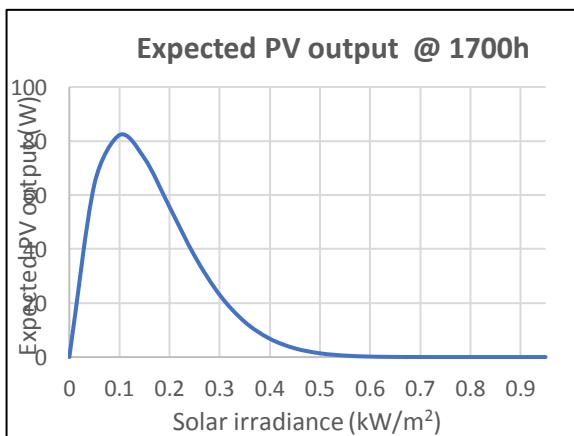


Figure 5.1 (e): Expected PV output @ 5 p.m. Figure 5.1 (f): Expected PV output @ 8 p.m.

Figure 5.1(a) – 5.1(f): Expected PV output for different time snaps (For Hambantota PV farm)

### 5.1.2. Mapping Procedure of SPV Generation

By taking the summation of all these 48 graphs and plotting them against time axis, the aggregated daily PV output curve can be obtained. Figure 5.2 illustrates the curve obtained in that manner.

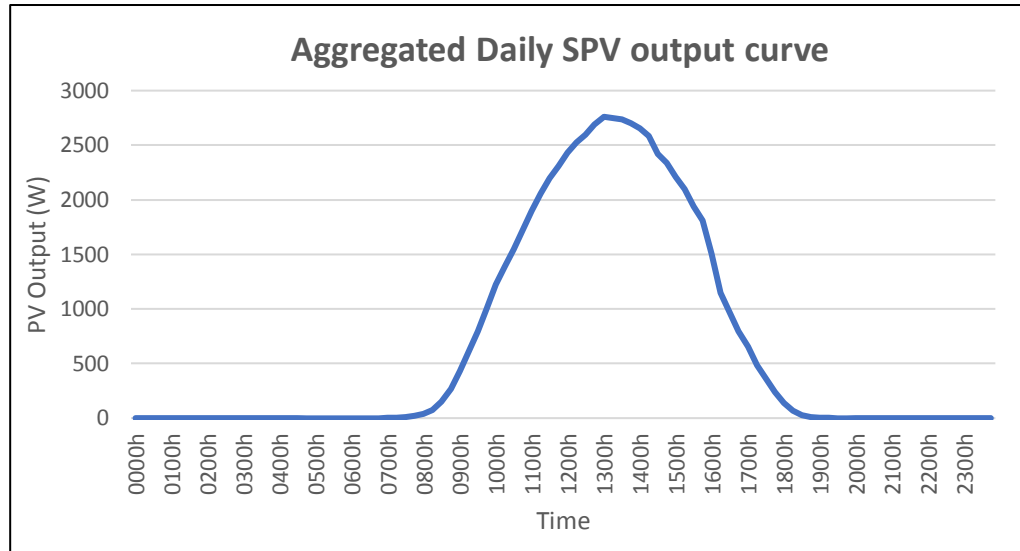


Figure 5.2: Aggregated daily SPV output curve (For Hambantota PV farm)

In the Chapter 4, the calculation of optimal DG sizes were done considering a snap shot of time for peak loading. For example, the optimal DG capacity calculated for busbar 18 was 652 kW (with no BESS) according to the loss and voltage sensitivity-based method. But practically, the DG unit at busbar 18 will be outputting a SPV generation less than or equal to 652kW for all time due to the intermittency nature of SPV generation. This is same for all the other DG units as well. In order to account for this one, mapping of the SPV generation of Hambantota PV farm is done for all the DG units connected in the considered network (i.e. IEEE-33 network). Thus, the resulting SPV curves obtained for the PV units connected for the IEEE-33 network can be obtained as shown in Figure 5.3. According to Figure 5.3, it can be seen 3 different peaks for the curves. That is due to the fact that 3 PV units have different maximum PV sizes which were calculated from the novel methodology presented in Chapter 4.

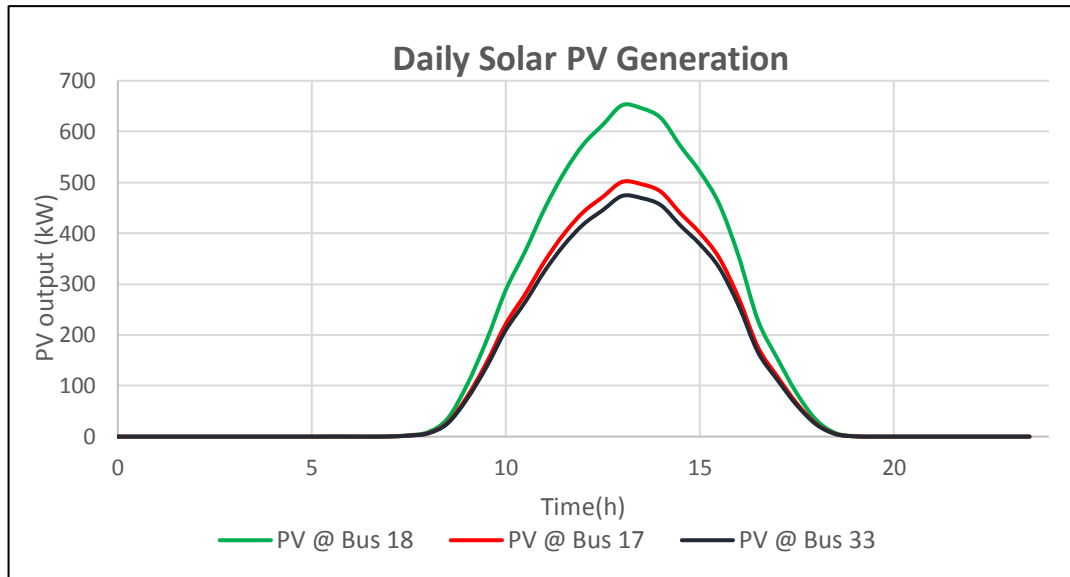


Figure 5.3: Total daily SPV output curves of the PV units (with No BESS) in the IEEE-33 network.

## 5.2. Modelling of Load Curves

In previous chapters, an instant of time for peak loading was considered for determining the optimal DG locations and capacities. However, in practical case the loads vary throughout the day. Hence, in order to account for this time varying nature of loads, load changing patterns need to be considered for obtaining realistic results. For doing this, following three different load patterns are taken into account and their curves were mapped with the constant peak loads in the IEEE-33 network.

- 1) Mix daily load profile
- 2) Residential load profile having a night peak
- 3) Commercial load profile having a day peak

### 5.2.1. Mapping Procedure of Load Curves

For modelling the mix daily load profile data from [87] are extracted. The other two load profiles are modelled using the data given in [88]. The residential load profile is obtained by modelling the load consumption in a typical rural area while the commercial load profile is obtained by modelling the load consumption in an urban area in Sri Lanka. For each curve, their typical values are obtained from their references, and then those values are normalized with respect to their peak values. The mix daily load profile represents the typical electricity consumption in Sri Lanka. It

consists of a slight morning peak, a higher day peak and the highest consumption during nighttime. According to Figure 5.5 and 5.6, it can be observed that the residential load profile has a night peak and the commercial load profile consists of a day peak respectively. These curves are mapped with the constant loads of IEEE-33 network in order to make them time varying. That is, for the three cases it is assumed that all the IEEE-33 network loads are;

- 1) Mix of all load types
- 2) Only residential loads
- 3) Only commercial loads

The resulting normalized curves obtained for the whole network are given by Figure 5.4, 5.5 and 5.6 for the three load profiles respectively.

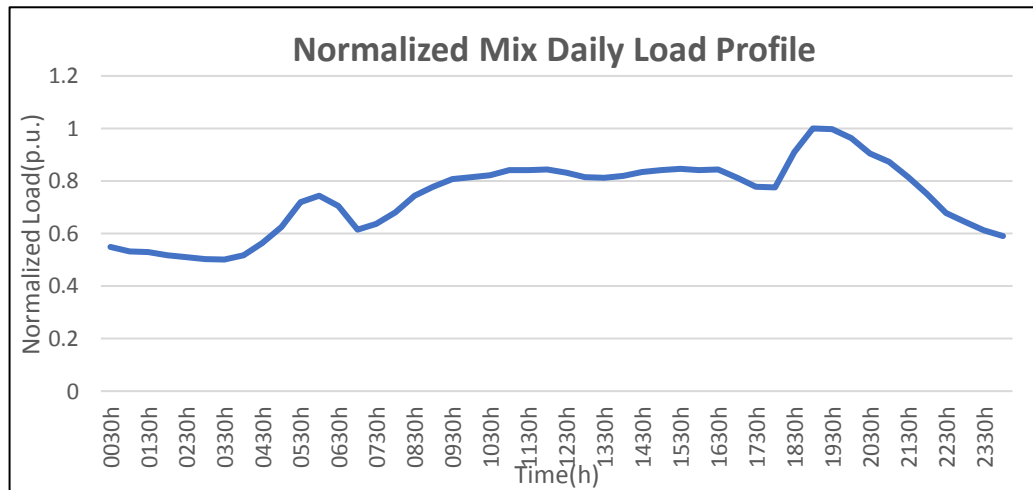


Figure 5.4: Normalized mix daily load profile [87]

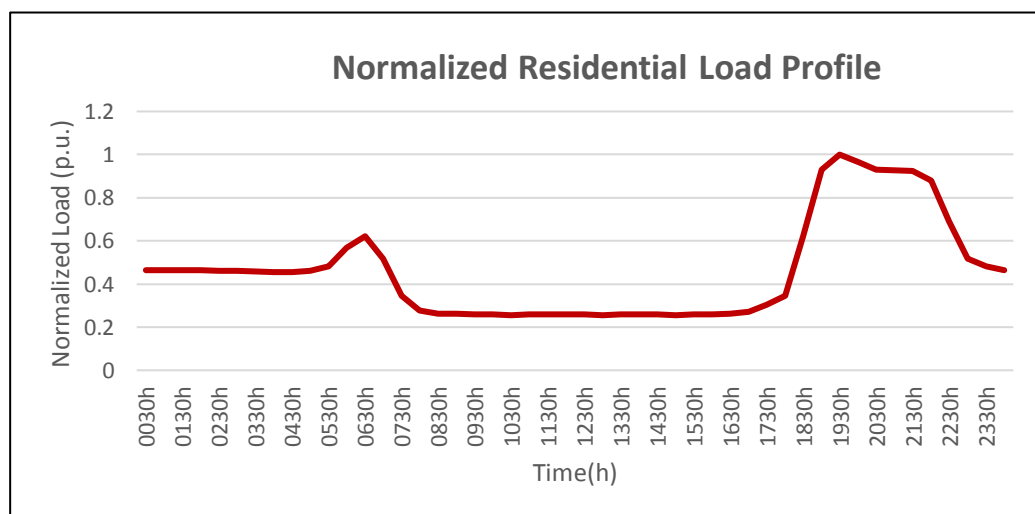


Figure 5.5: Normalized residential load profile [88]

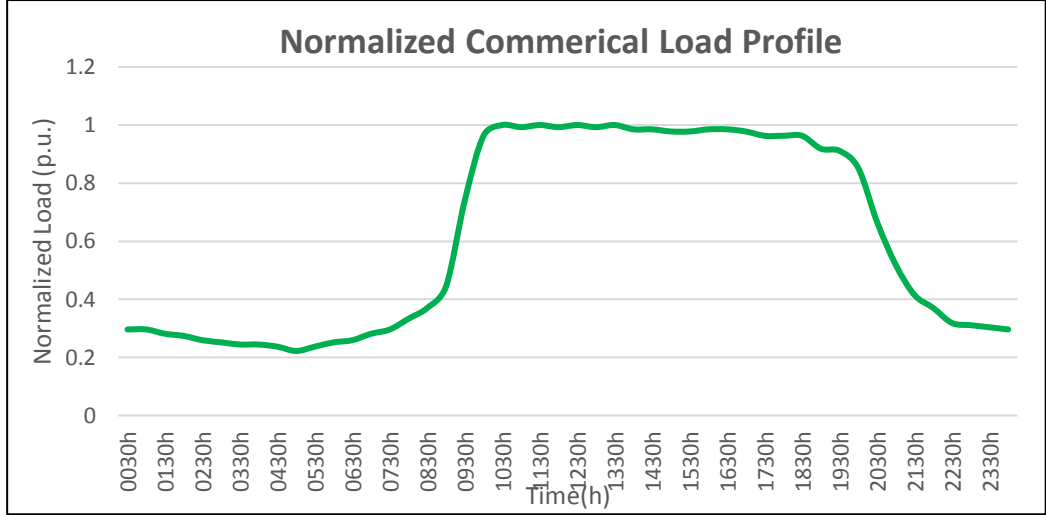


Figure 5.6: Normalized commercial load profile [88]

### 5.3. Analytical Method for PV & BESS Sizing

This section presents the analytical method proposed for determining the capacities of PV and BESS units. The steps followed in this procedure are given as follows.

#### Step 1: Determination of time spans for peak solar period and off-peak solar period

As the first step, the time ranges for peak solar and off-peak solar periods need to be determined. Peak solar period is taken as a particular time duration in day time, in which the SPV generation is significantly high while the off-peak solar period is taken as the rest of the time in a day, usually in night time in which the SPV generation is significantly low. For doing this, total percentage SPV generation at an instant of time is calculated with respect to total installed SPV capacity. This parameter is named as  $\%SPV_{actual}$ . Thus,  $\%SPV_{actual}$  is used as the parameter which determines the spans of peak solar period and off-peak solar period. The time of the day in which SPV generation exceeds  $\%SPV_{actual}$  is taken as T1 and the time of the day in which SPV generation falls below  $\%SPV_{actual}$  is taken as T2. Hence, the time span from T1 to T2 is taken as the peak solar period and rest of the time is taken as the off-peak solar period.

$$\%SPV_{actual} = \frac{P_{PV,Gen}}{P_{PV,Installed}} \times 100\% \quad (5.9)$$

Here  $P_{PV,Gen}$  is the total SPV generation of all the PV units at a particular instant of time and  $P_{PV,Installed}$  is the total SPV installed capacity. Thus, the peak

solar period and off-peak solar periods are defined as given in (5.10) and (5.11).

Definitions of the above parameters are graphically illustrated by Figure 5.7.

- During Peak solar period  $\rightarrow \frac{P_{PV,Gen}}{P_{PV,Installed}} \times 100\% \geq \%SPV_{actual}$  (5.10)

- During Off-peak solar period  $\rightarrow \frac{P_{PV,Gen}}{P_{PV,Installed}} \times 100\% \leq \%SPV_{actual}$  (5.11)

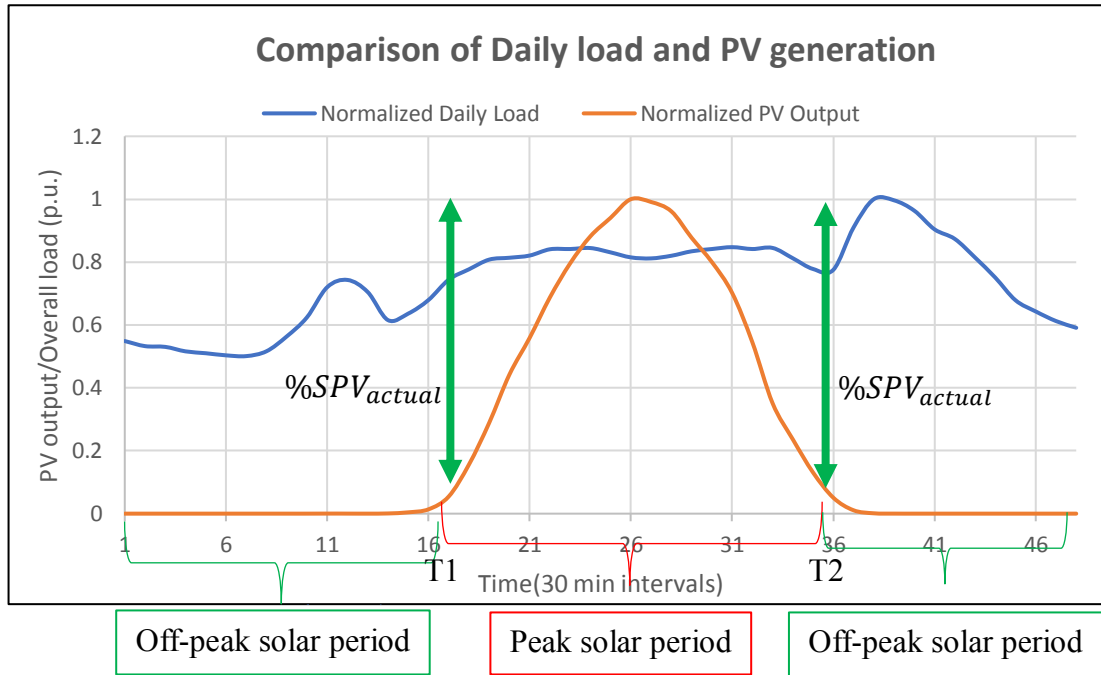


Figure 5.7: Illustration of the definitions of peak solar period and off-peak solar period

**Step 2: Calculate the total daily energy consumption and peak solar period energy consumption**

As the next step, the total daily energy consumption and peak solar period energy consumption need to be calculated. This is done by determining the area under the daily load curve. The total daily energy consumption can be calculated by considering the whole area under the load curve. The peak solar period energy consumption can be estimated by taking the area under the load curve between T1 and T2 time interval.

**Step 3: Define the BESS capacity in terms of off-peak solar period energy consumption, SOC limits and Load Proportionality Factor**

Based on the methodology presented in Chapter 3 for determining the optimal DG locations, their locations may be situated in different branches of the considered network. For the IEEE-33 network, busbar 18,17 and 33 are identified as the optimal DG and BESS locations. Here, the busbars 18 and 17 are located close by to each other in the same branch while busbar 33 is in another separate branch. Due to this distributed nature of DG and BESS locations, the considered network can be subdivided into certain load areas. In this way, the IEEE-33 network can be divided into two areas as Area 1 and Area 2 as shown in Figure 5.8. We will define the Area 1 as the branch of the network which consists of busbar 26 to busbar 33 while Area 2 as the rest of the network. The reason for considering only two areas is that, since BESS unit at busbar 33 is in a separate branch while the other two BESS units are located adjacent to each other in the same branch. In case if the three BESS units are at three different branches, obviously the network should be subdivided into three main areas.

For each of these areas, a novel parameter namely “Load Proportionality Factor” (LPF) is defined in terms of the total peak load in that particular area and the total peak load in the network. This is mathematically illustrated by (5.12).

$$Load\ Proportionality\ Factor\ in\ i^{th}\ area = \frac{Peak\ Load\ in\ i^{th}\ area}{Total\ Peak\ Load} \quad (5.12)$$

(LPF<sub>i</sub>)

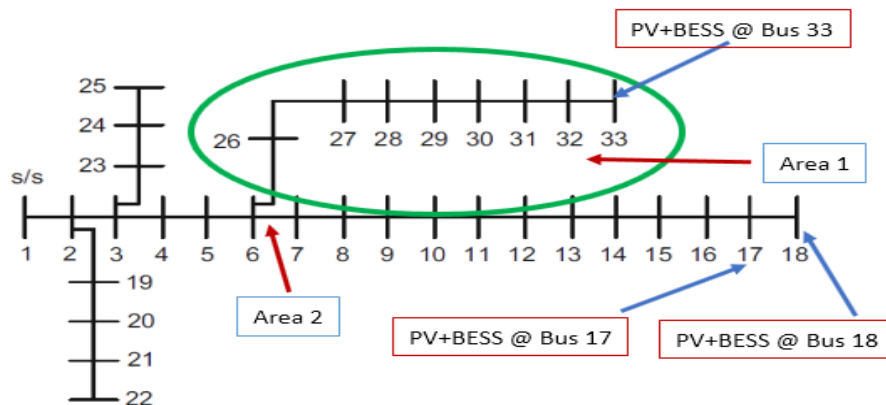


Figure 5.8: Load areas of the IEEE-33 test bus system

For the IEEE-33 network the ( $LPF_i$ ) values for the two areas can be calculated as shown below.

- Total peak load in Area 1 = 1075 kW
- Total peak load in Area 2 = 2640 kW
- Total peak load in the network = 3715 kW

Hence,

$$\text{Load Proportionality Factor in Area 1} = \frac{1075 \text{ kW}}{3715 \text{ kW}} = 0.2894$$

( $LPF_1$ )

$$\text{Load Proportionality Factor in Area 2} = \frac{2640 \text{ kW}}{3715 \text{ kW}} = 0.7106$$

( $LPF_2$ )

- As the next step the State of Charge (SOC) limits of BESS units are defined. Furthermore, it is assumed that all the BESS units have the same SOC limits.

Take,  $SOC_{min}=10\%$  and  $SOC_{max}=100\%$

- Assume only a portion of daily off-peak solar period energy consumption is expected to be served by each BESS say " $\eta$ "

Then a general expression for BESS capacity in terms of off-peak solar period energy consumption, SOC limits of BESS units and Load Proportionality Factors can be stated as given in (5.13).

$$\text{BESS Capacity of Area } i = \frac{2 \times LPF_i \times \eta \times (\text{Total Daily Energy} - \text{Solar peak period Daily Energy})}{(SOC_{max} - SOC_{min})} \quad (5.13)$$

In this way, for the IEEE-33 network two area BESS capacities can be calculated. Moreover, since BESS unit @ busbar 18 and BESS unit @ busbar 17 are

adjacent and located in the same area (i.e. Area 2), it is reasonable to assume they have the same BESS capacities.

Hence, the mathematical relationships which gives the BESS sizes for each unit can be obtained as given below.

- *BESS Size @ Bus 33 = BESS Capacity of Area 1*
- *BESS Size @ Bus 18 = BESS Size @ Bus 17 = 0.5xBESS Capacity of Area 2*

### 5.3.1. Sample Calculation

A sample calculation done in calculating the PV and BESS sizes based on the proposed methodology is illustrated below.

Assume that PV and BESS sizing need to be done for the IEEE-33 network considering the mix daily load profile behavior. Consider the case of  $\%SPV_{actual} = 5\%$ . Moreover, take  $\eta = 20\%$  case (i.e. 20% of the off-peak solar period energy consumption is expected to be supplied by BESS energy). Consider the PV and BESS unit at busbar 33 for the following calculations.

- PV size @ bus 33 (No BESS) = 474 kW

This value is taken from the calculation done based on the DG sizing methodology presented in Chapter 4.

- Total daily PV energy generated by the PV unit @ bus 33 (No BESS) =2718 kWh (4.2%)

This is the total daily energy generated by the PV unit before integrating the BESS unit. This is calculated by considering the area under the SPV power output curve. The energy yield is presented as a percentage of the total daily energy consumption by the loads in the IEEE-33 network which is approximately about 64870 kWh.

- Total daily PV energy generated by the PV unit @ bus 33 (with BESS) =4797 kWh (7.4%)

This is the total daily energy generated by the PV unit after integrating the BESS unit. The increase of the energy yield is due to the fact that now the PV unit has to generate more power for charging the BESS unit during the peak solar period which is required for serving a 20% energy consumption in the off-peak solar period. The energy yield is presented as a percentage of the total daily energy consumption by the loads in the IEEE-33 network which is approximately about 64870 kWh.

- Capacity of the BESS unit @ bus 33 = 4500 kWh

This is the approximated capacity value of the BESS unit @ bus 33 which is determined by substituting the required values for (5.13).

- PV size @ bus 33 (with BESS) = 836 kW

This is the new PV size (approximated value) required @ bus 33 for having a BESS unit at the same PV location. The PV size is approximated by assuming a proportional relationship as follows.

$$PV \text{ size (with BESS)} \approx \frac{PV \text{ size (No BESS)} \times PV \text{ energy yield (with BESS)}}{PV \text{ energy yield (No BESS)}} \quad (5.14)$$

By substituting the values for the PV unit @ bus 33

$$PV \text{ size (with BESS)} = \frac{474 \text{ kW} \times 4797 \text{ kWh}}{2718 \text{ kWh}} \approx 836 \text{ kW}$$

Hence, these set of calculations can be done for the PV and BESS units at other optimal busbar locations as well. Results obtained for different cases with different load profiles are given by Table (5.2) to (5.6).

Table 5.2: Case I ( $\eta = 20\%$ , *Mix daily load profile*)

	<b>Bus 33</b>	<b>Bus 18</b>	<b>Bus 17</b>	<b>Total Energy</b>
PV Size (No BESS)	474 kW	652 kW	500 kW	
PV Energy (No BESS)	2718 kWh (4.2%)	3743 kWh (5.8%)	2877 kWh (4.4%)	9338 kWh (14.4%)
PV Size (with BESS)	$\frac{474 \times 4797}{2718} = 836$ kW	$\frac{652 \times 6296}{3743} = 1100$ kW	$\frac{500 \times 5430}{2877} = 950$ kW	
BESS Capacity	4500 kWh	5700 kWh	5700 kWh	
Total PV Energy	4797 kWh (7.4%)	6296 kWh (9.7%)	5430 kWh (8.4%)	16523 kWh (25.5%)
Total Load Energy Consumption				64870 kWh

Table 5.3: Case II ( $\eta = 25\%$ , *Mix daily load profile*)

	<b>Bus 33</b>	<b>Bus 18</b>	<b>Bus 17</b>	<b>Total Energy</b>
PV Size (No BESS)	474 kW	652 kW	500 kW	
PV Energy (No BESS)	2718 kWh (4.2%)	3743 kWh (5.8%)	2877 kWh (4.4%)	9338 kWh (14.4%)
PV Size (with BESS)	930 kW	1200 kW	1050 kW	
BESS Capacity	5800 kWh	7100 kWh	7100 kWh	
Total PV Energy	5318 kWh (8.2%)	6934 kWh (10.7%)	6068 kWh (9.4%)	18320 kWh (28.2%)
Total Load Energy Consumption				64870 kWh

Table 5.4: Case III ( $\eta = 30\%$ , *Mix daily load profile*)

	<b>Bus 33</b>	<b>Bus 18</b>	<b>Bus 17</b>	<b>Total Energy</b>
PV Size (No BESS)	474 kW	652 kW	500 kW	
PV Energy (No BESS)	2718 kWh (4.2%)	3743 kWh (5.8%)	2877 kWh (4.4%)	9338 kWh (14.4%)
PV Size (with BESS)	1020 kW	1320 kW	1170 kW	
BESS Capacity	6900 kWh	8500 kWh	8500 kWh	
Total PV Energy	5837 kWh (9.0%)	7572 kWh (11.7%)	6706 kWh (10.3%)	18320 kWh (28.2%)
Total Load Energy Consumption				64870 kWh

Table 5.5: Case IV ( $\eta = 20\%$ , *Residential load profile*)

	<b>Bus 33</b>	<b>Bus 18</b>	<b>Bus 17</b>	<b>Total Energy</b>
PV Size (No BESS)	474 kW	652 kW	500 kW	
PV Energy (No BESS)	2718 kWh (6.8%)	3743 kWh (9.3%)	2877 kWh (7.2%)	9338 kWh (23.3%)
PV Size (with BESS)	780 kW	1030 kW	880 kW	
BESS Capacity	3950 kWh	4850 kWh	4850 kWh	
Total PV Energy	4498 kWh (11.2%)	5927 kWh (14.8%)	5061 kWh (12.6%)	15486 kWh (38.6%)
Total Load Energy Consumption				40130 kWh

Table 5.6: Case V ( $\eta = 20\%$ , Commercial load profile)

	Bus 33	Bus 18	Bus 17	Total Energy
PV Size (No BESS)	474 kW	652 kW	500 kW	
PV Energy (No BESS)	2718 kWh (6.7%)	3743 kWh (9.2%)	2877 kWh (7.0%)	9338 kWh (22.9%)
PV Size (with BESS)	540 kW	740 kW	590 kW	
BESS Capacity	900 kWh	1100 kWh	1100 kWh	
Total PV Energy	3124 kWh (7.7%)	4243 kWh (10.4%)	3377 kWh (8.3%)	10744 kWh (26.3%)
Total Load Energy Consumption				40810 kWh

#### 5.4. Verification of Results for PV Sizes (with BESS)

The verification of the results obtained for BESS capacities that are integrated for optimal PV locations was done using the IEEE-33 network. The results obtained by the analytical method are compared with the results obtained from GA algorithm considering the required constraints. A summary of the results is tabulated in Table 5.7.

Table 5.7: Comparison of PV sizes (with BESS)

	Case I		Case II		Case III		Case IV		Case V	
	Novel Method (kW)	GA Method (kW)								
Bus 33	836	822	930	947	1020	1018	780	789	540	545
Bus 18	1100	1077	1200	1173	1320	1309	1030	1001	740	729
Bus 17	950	934	1050	1059	1170	1195	880	885	590	608

When considering the overall results obtained for PV sizes (with BESS), it can be observed that the sizes of PV units are increased than the PV unit sizes obtained for without BESS case as given in Table 4.1. The reason is that with BESS integrated, PV units have to generate more power during the peak solar period time to be stored in their respective BESS units.

When considering Case I ( $\eta = 20\%$ , *Overall daily load profile*) and Case IV ( $\eta = 20\%$ , *Residential load profile*), they are intended for serving the same portion of energy during the off-peak solar period but with different load profiles. However, the PV and BESS sizes for the Case I were high when compared with Case IV. The reason for this is their difference in load profiles. In Case I, during the peak solar period also there is a significant day time load. Because of that, the sizes of PV units need to be higher for serving that load. But in Case IV, there is hardly any peak solar period load and hence the existing PV sizes (PV sizes before integrating BESS units) or slightly higher sizes can manage the load.

When comparing Case I ( $\eta = 20\%$ , *Overall daily load profile*), Case II ( $\eta = 25\%$ , *Overall daily load profile*) and Case III ( $\eta = 30\%$ , *Overall load profile*), it is clearly seen that when "n" is increased, the sizes of PV units and BESS units are also increased. That is because when "n" is increased, BESS units should be capable of serving more energy during off-peak solar period. Hence, the additional energy that needs to be generated by PV units and stored in BESS units also increase. As a result of that, sizes of PV and BESS units are increased.

Moreover, it was observed that for Case V ( $\eta = 20\%$ , *Commercial load profile*), which considered a commercial load profile recorded the least PV and BESS sizes (as given in Table 5.6 and 5.7). The reason for this is that for commercial load profiles they have a day peak demand and hence the existing PV sizes are capable of serving that load. Because of that only less demand is available in the off-peak solar period and the amount of energy that need to be stored in BESS is very low. Therefore, the increase of PV sizes is very low, and less BESS capacity is required for each unit.

## **5.5. Summary**

In this chapter a novel analytical method for determining BESS capacities was presented. Detailed Solar PV output modelling was required and the SPV output was mapped with the PV generation from the respective PV units integrated in the IEEE-33 network. From the loads perspective, three different load profiles (mix daily load profile, residential load profile and commercial load profile) were taken into account and they were mapped to the constant loads in the considered distribution network. By these approaches, the time varying nature of SPV generation and loads were adopted for the IEEE-33 bus system.

Then the step by step procedure in calculating the BESS sizes was presented. The BESS capacities were determined in terms of Load Proportionality Factor, portion of off-peak solar period energy consumption that is expected to be supplied by BESS energy and the SOC limits of BESS units. Accordingly, the PV sizes and their respective BESS capacities were determined for five different cases. A synopsis of the results obtained is given by Table 5.2 to Tale 5.7.

## CHAPTER 6

### OPTIMAL POWER DISPATCH SCHEDULE

The previous chapters mainly focused on optimizing the DG location, DG size (which are the first two pillar of DG allocation) and sizing of BESS units. In this chapter, optimizing the power dispatch which is the third pillar of DG allocation is discussed. The necessity of dispatching power is highlighted for some of the DG technologies such as SPV and wind power generation due to their intermittency and non-dispatchable nature. Since the DG technology was specifically focused on SPV generation in the previous chapter, the same DG technology is considered in presenting a methodology for optimizing the power dispatch of BESS units. Moreover, as the solar data and load data were extracted in 30-minute intervals, it is assumed that a decision about dispatching power from BESS units is also taken for every 30 minutes.

#### 6.1. Mathematical Background

Before moving on to present about the optimal BESS dispatch algorithm, it is necessary to define certain mathematical parameters which are widely used in this section. At first, it is required to define the minimum charging/discharging rates of each BESS. It is defined as given in (6.1).

$$CRateB_{i,min} = \frac{(Daily\ energy\ expected\ to\ be\ served\ by\ BESS\ @\ i^{th}\ bus)/2}{24h} \quad (6.1)$$

As a sample calculation, for the IEEE-33 network consider the case of  $\eta = 20\%$ . Hence, the minimum charge/discharge rates for the three BESS units are calculated as given below.

For the BESS unit at busbar 33,

$$CRateB_{33,min} = \frac{(4797kWh - 2718kWh)/2}{24h} \approx 40kW$$

For the BESS unit at busbar 18,

$$CRateB_{18,min} = \frac{(6296kWh - 3743kWh)/2}{24h} \approx 50kW$$

For the BESS unit at busbar 17,

$$CRate_{B_{17},min} = \frac{(5430kWh - 2877kWh)/2}{24h} \approx 50kW$$

In this manner, the minimum charge/discharge rates of all the BESS units for different cases can be calculated. In the process of charging BESS units, it is considered that a fixed portion of PV generation is used for charging the BESS units. The fraction of PV generation that is used for charging the BESS units is taken as " $\alpha$ ".

## 6.2. BESS Dispatch Algorithm

The BESS dispatch algorithm presented in this chapter is based on some key parameters such as total active power load ( $Total P_{load}$ ), total PV generation ( $P_{PV,Gen}$ ), SOC limits of BESS units ( $SOC_{min}$  and  $SOC_{max}$ ),  $\eta$  (Fraction of daily load consumption) and  $\alpha$  (Fraction of PV generation used for charging BESS units). The flow chart explaining the BESS dispatch algorithm presented in this chapter is given by Figure 6.1.

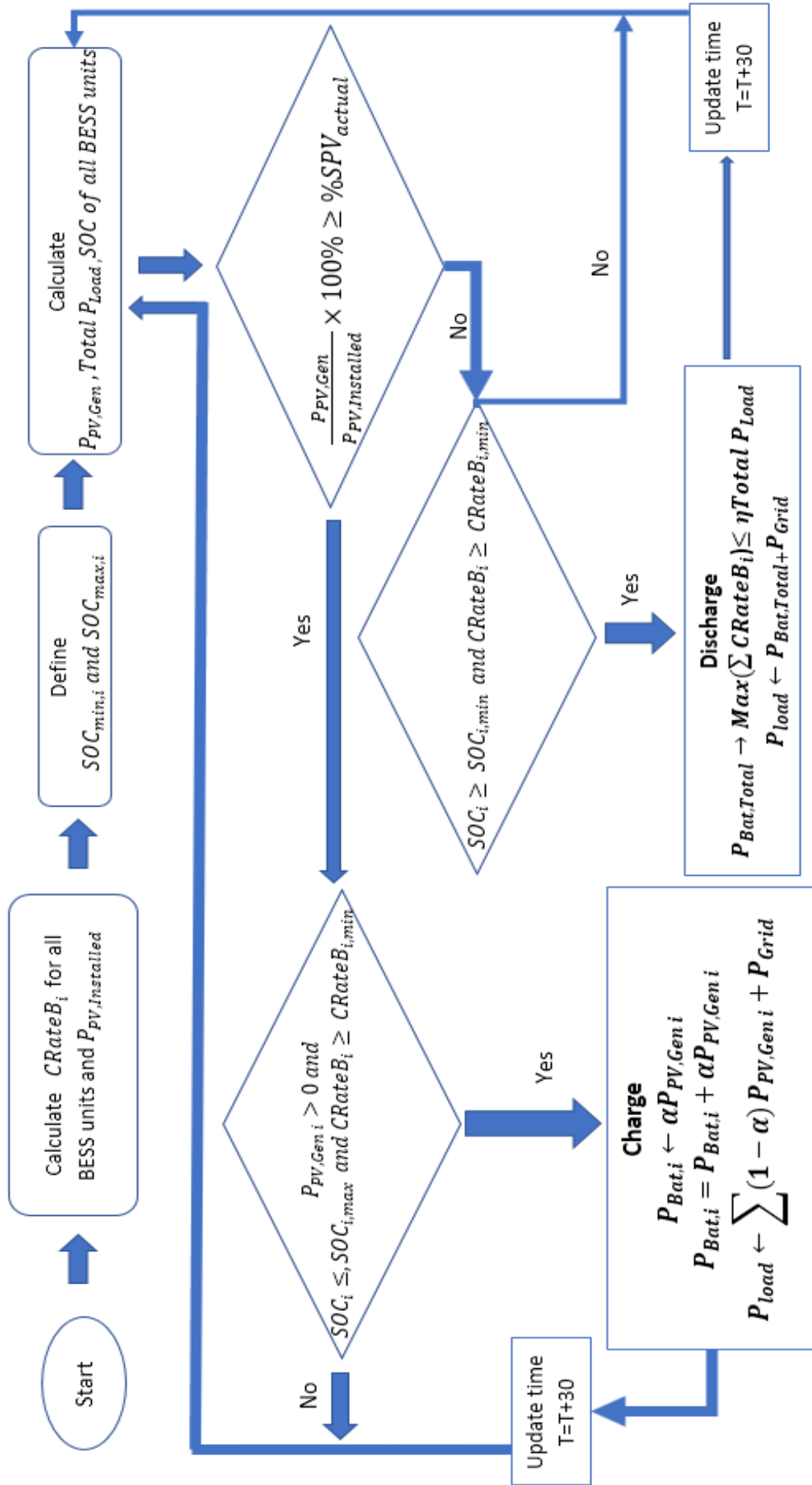


Figure 6.1: BESS dispatch algorithm

The algorithm given in Figure 6.1 can be illustrated in a more detailed manner as given below.

- ❖ Calculate the minimum charge/discharge rates of each BESS, total installed PV capacity, total PV generation, total active power load, SOC of all BESS units.
- ❖ Define the SOC limits of all BESS units.
- ❖ If it is in the peak solar period, check the conditions for charging are satisfied.
- ❖ If it is possible to charge, use a portion of PV generation ( $\alpha$ ) to charge the BESS. The load is supplied by the rest of PV generation and power from the grid.
- ❖ Update the values of total PV generation, total active power load, SOC of all BESS units after 30 minutes.
- ❖ If it is not possible to charge, check the conditions for discharging are satisfied.
- ❖ If it is possible to discharge, discharge the maximum amount of energy possible from each BESS which satisfies the portion of energy expected to be supplied in the off-peak solar period. The deficit of power needed to supply the load is given by the grid.
- ❖ Update the values of total PV generation, total active power load, SOC of all BESS units after 30 minutes.
- ❖ Continue the procedure of power dispatch as a loop.

### **6.3. Simulation Results**

The proposed methodology for dispatching the power of BESS units was applied for the standard IEEE-33 test bus system by considering three load profiles (mix daily load profile, residential load profile and commercial load profile) in order to justify the acceptability of it. A summary of the results obtained for different load profiles for a particular case is given below.

#### **6.3.1. Charge/Discharge Rate of BESS**

The charge/discharge rate behavior for three load profiles are given by Figure 6.2, 6.3 and 6.4. For all the load profiles, the case of  $\eta = 20\%$  and  $\alpha = 50\%$  are considered.

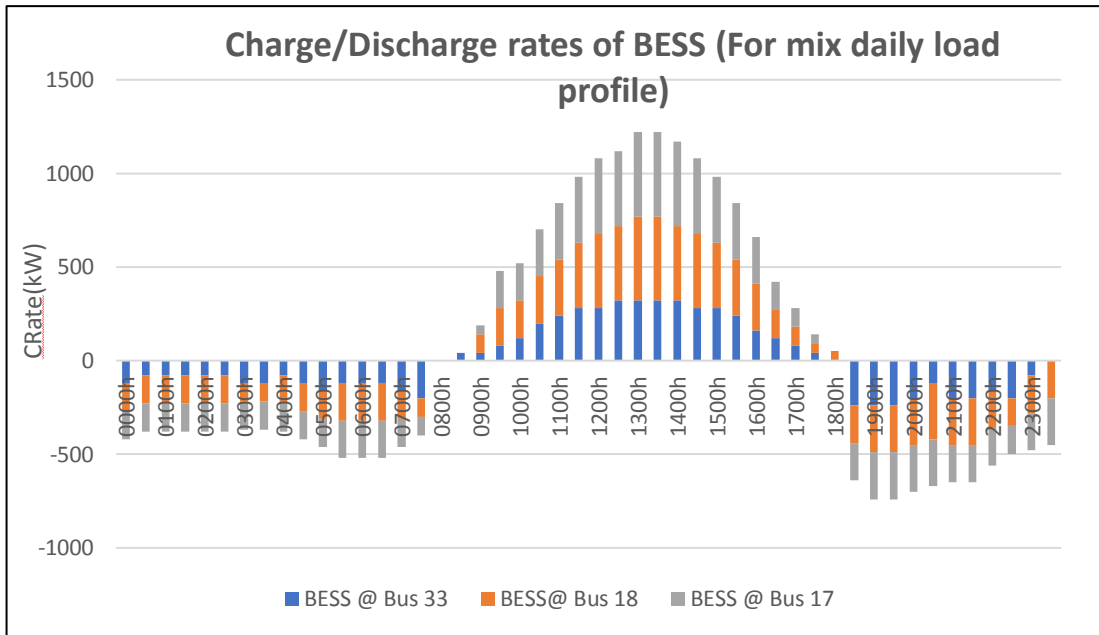


Figure 6.2: Charge/Discharge rates of BESS units (For mix daily load profile)

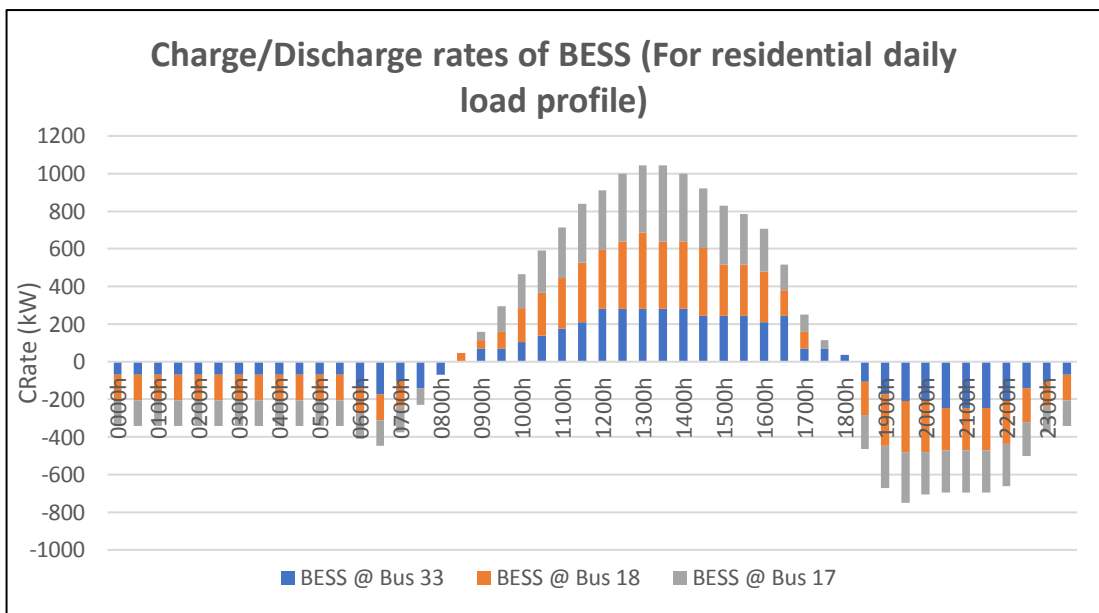


Figure 6.3: Charge/Discharge rates of BESS units (For residential daily load profile)

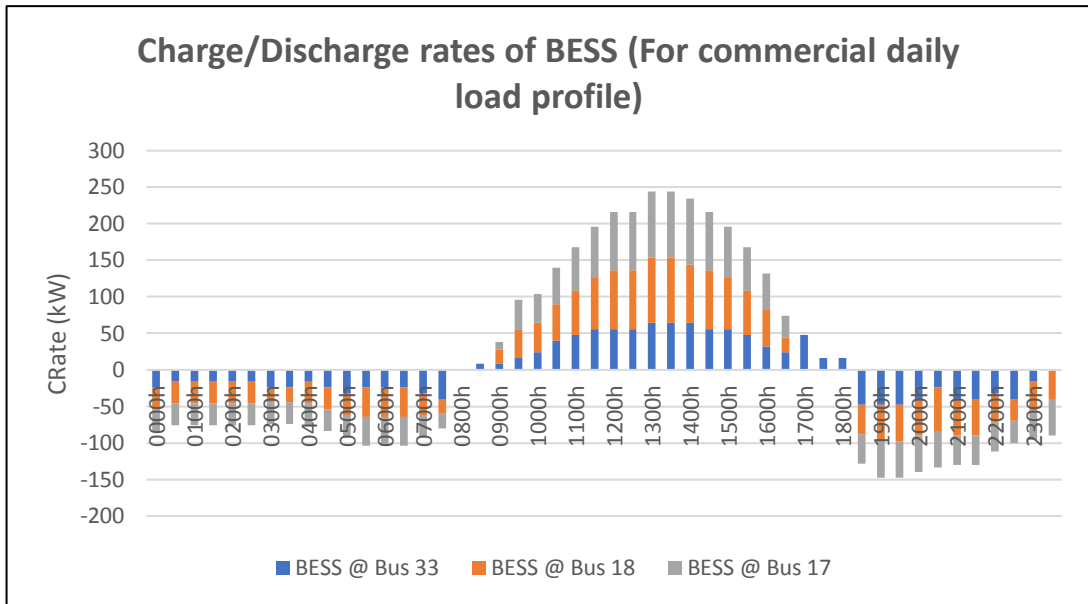


Figure 6.4: Charge/Discharge rates of BESS units (For commercial daily load profile)

When comparing the graphs obtained for the three load profiles it can be observed that total charge/discharge rates of BESS units for the mix load profile and residential load profile are higher when compared with the commercial load profile. The reason for this is that in the commercial load profile the peak load is in the solar peak period and there is hardly any load during the off-peak solar period. Hence, the amount of energy that needs to be stored during the peak solar period and dispatched during the off-peak solar period is very low. But with the other two load profiles, since the peak load is during the off-peak solar period, the BESS units are needed to be charged more during the peak solar period and dispatched during the off-peak solar period.

### 6.3.2. SOC Variation of BESS Units

The SOC variation of BESS units for the three load profiles are given by Figure 6.5, 6.6 and 6.7. For all the load profiles, the case of  $\eta = 20\%$  and  $\alpha = 50\%$  are considered.

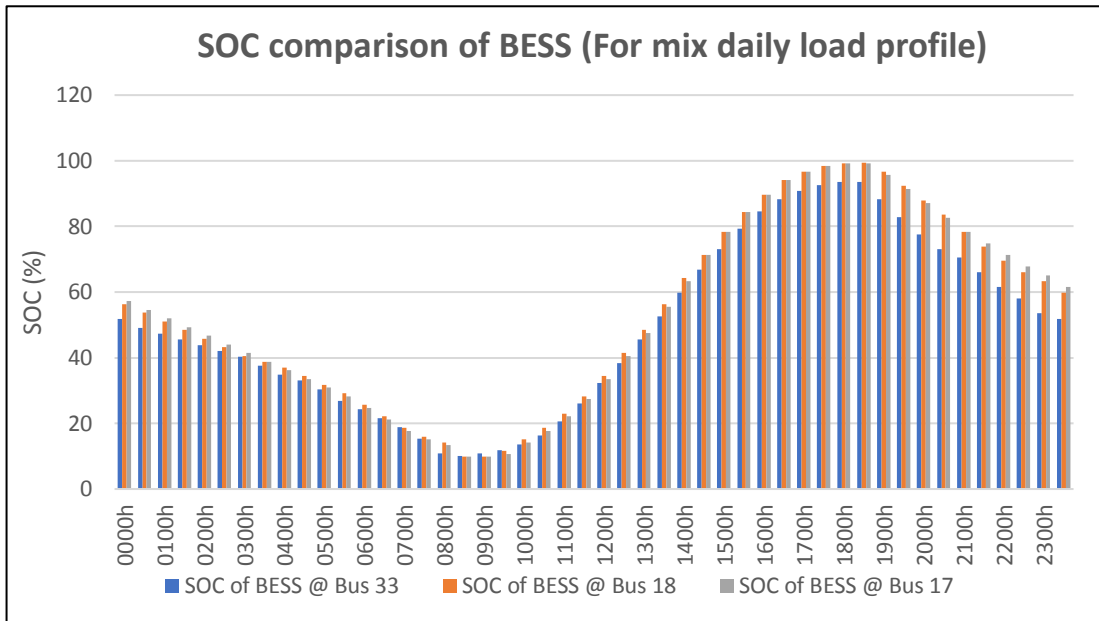


Figure 6.5: SOC variation of BESS units (For mix daily load profile)

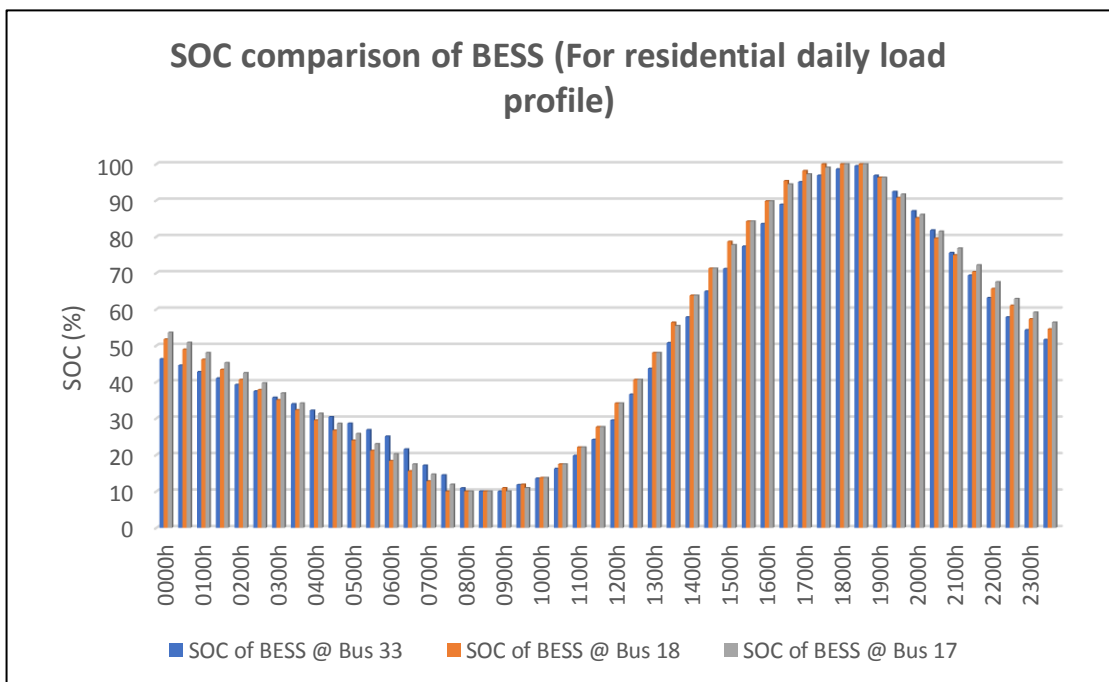


Figure 6.6: SOC variation of BESS units (For residential daily load profile)

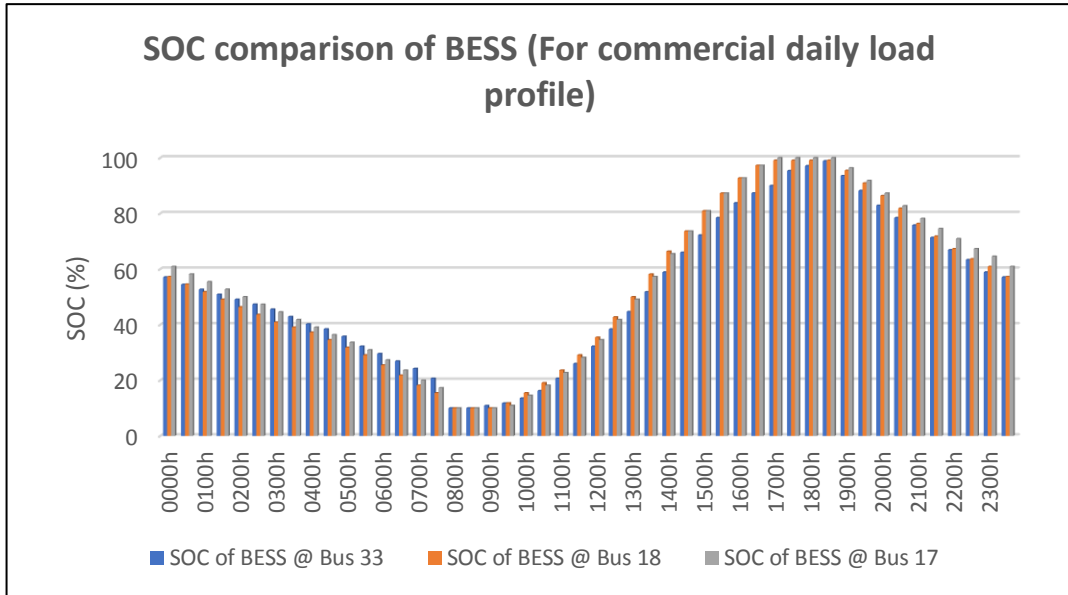


Figure 6.7: SOC variation of BESS units (For commercial daily load profile)

When comparing the three SOC curves, it can be clearly seen that all the curves have followed the same pattern. That is, during the peak solar period the SOC levels have gradually increased as the BESS units are charged during this time. During the off-peak solar period, the SOC levels have gradually decreased since the BESS units are discharged during this time period.

### 6.3.3. Active Power Loss Variation

The active power loss variation for the three load profiles are given by Figure 6.8, 6.9 and 6.10. For all the load profiles, the case of  $\eta = 20\%$  and  $\alpha = 50\%$  are considered. The power loss variations are considered for the base case, PV integrated case and PV & BESS integrated cases.

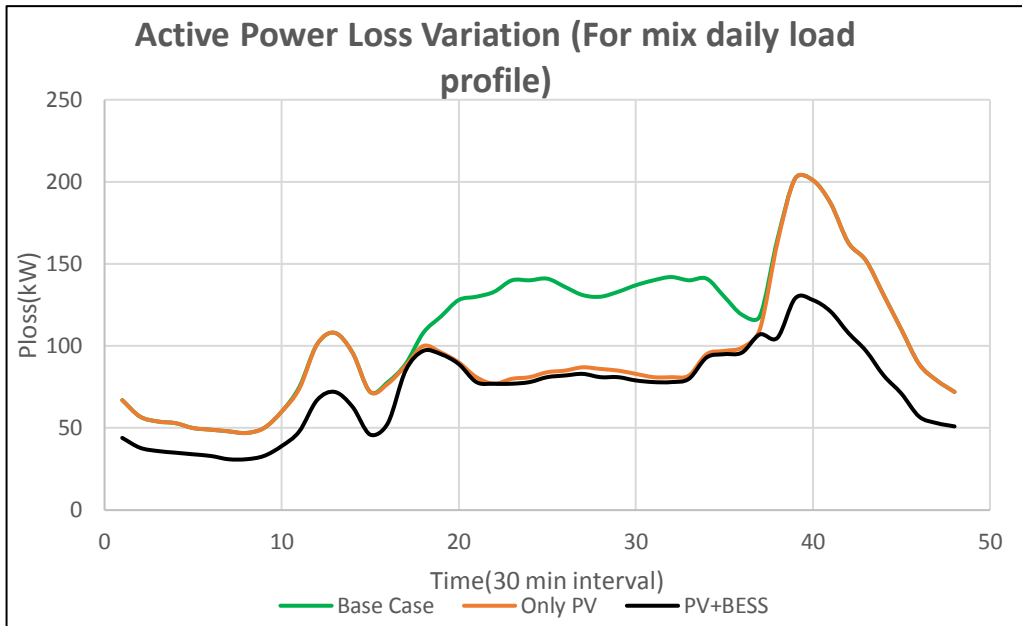


Figure 6.8: Active power loss variation (For mix daily load profile)

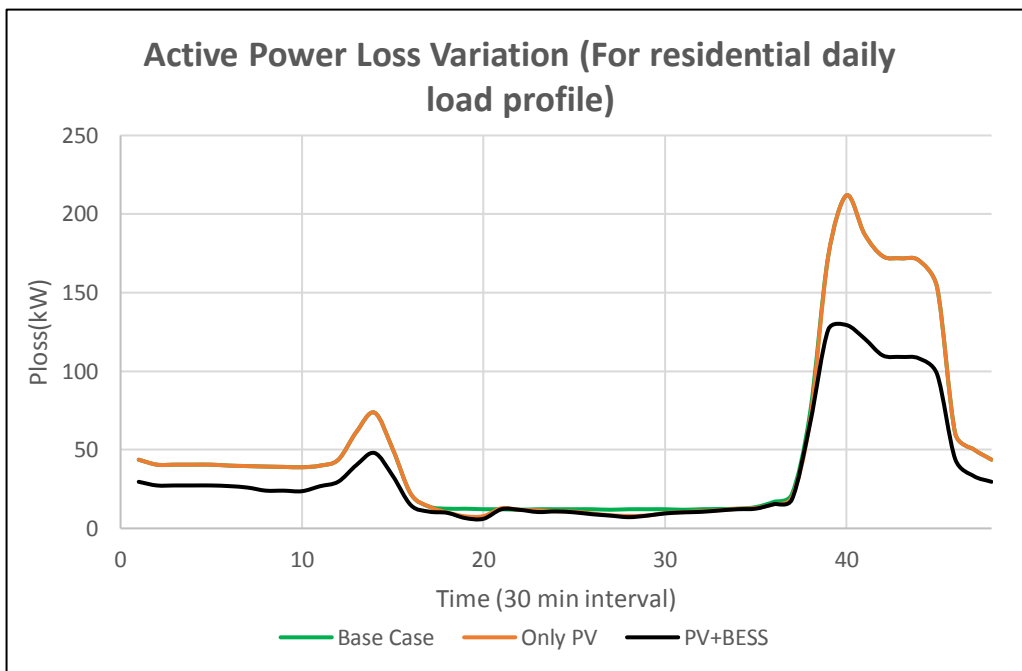


Figure 6.9: Active power loss variation (For residential daily load profile)

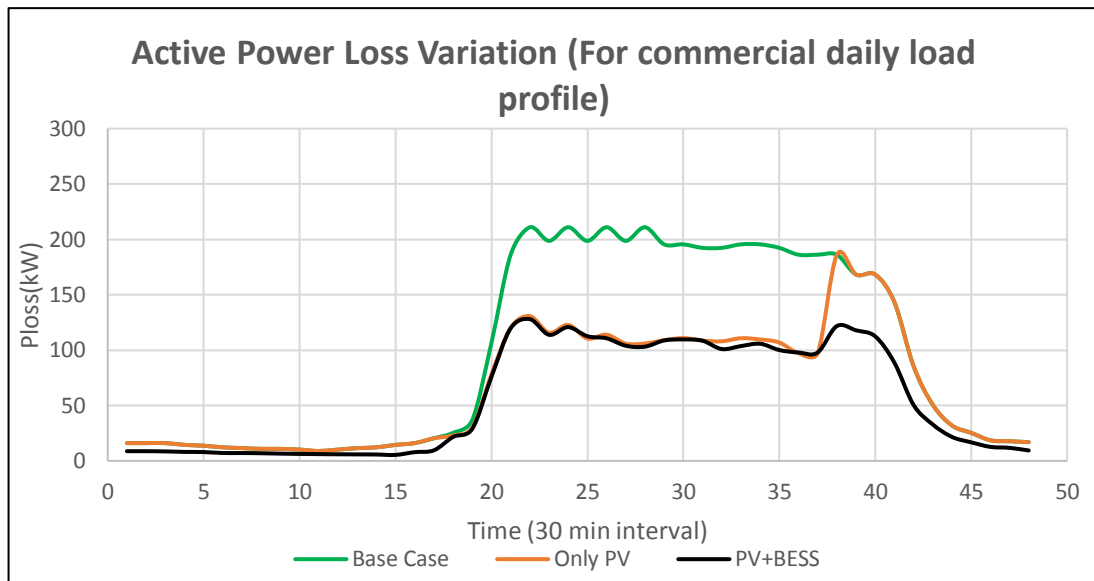


Figure 6.10: Active power loss variation (For commercial daily load profile)

When considering the active power loss variation for the mix daily load profile, it can be observed that losses are minimized during the PV and BESS integrated case. During the off-peak solar period, both base case and PV case have produced almost the same active power losses as there is hardly any PV generation during that time. In that particular period, the losses are minimized with the PV+BESS case as the BESS units are dispatching power during that time which helps to reduce the power taken from the grid. In contrast, during the peak solar period, it can be seen that losses are minimized by both Only PV and PV+BESS cases in a similar manner. That is because, during this period of the day, excessive PV generation is used for charging the BESS units while usual PV generation is utilized for reducing the power taken from the grid and thereby reduce the losses.

For the case of active power loss variation of residential load profile, it can be clearly seen that once again the losses are minimized with the PV+BESS case. During the off-peak solar period, both base case and PV case have produced almost the same active power losses as there is hardly any PV generation during that time. Nevertheless, lesser active power losses are recorded with the PV+BESS case as the BESS units are dispatching power during that time. During the peak solar period, almost the same power loss variations are shown by all the three cases but still the least power loss variation is given by PV+BESS case. The reason for this similar behavior

of loss variation during the peak solar period is that there is very low load consumption during this time of the day.

When considering the active power loss variation for the commercial daily load profile, here also it can be observed that losses are minimized during the PV and BESS integrated case. During the peak solar period, the losses are reduced with the Only PV and PV+BESS case when compared with the base case. This is due to the abundant PV generation during this time of the day. However, during the off-peak solar period it can be observed that although the losses are reduced with the PV+BESS case when compared with the base case and Only PV case, there is hardly any difference between the loss reduction. Availability of a very low commercial load during this time period has affected to experience such a behavior of loss variation.

Table 6.1 Daily energy loss comparison for different load profiles

	Daily Energy Loss		
	Mix Load	Residential Load	Commercial Load
<b>Base Case</b>	2635 kWh (4.06%)	1196 kWh (2.98%)	2324 kWh (5.69%)
<b>Only PV</b>	2195 kWh (3.38%)	1174 kWh (2.93%)	1568 kWh (3.84%)
<b>PV+BESS (<math>\eta = 20\%</math>, <math>\alpha = 50\%</math>)</b>	1279 kWh (1.97%)	812 kWh (2.02%)	1341 kWh (3.29%)

A summary of the daily energy losses is given in Table 6.1. From the values obtained for different cases it can be seen that with the PV+BESS case has given the minimum energy losses. Nevertheless, the best energy loss percentage reduction is given by the commercial load case when compared with mix load and residential load cases. It is about 2.40% energy loss reduction with respect to the base case. The least energy loss reduction is given by the residential load case and it is about 0.96% energy loss reduction with respect to the base case.

### 6.3.4. Voltage Profile Variation

The variation of busbar voltages for the three load profiles are given by Figure 6.11(a) to Figure 6.13(c) for three different time stamps. For all the load profiles, the case of  $\eta = 20\%$  and  $\alpha = 50\%$  are considered. Moreover, the busbar voltages are considered for the base case, PV integrated case and PV & BESS integrated cases.

#### Variation of Busbar Voltages for the Mix Daily Load Profile

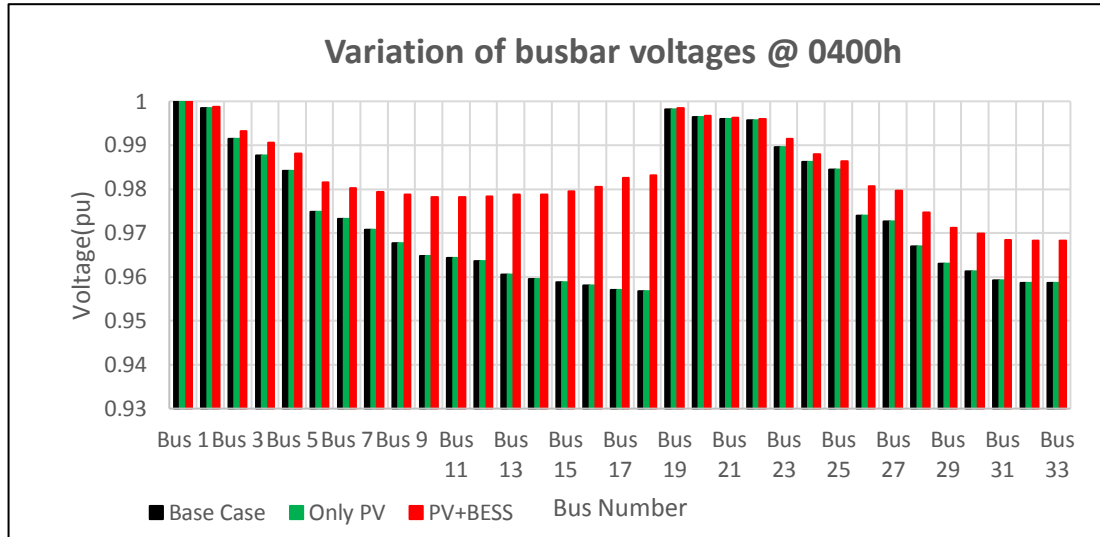


Figure 6.11(a): Variation of busbar voltages @ 4 a.m. (For mix daily load profile)

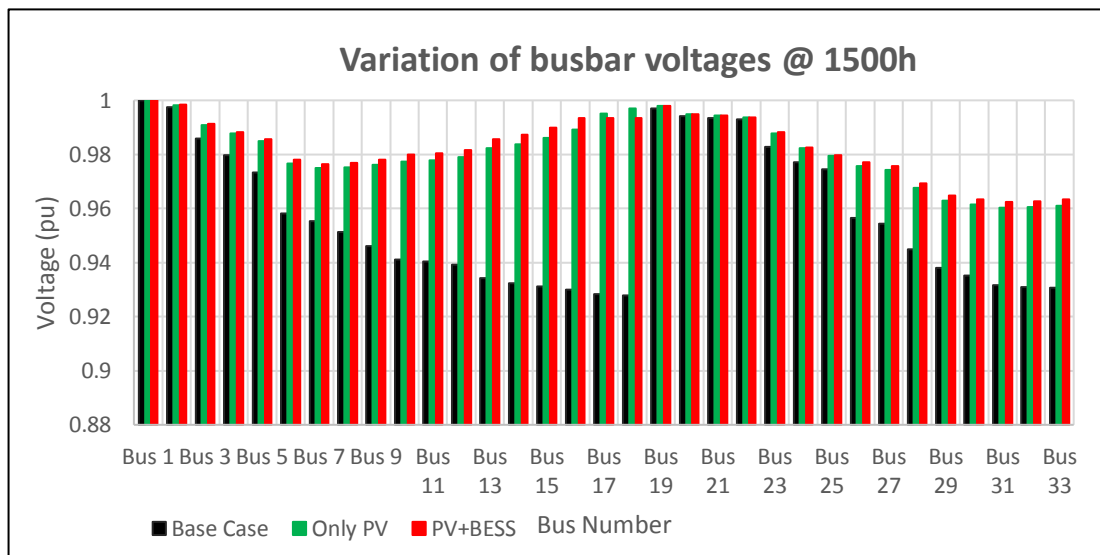


Figure 6.11(b): Variation of busbar voltages @ 3 p.m. (For mix daily load profile)

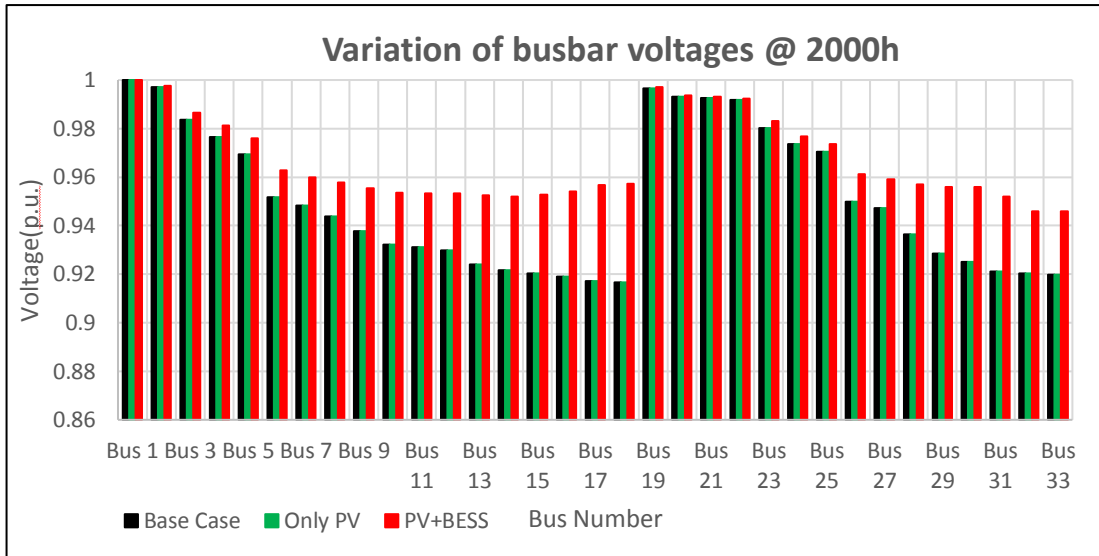


Figure 6.11(c): Variation of busbar voltages @ 8 p.m. (For mix daily load profile)

Figure 6.11(a)-6.11(c): Variation of busbar voltages for different time snaps (For mix daily load profile)

When comparing the voltage profiles taken at three different time stamps of a day, it can be concluded that the best voltage profiles are obtained from PV+BESS case. During the off-peak solar period, both base case and only PV case have almost the same voltage profile (Figure 6.11(a) and 6.11(c)) as there is hardly any PV generation during that period of the day. But during the peak solar period, the three different voltage profiles for base case, only PV case and PV+BESS case can be observed. During this period, the best voltage profile is once again given by the PV+BESS case which suggests the acceptability of the proposed methodology.

### Variation of Busbar Voltages for the Residential Daily Load Profile

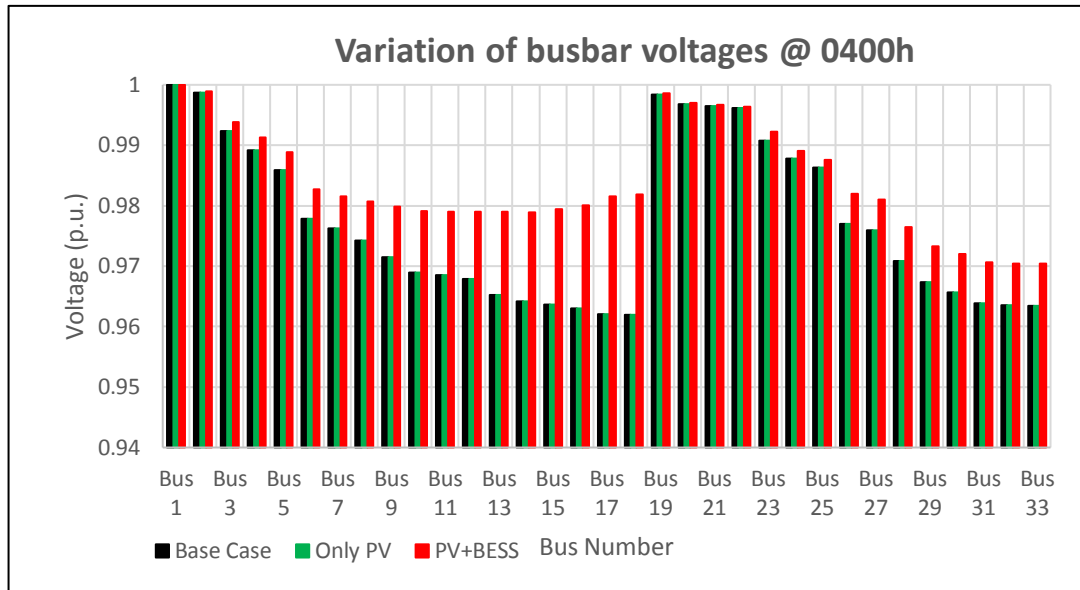


Figure 6.12(a) Variation of busbar voltages @ 4 a.m. (For residential daily load profile)

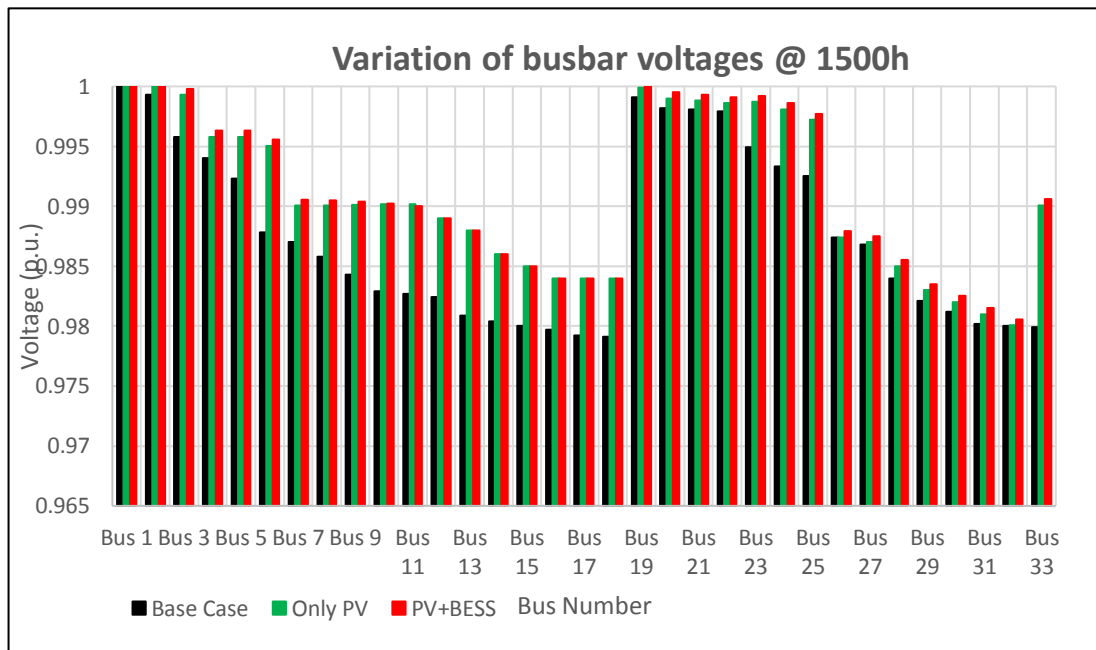


Figure 6.12(b) Variation of busbar voltages @ 3 p.m. (For residential daily load profile)

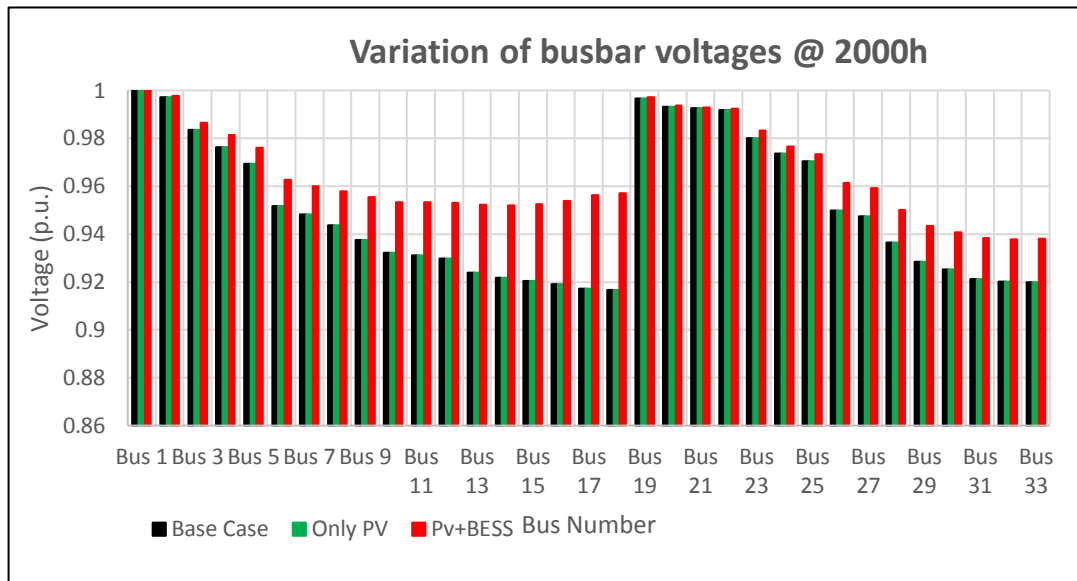


Figure 6.12(c) Variation of busbar voltages @ 8 p.m. (For residential daily load profile)

Figure 6.12(a)-6.12(c): Variation of busbar voltages for different time snaps (For residential daily load profile)

When comparing the voltage profiles taken at three different time stamps of a day, it can be concluded that the best voltage profiles are obtained from PV+BESS case. However, there is hardly any difference between the base case and only PV case voltage profiles given in Figure 6.12(a) and 6.12(c) as those voltage profiles are taken during off-peak solar periods. But during the peak solar period, the three different voltage profiles for base case, only PV case and PV+BESS case can be observed. During this period, the best voltage profile is once again given by the PV+BESS case.

### Variation of Busbar Voltages for the Commercial Daily Load Profile

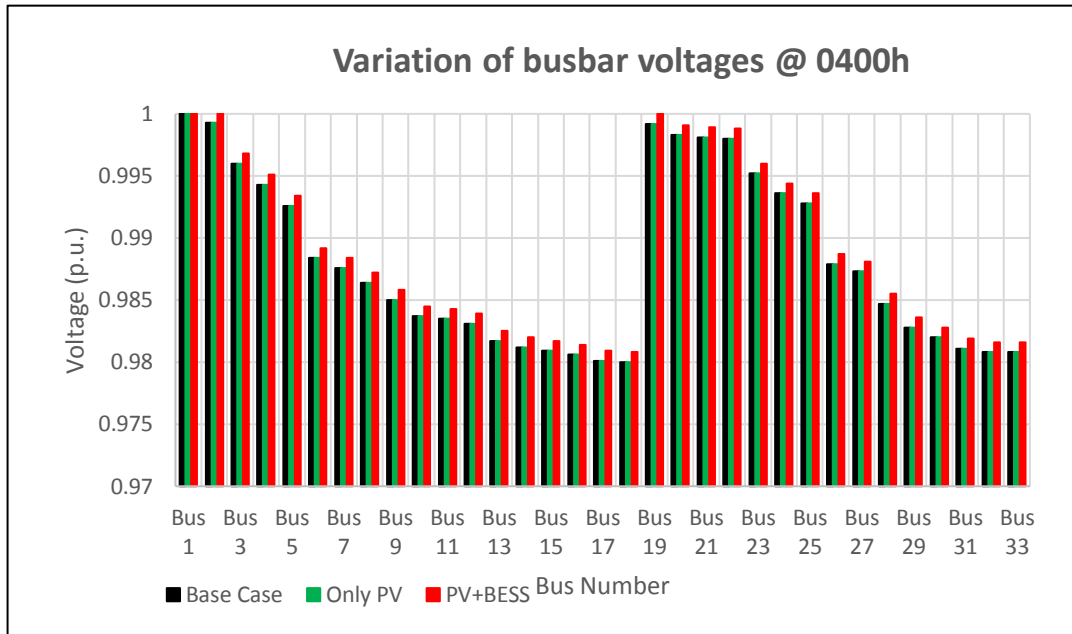


Figure 6.13(a) Variation of busbar voltages @ 4 a.m. (For commercial daily load profile)

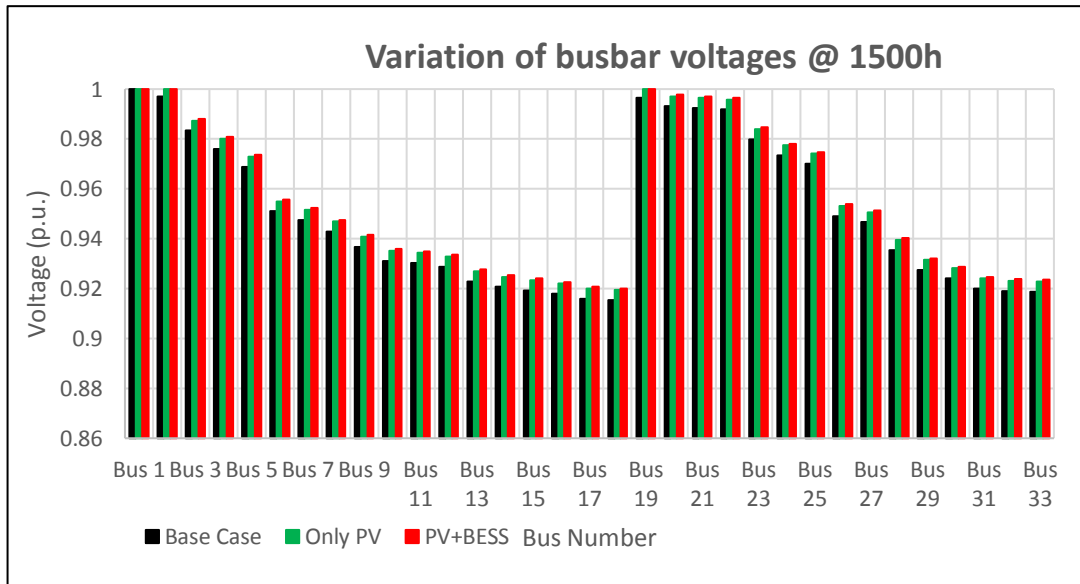


Figure 6.13(b) Variation of busbar voltages @ 3 p.m. (For commercial daily load profile)

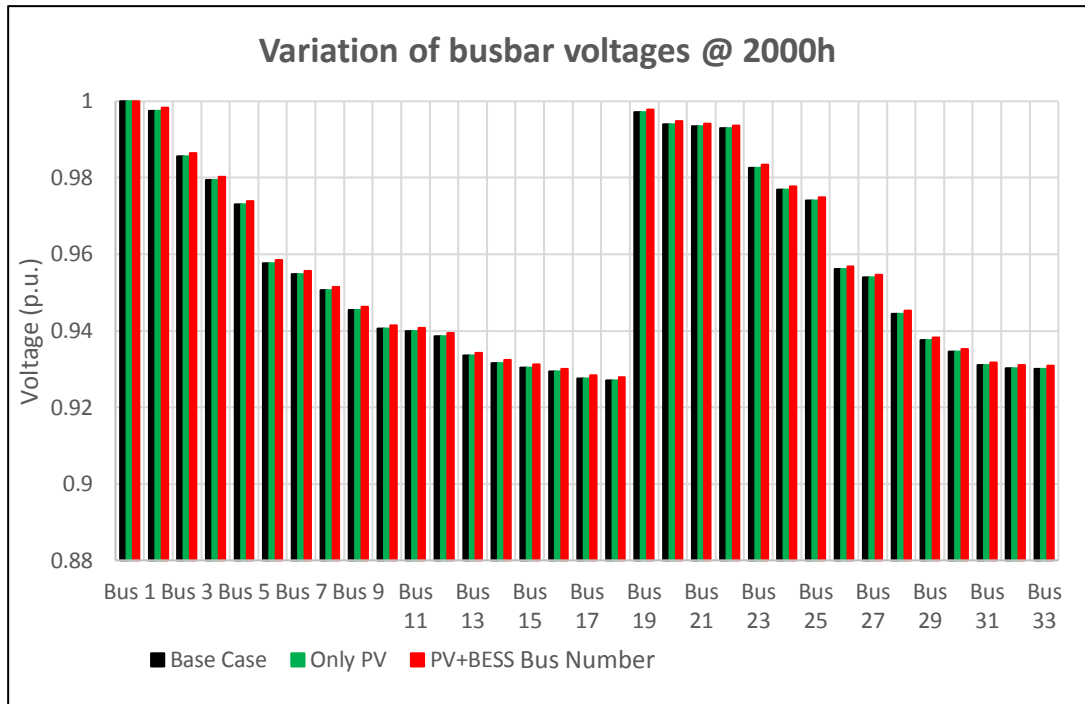


Figure 6.13(c) Variation of busbar voltages @ 8 p.m. (For commercial daily load profile)

Figure 6.13(a)-6.13(c): Variation of busbar voltages for different time snaps (For commercial daily load profile)

When comparing the voltage profiles taken at three different time stamps of a day, it can be concluded that the best voltage profiles are obtained from PV+BESS case. However, there is hardly any difference between the Base case and Only PV case voltage profiles given in Figure 6.13(a) and 6.13(b). Figure 6.13(c) shows that all the three profiles are behaving in a similar manner so that it is difficult to observe any difference between each profile. The reason for this behavior is that during off-peak solar period commercial load consumption is very low when compared with the load consumption during the peak solar period.

#### 6.4. Summary

In this chapter, a novel algorithm for operating BESS units integrated for a distribution network was presented. At first, the minimum charge/discharge rate of BESS units was defined in terms of daily energy expected to be served by the BESS units and the number of hours per day. The BESS dispatch algorithm was based on

some key parameters such as total active power load ( $Total P_{load}$ ), total PV generation ( $Total PV_B$ ), SOC limits of BESS units ( $SOC_{min}$  and  $SOC_{max}$ ),  $\eta$  (Fraction of daily load consumption) and  $\alpha$  (Fraction of PV generation used for charging BESS units). The decision chart of the BESS dispatch algorithm was presented along with a sample illustration. Variation of charge/discharge rates of BESS, SOC variation, active power loss variation and busbar voltage profile comparisons were analyzed for different scenarios considered. The results suggested that the PV and BESS integrated case was able to give the best results in terms of minimizing active power losses and voltage deviations.

## CHAPTER 7

### CONCLUSIONS AND FUTURE WORK

#### 7.1. Conclusions

Integration of DG units for power networks has occupied a great interest in the modern power industry due to their numerous varieties of merits over the conventional methods of power generation. However, the decision about DG allocation (i.e. location, size and power dispatch) is usually taken by the investors and/or power utilities depending on several conditions. Thus, there may be instances of inappropriate allocation of DG units which can affect the system performance undesirably. Therefore, it is essential to optimize DG allocation to harness the best expected results of it.

In this thesis, a novel method based on loss and voltage sensitivities was developed for determining the optimal DG location. A novel index named “LVSI (Loss-Voltage Sensitivity Index)” was defined in terms of Loss Sensitivity Index (LSI) and Voltage Sensitivity Index (VSI) as the objective function and solved it at the base case for determining the optimal DG location. The proposed scheme was tested by using standard IEEE-6 and IEEE-33 test bus systems. The results justified the acceptability of the proposed methodology.

As the next step, two different approaches were presented for determining the optimal DG sizes. In the first method, once again the combined effect of LSI and VSI were taken into account for formulating a novel objective function such that active power losses and voltage deviations are minimized. By solving the objective function, an expression for optimal DG size was obtained. The second method was based on developing an objective function in terms of active power losses and voltage deviations so that those parameters are minimized in the optimization process. Moreover, the objective function was solved based on Lagrange Multiplier Method (LMM). When the DG penetration level is given, this method could be used for determining the optimal DG sizes. The validity of the proposed methodologies were tested on IEEE-6 and IEEE-33 test bus systems. Furthermore, the values obtained for optimal DG sizes were compared with the results obtained through Genetic Algorithm (GA) for further verification and the results justified the accuracy of the proposed methodologies.

A novel approach for determining the BESS capacities for serving a portion of peak load was presented as the next step. For simplicity, the DG technology was specified for SPV generation. Although in the methodologies presented for optimizing DG location and size considered a snapshot of time at peak loading, the time varying nature of loads and DG output were adopted in this approach for achieving realistic results. For doing that, raw solar data collected from a PV farm in Hambantota area and three typical load curves (mix load, residential load and commercial load) were used. Those curves were mapped with the constant loads and PV generation of the considered distribution network. Then a method based on Load Proportionality Factor (LPF), State of Charge (SOC), portion of daily off-peak solar period energy consumption expected to be served by BESS was presented for determining the BESS capacities. The proposed method was tested under five cases by varying the portion of daily off-peak solar period energy consumption expected to be served by BESS ( $\eta$ ) and type of load profile. The results justified that with the proposed scheme, the network energy losses and voltage deviations were minimized.

As the final approach, a BESS dispatch algorithm was presented such that energy storing and dispatching of BESS units are done in a manner such that the network power losses and voltage deviations are minimized. The results were obtained for charging/discharging of BESS units, their SOC variation, active power losses and voltage profile variation. Here also, the results were analyzed for three different load profiles and the results justified the acceptability of the proposed scheme.

By considering the results obtained for optimizing DG location, size BESS capacities and power dispatch, it can be concluded that those methodologies were efficient and accurate enough to produce the expected results (i.e. minimizing active power losses and enhancing voltage profile).

## **7.2. Future Work**

As a future work, the time varying nature of loads and DG output can be adopted so that more accurate and realistic results can be obtained for DG location and size since usually optimal DG sizing and location determination are done considering the peak load condition. Furthermore, in the BESS sizing and optimal power dispatch approaches, it considered only a single DG technology as SPV generation. But as a future work, it is better to analyze a mix of DG technologies operating together so that

a better understanding about the behavior of DG technologies and their outputs can be gained.

Usually the Distribution System Operators (DSOs) are interested in network performance aspects such as minimizing active power losses and voltage deviations. However, they are also concerned about operating the system with the minimum cost. As a future work, it is better to a study considering the cost of operation as well. For that case, constraints for DG location, sizes and BESS capacities can be imposed in order to get a compromise between the network operation cost and network performance aspects.

In the optimal BESS dispatch schedule procedure, the presented method considered that BESS units were charged during the peak solar period only while using a fixed portion of PV generation (" $\alpha$ ") to charge the batteries. However, an adoptive methodology can be developed such that the charging periods and charging proportion are not fixed so that they are determined based on the network situation at that moment. Moreover, better results can be obtained with a methodology such that DG and BESS units are locally communicating with each other to decide the dispatch decision.

## REFERENCES

- [1] P.S. Georgilakis and N.D. Hatziargyriou, "Optimal distributed generation placement in power distribution networks: Models, methods, and future research," *IEEE Transactions on Power Systems*, vol. 28, no. 3, pp. 3420–3428, 2013.
- [2] K.B.J. Anuradha, U. Jayatunga, and H.Y.R. Perera, "Voltage-Loss Sensitivity Based Approach for Optimal DG Placement in Distribution Networks," *2019 IEEE International Conference on Industrial and Information Systems (ICIIS)*, 2019.
- [3] L. F. Ochoa, C. J. Dent, and G. P. Harrison, "Distribution network capacity assessment: Variable DG and active networks," *IEEE Transactions on Power Systems*, vol. 25, no. 1, pp. 87–95, Feb. 2010.
- [4] C. Wang and M. Nehrir, "Analytical Approaches for Optimal Placement of Distributed Generation Sources in Power Systems," *IEEE Transactions on Power Systems*, vol. 19, no. 4, pp. 2068-2076, 2004.
- [5] G. Celli, E. Ghiani, S. Mocci, and F. Pilo, "A multiobjective evolutionary algorithm for the sizing and siting of distributed generation," *IEEE Transactions on Power Systems*, vol. 20, no. 2, pp. 750–757, 2005.
- [6] S.H. Lee and J.W. Park, "Selection of optimal location and size of multiple distributed generations by using kalman filter algorithm," *IEEE Transactions on Power Systems*, vol. 24, no. 3, pp. 1393–1400, 2009.
- [7] G.P. Harrison, A. Piccolo, P. Siano and A.R. Wallace "Hybrid GA and OPF evaluation of network capacity for distributed generation connections," *Electric Power Systems Research*, vol. 78, no. 3, pp. 392– 398, 2008.
- [8] L. Wang and C. Singh "Reliability-Constrained Optimum Placement of Reclosers and Distributed Generators in Distribution Networks Using an Ant Colony System Algorithm," *IEEE Transactions on Systems, Man, and Cybernetics, Part C (Applications and Reviews)*, vol. 38, no. 6, pp. 757-764, 2008.
- [9] D. Singh, D. Singh, and K.S. Verma, " Multiobjective Optimization for DG Planning With Load Models," *IEEE Transactions on Power Systems*, vol. 24, no. 1, pp. 427-436, 2009.
- [10] P. Prakash and D. K. Khatod, "Optimal sizing and siting techniques for distributed generation in distribution systems: A review," *Renewable and Sustainable Energy Reviews*, vol. 57, pp. 111–130, 2016.
- [11] D.H. Popovic, J. Greatbanks, M. Begovic, and A. Pregelj, "Placement of distributed generators and reclosers for distribution network security and reliability," *International Journal of Electrical Power Energy Systems*, vol. 27, no. 5-6, pp. 398-408, 2005.
- [12] G. Carpinelli, G. Celli, F. Pilo, and A. Russo, "Embedded generation planning under uncertainty including power quality issues," *European Transactions on Electrical Power*, vol. 13, no. 6, pp. 381–389, 2003.

- [13] S. Kotamarty, S. Khushalani, and N. Schulz, “Impact of distributed generation on distribution contingency analysis,” *Electric Power Systems Research*, vol. 78, no. 9, pp. 1537-1545, 2008.
- [14] A. Keane and M. O’Malley, “Optimal allocation of embedded generation on distribution networks,” *IEEE Transactions on Power Systems*, vol. 20, no.3, pp. 1640–1646, Aug. 2005.
- [15] A. Keane and M. O’Malley, “Optimal utilization of distribution networks for energy harvesting,” *IEEE Transactions on Power Systems*, vol. 22, no. 1, pp. 467–475, Feb. 2007.
- [16] B. Singh, V. Mukherjee, and P. Tiwari, “A survey on impact assessment of DG and FACTS controllers in power systems,” *Renewable and Sustainable Energy Reviews*, vol. 42, pp. 846–882, 2015.
- [17] Y. M. Atwa and E. F. El-Saadany, “Probabilistic approach for optimal allocation of wind-based distributed generation in distribution systems,” *IET Renewable Power Generation*, vol. 5, no. 1, pp. 79–88, Jan. 2011.
- [18] S. Porkar, P. Poure, A. Abbaspour-Tehrani-Fard, and S. Saadate, “Optimal allocation of distributed generation using a two-stage multi-objective mixed-integer-nonlinear programming,” *European Transactions on Electrical Power*, vol. 21, no. 1, pp. 1072–1087, Jan. 2011.
- [19] A. Kumar and W. Gao, “Optimal distributed generation location using mixed integer non-linear programming in hybrid electricity markets,” *IET Generation, Transmission and Distribution*, vol. 4, no. 2, pp. 281–298, Feb. 2010.
- [20] W. El-Khattam, Y. G. Hegazy, and M. M. A. Salama, “An integrated distributed generation optimization model for distribution system planning,” *IEEE Transactions on Power Systems*, vol. 20, no. 2, pp. 1158–1165, May 2005.
- [21] R.S.A. Abri, E.F. El-Saadany, and Y.M. Atwa, “Optimal Placement and Sizing Method to Improve the Voltage Stability Margin in a Distribution System Using Distributed Generation,” *IEEE Transactions on Power Systems*, vol. 28, no. 1, pp. 326-334, 2013.
- [22] S. Kaur, G. Kumbhar, and J. Sharma, “A MINLP technique for optimal placement of multiple DG units in distribution systems,” *International Journal of Electrical Power & Energy Systems*, vol. 63, pp. 609–617, 2014.
- [23] Y. M. Atwa, E. F. El-Saadany, M. M. A. Salama, and R. Seethapathy, “Optimal renewable resources mix for distribution system energy loss minimization,” *IEEE Transactions on Power Systems*, vol. 25, no. 1, pp. 360–370, Feb. 2010.
- [24] C. J. Dent, L. F. Ochoa, and G. P. Harrison, “Network distributed generation capacity analysis using OPF with voltage step constraints,” *IEEE Trans. Power Syst.*, vol. 25, no. 1, pp. 296–304, Feb. 2010.

- [25] L. F. Ochoa and G. P. Harrison, "Minimizing energy losses: Optimal accommodation and smart operation of renewable distributed generation," *IEEE Trans. Power Syst.*, vol. 26, no. 1, pp. 198–205, Feb. 2011.
- [26] P. N. Vovos, G. P. Harrison, A. R. Wallace, and J. W. Bialek, "Optimal power flow as a tool for fault level-constrained network capacity analysis," *IEEE Trans. Power Syst.*, vol. 20, no. 2, pp. 734–741, May 2005.
- [27] M. F. AlHajri, M. R. AlRashidi, and M. E. El-Hawary, "Improved sequential quadratic programming approach for optimal distribution generation deployments via stability and sensitivity analyses," *Electrical Power Component Systems*, vol. 38, no. 14, pp. 1595–1614, Dec. 2010.
- [28] R. Wang, P. Wang, and G. Xiao, "A robust optimization approach for energy generation scheduling in microgrids," *Energy Conversion and Management*, vol. 106, pp. 597–607, 2015.
- [29] N. Khalesi, N. Rezaei, and M.-R. Haghifam, "DG allocation with application of dynamic programming for loss reduction and reliability improvement," *International Journal of Electrical Power & Energy Systems*, vol. 33, no. 2, pp. 288–295, Feb. 2011.
- [30] O. Gandhi, C. D. Rodriguez-Gallegos, and D. Srinivasan, "Review of optimization of power dispatch in renewable energy system," *2016 IEEE Innovative Smart Grid Technologies - Asia (ISGT-Asia)*, 2016.
- [31] R. A. Jabr and B. C. Pal, "Ordinal optimization approach for locating and sizing of distributed generation," *IET Generation, Transmission & Distribution*, vol. 3, no. 8, pp. 713–723, Aug. 2009.
- [32] S. Kansal, B. Sai, B. Tyagi, and V. Kumar, "Optimal placement of wind-based generation in distribution networks," *IET Conference on Renewable Power Generation (RPG 2011)*, 2011.
- [33] R. Jabr and B. Pal, "Ordinal optimization approach for locating and sizing of distributed generation," *IET Generation, Transmission & Distribution*, vol. 3, no. 8, pp. 713–723, Jan. 2009.
- [34] P. Vovos and J. Bialek, "Direct incorporation of fault level constraints in optimal power flow as a tool for network capacity analysis," *IEEE Trans. Power Syst.*, vol. 20, no. 4, pp. 2125–2134, Nov. 2005.
- [35] N. S. Rau and Y.-H. Wan, "Optimum location of resources in distributed planning," *IEEE Transactions on Power Systems*, vol. 9, no. 4, pp. 2014–2020, Nov. 1994.
- [36] S. Sivanandam and S. Deepa, *Introduction to Genetic Algorithms*. Springer, 2008.
- [37] J.-H. Teng, S.-W. Luan, D.-J. Lee, and Y.-Q. Huang, "Optimal Charging/Discharging Scheduling of Battery Storage Systems for Distribution Systems Interconnected With Sizeable PV Generation Systems," *IEEE Transactions on Power Systems*, vol. 28, no. 2, pp. 1425–1433, 2013.

- [38] D. Singh, D. Singh, and K.-S. Verma, "Multiobjective optimization for DG planning with load models," *IEEE Transactions on Power Systems*, vol. 24, no. 1, pp. 427–436, Feb. 2009.
- [39] R. K. Singh and S. K. Goswami, "Optimum siting and sizing of distributed generations in radial and networked systems," *Electrical Power Component Systems*, vol. 37, no. 2, pp. 127–145, Jan. 2009.
- [40] C. L. T. Borges and D. M. Falcão, "Optimal distributed generation allocation for reliability, losses, and voltage improvement," *International Journal of Electrical Power & Energy Systems*, vol. 28, no. 6, pp. 413–420, Jul. 2006.
- [41] J.-H. Teng, Y.-H. Liu, C.-Y. Chen, and C.-F. Chen, "Value-based distributed generator placements for service quality improvements," *International Journal of Electrical Power & Energy Systems*, vol. 29, no. 3, pp. 268–274, Mar. 2007.
- [42] J. M. López-Lezama, J. Contreras, and A. Padilha-Feltrin, "Location and contract pricing of distributed generation using a genetic algorithm," *International Journal of Electrical Power & Energy Systems*, vol. 36, no. 1, pp. 117–126, Mar. 2012.
- [43] K.-H. Kim, Y.-J. Lee, S.-B. Rhee, S.-K. Lee, and S.-K. You, "Dispersed generator placement using fuzzy-GA in distribution systems," *IEEE Power Engineering Society Summer Meeting*, Jul. 2002, pp. 1148–1153.
- [44] L. F. Ochoa, A. Padilha-Feltrin, and G. P. Harrison, "Time-series-based maximization of distributed wind power generation integration," *IEEE Transactions on Energy Conversion*, vol. 23, no. 3, pp. 968–974, Sep. 2008.
- [45] B. Yuce, Y. Rezgui, and M. Mourshed, "ANN-GA smart appliance scheduling for optimized energy management in the domestic sector," *Energy and Buildings*, vol. 111, pp. 311–325, 2016.
- [46] R.-H. Liang and J.-H. Liao, "A Fuzzy-Optimization Approach for Generation Scheduling with Wind and Solar Energy Systems," *IEEE Transactions on Power Systems*, vol. 22, no. 4, pp. 1665–1674, 2007.
- [47] R. Mehta, D. Srinivasan, A. M. Khambadkone, J. Yang, and A. Trivedi, "Smart Charging Strategies for Optimal Integration of Plug-in Electric Vehicles within Existing Distribution System Infrastructure," *IEEE Transactions on Smart Grid*, vol. 3053, no. c, pp. 1–1, 2016.
- [48] J. Kennedy and R. Eberhart, "Particle swarm optimization," *Neural Networks, 1995. Proceedings., IEEE International Conference on*, vol. 4, pp. 1942–1948 vol.4, 1995.
- [49] C. D. Rodriguez-Gallegos, K. Rahbar, M. Bieri, O. Gandhi, T. Reindl, and S. K. Panda, "Optimal PV and storage sizing for PV-battery-diesel hybrid systems," *IECON 2016 - 42nd Annual Conference of the IEEE Industrial Electronics Society*, 2016.
- [50] A. M. El-Zonkoly, "Optimal placement of multi-distributed generation units including different load models using particle swarm optimization," *IET Generation, Transmission & Distribution*, vol. 5, no. 7, pp. 760–771, Jul. 2011.

- [51] V.R. Pandi, H.H. Zeineldin, and W. Xiao, “Determining Optimal Location and Size of Distributed Generation Resources Considering Harmonic and Protection Coordination Limits,” *IEEE Transactions on Power Systems*, vol. 28, no. 2, pp. 1245–1254, 2013.
- [52] M. Gomez-Gonzalez, A. López, and F. Jurado, “Optimization of distributed generation systems using a new discrete PSO and OPF,” *Electrical Power Systems Resources*, vol. 84, no. 1, pp. 174–180, Mar. 2012.
- [53] M. H. Moradi and M. Abedini, “A combination of genetic algorithm and particle swarm optimization for optimal DG location and sizing in distribution systems,” *International Journal of Electrical Power & Energy Systems*, vol. 34, no. 1, pp. 66–74, Jan. 2012.
- [54] W. Prommee and W. Ongsakul, “Optimal multiple distributed generation placement in microgrid system by improved reinitialized social structures particle swarm optimization,” *European Transactions on Electrical Power*, vol. 21, no. 1, pp. 489–504, Jan. 2011.
- [55] B. Zhao, C. Guo, and Y. Cao, “A Multiagent-Based Particle Swarm Optimization Approach for Optimal Reactive Power Dispatch,” *IEEE Transactions on Power Systems*, vol. 20, no. 2, pp. 1070–1078, 2005.
- [56] Z. Ziadi, S. Taira, M. Oshiro, and T. Funabashi, “Optimal power scheduling for smart grids considering controllable loads and high penetration of photovoltaic generation,” *IEEE Transactions on Smart Grid*, vol. 5, no. 5, pp. 2350–2359, 2014.
- [57] C. D. Rodriguez-Gallegos, M. S. Alvarez-Alvarado, O. Gandhi, D. Yang, W. Zhang, T. Reindl, and S. K. Panda, “Placement and sizing optimization for PV-battery-diesel hybrid systems,” *2016 IEEE International Conference on Sustainable Energy Technologies (ICSET)*, 2016.
- [58] L. Wang and C. Singh, “Reliability-Constrained Optimum Placement of Reclosers and Distributed Generators in Distribution Networks Using an Ant Colony System Algorithm,” *IEEE Transactions on Systems, Man, and Cybernetics, Part C (Applications and Reviews)*, vol. 38, no. 6, pp. 757–764, 2008.
- [59] F. S. Abu-Mouti and M. E. El-Hawary, “Optimal distributed generation allocation and sizing in distribution systems via artificial bee colony algorithm,” *IEEE Transactions on Power Delivery*, vol. 26, no. 4, pp. 2090–2101, Oct. 2011.
- [60] J. A. Martinez and G. Guerra, “A Parallel Monte Carlo Method for Optimum Allocation of Distributed Generation,” *IEEE Transactions on Power Systems*, vol. 29, no. 6, pp. 2926–2933, 2014.
- [61] Z. Liu, F. Wen, and G. Ledwich, “Optimal Siting and Sizing of Distributed Generators in Distribution Systems Considering Uncertainties,” *IEEE Transactions on Power Delivery*, vol. 26, no. 4, pp. 2541–2551, 2011.
- [62] F. Glover and M. Laguna, *Tabu Search*. Boston, MA: Springer US, 1997.

- [63] K. Nara, Y. Hayashi, K. Ikeda, and T. Ashizawa, "Application of tabu search to optimal placement of distributed generators," *2001 IEEE Power Engineering Society Winter Meeting. Conference Proceedings (Cat. No.01CH37194)*.
- [64] M.E.H. Golshan and S.A. Arefifar "Optimal allocation of distributed generation and reactive sources considering tap positions of voltage regulators as control variables," *European Transactions on Electrical Power*, vol. 17, no. 3, pp. 219–239, 2007.
- [65] C. Novoa and T. Jin, "Reliability centered planning for distributed generation considering wind power volatility," *Electrical Power Systems Resources*, vol. 81, no. 8, pp. 1654–1661, Aug. 2011.
- [66] A. Takeuchi, T. Hayashi, Y. Nozaki, and T. Shimakage, "Optimal scheduling using metaheuristics for energy networks," *IEEE Transactions on Smart Grid*, vol. 3, no. 2, pp. 968–974, 2012.
- [67] T. Sousa, H. Morais, Z. Vale, P. Faria, and J. Soares, "Considering Vehicle-to-Grid: A Simulated Annealing Approach," *IEEE Transactions on Smart Grid*, vol. 3, no. 1, pp. 535–542, 2012.
- [68] L.D.Arya, A. Koshti, and S. C. Choube, "Distributed generation planning using differential evolution accounting voltage stability consideration," *International Journal of Electrical Power & Energy Systems*, vol. 42, no. 1, pp. 196–207, Nov. 2012.
- [69] H.L. Willis, "Analytical methods and rules of thumb for modeling DG-distribution interaction," *IEEE Power Engineering Society Summer Meeting*, vol. 3, 2000, pp.1643–1644.
- [70] D.Q. Hung and N. Mithulananthan, "Multiple distributed generator placement in primary distribution networks for loss reduction," *IEEE Transactions on Industrial Electronics*, vol. 60, no. 4, pp. 1700–1708, 2013.
- [71] N. Rau and Y.H. Wan, "Optimum location of resources in distributed planning," *IEEE Transactions on Power Systems*, vol. 9, no. 4, pp. 2014– 2020, 1994.
- [72] P. Seshadri, and A. Patton "Bus voltage sensitivity: an instrument for pricing voltage control service," *1999 IEEE Power Engineering Society Summer Meeting. Conference Proceedings (Cat. No.99CH36364)*, pp. 703–707, 1999.
- [73] A. Venkataramana, J. Carr and R.S. Ramshaw "Optimal Reactive Power Allocation," *IEEE Transactions on Power Systems*, vol. 2, no. 1, pp. 138–144, 1987.
- [74] J. Sardi, and N. Mithulananthan and D.Q. Hung, "A loss sensitivity factor method for locating ES in a distribution system with PV units," *2015 IEEE PES Asia-Pacific Power and Energy Engineering Conference (APPEEC),2015*.
- [75] H. Saadat "Power Flow Analysis," *Power System Analysis*, Boston, USA:McGraw Hill, Inc., 2002, pp. 232–234.

- [76] N. M. Nor, A. Ali, T. Ibrahim, and M. F. Romlie, "Battery Storage for the Utility-Scale Distributed Photovoltaic Generations," *IEEE Access*, vol. 6, pp. 1137–1154, 2018.
- [77] N. Acharya, P. Mahat, and N. Mithulananthan, "An analytical approach for DG allocation in primary distribution network," *International Journal of Electrical Power & Energy Systems*, vol. 28, no. 10, pp. 669–678, 2006.
- [78] T.R. Mendonca, M.E. Collins, M.F. Pinto, and T.C. Green, "Decentralisation of power flow solution for facilitating active network management," *CIREN - Open Access Proceedings Journal*, vol. 2017, no. 1, pp. 1669-1672, 2017.
- [79] Y. Yang, S. Bremner, C. Menictas, K. Meng, Z. Y. Dong, and M. Kay, "An economic optimization for BESS sizing in a hybrid PV and wind power plant," *2017 IEEE Innovative Smart Grid Technologies - Asia (ISGT-Asia)*, 2017.
- [80] A. Takeuchi, T. Hayashi, Y. Nozaki, and T. Shimakage, "Optimal scheduling using metaheuristics for energy networks," *IEEE Transactions on Smart Grid*, vol. 3, no. 2, pp. 968–974, 2012.
- [81] E. Kuznetsova, Y. F. Li, C. Ruiz, and E. Zio, "An integrated framework of agent-based modelling and robust optimization for microgrid energy management," *Applied Energy*, vol. 129, pp. 70–88, 2014.
- [82] L. Bitencourt, A. Schetinger, B. Borba, D. Dias, R. Maciel, and B. Dias, "Maximum PV Penetration Under Voltage Constraints Considering Optimal Sizing of BESS on Brazilian Secondary Distribution Network," *IEEE Latin America Transactions*, vol. 14, no. 9, pp. 4063–4069, 2016.
- [83] X. Jiang, X. Zheng, G. Chen, and Y. Miao, "Optimization of BESS Locating and Sizing for the Grid under the Market Mechanism," *2018 International Conference on Power System Technology (POWERCON)*, 2018.
- [84] E. I. Vrettos and S. A. Papathanassiou, "Operating Policy and Optimal Sizing of a High Penetration RES-BESS System for Small Isolated Grids," *IEEE Transactions on Energy Conversion*, vol. 26, no. 3, pp. 744–756, 2011.
- [85] System control report on "Log Data" on 03/08/2018, Ceylon Electricity Board, 2018
- [86] Z. M. Salameh, B. S. Borowy, and A. R. A. Amin, "Photovoltaic module-site matching based on the capacity factors," *IEEE Transactions on Energy Conversion*, vol. 10, no. 2, pp. 326–332, Jun. 1995.
- [87] "Long Term Generation Expansion Plan (2020-2039)", Ceylon Electricity Board, 2019.
- [88] W. D. A. S. Wijayapala, S. R. K. Gamage, and H. M. S. L. G. Bandara, "Determination of Capitalization Values for No Load Loss and Load Loss in Distribution Transformers," *Engineer: Journal of the Institution of Engineers, Sri Lanka*, vol. 49, no. 3, p. 11, 2016.

## APPENDIX – A – DERIVATION OF JACOBIAN MATRIX

For a  $N$  busbar system, the real power and reactive power associated with busbar " $i$ " can be expressed as given in (I.1) and (I.2) respectively.

$$P_i = \sum_{j=1}^n |V_i| |V_j| |Y_{ij}| \cos(\theta_{ij} - \delta_i + \delta_j) \quad (\text{I.1})$$

$$Q_i = - \sum_{j=1}^n |V_i| |V_j| |Y_{ij}| \sin(\theta_{ij} - \delta_i + \delta_j) \quad (\text{I.2})$$

Where;

- $n$ : No. of busbars connected to busbar " $i$ "
- $|V_i|$  Voltage magnitude of busbar " $i$ "
- $|V_j|$  Voltage magnitude of busbar " $j$ "
- $|Y_{ij}|$  Bus admittance magnitude of line " $ij$ "
- $\delta_i$  Phase angle of voltage in busbar " $i$ "
- $\delta_j$  Phase angle of voltage in busbar " $j$ "
- $\theta_{ij}$  Bus admittance angle of line " $ij$ "

The set of nonlinear equations obtained from (I.1) and (I.2) for all the busbars in terms of voltage magnitudes and phase angles, are then linearized neglecting the higher order terms of the Taylor's series expansion [75]. Thus, the conventional Jacobian matrix can be obtained which relates the changes in angles and voltages to changes in real and reactive power injections. Since busbar 1 is assumed to be the slack bus, it is not included in the Jacobian matrix. Equations given by (I.3) to (I.10) are used for determining the elements of the Jacobian matrix [75].

$$\frac{\partial P_i}{\partial \delta_i} = \sum_{j \neq i} |V_i| |V_j| |Y_{ij}| \sin(\theta_{ij} - \delta_i + \delta_j) \quad (\text{I.3})$$

$$\frac{\partial P_i}{\partial \delta_j} = - |V_i| |V_j| |Y_{ij}| \sin(\theta_{ij} - \delta_i + \delta_j) \quad i \neq j \quad (\text{I.4})$$

$$\frac{\partial P_i}{\partial |V_i|} = 2 |V_i| |Y_{ii}| \cos(\theta_{ii}) + \sum_{j \neq i} |V_j| |Y_{ij}| \cos(\theta_{ij} - \delta_i + \delta_j) \quad (\text{I.5})$$

$$\frac{\partial P_i}{\partial |V_j|} = |V_i| |Y_{ij}| \cos(\theta_{ij} - \delta_i + \delta_j) \quad i \neq j \quad (\text{I.6})$$

$$\frac{\partial Q_i}{\partial \delta_i} = \sum_{j \neq i} |V_i| |V_j| |Y_{ij}| \cos(\theta_{ij} - \delta_i + \delta_j) \quad (\text{I.7})$$

$$\frac{\partial Q_i}{\partial \delta_j} = -|V_i| |V_j| |Y_{ij}| \cos(\theta_{ij} - \delta_i + \delta_j) \quad i \neq j \quad (\text{I.8})$$

$$\frac{\partial Q_i}{\partial |V_i|} = -2 |V_i| |Y_{ii}| \sin(\theta_{ii}) - \sum_{j \neq i} |V_j| |Y_{ij}| \sin(\theta_{ij} - \delta_i + \delta_j) \quad (\text{I.9})$$

$$\frac{\partial Q_i}{\partial |V_j|} = -|V_i| |Y_{ij}| \sin(\theta_{ij} - \delta_i + \delta_j) \quad i \neq j \quad (\text{I.10})$$

## APPENDIX – B – PARAMETERS OF IEEE-6 BUS SYSTEM

- ❖ Voltage Base – 25 kV
- ❖ MVA Base – 100 MVA

Table II.1: Bus load data of IEEE-6 bus system

Bus Number	Nominal Load	
	P (MW)	Q (MVAr)
1	0.00	0.00
2	4.00	1.00
3	7.25	2.00
4	5.00	1.25
5	8.00	Not specified
6	5.00	1.50

Table II.2: Line data of IEEE-6 bus system

From	To	$Z_{\text{serial}}$ (p.u.)	$Y_{\text{shunt}}$ (p.u.)
1	2	$0.2238+j0.5090$	$j0.0012$
2	3	$0.2238+j0.5090$	$j0.0012$
3	4	$0.2238+j0.5090$	$j0.0012$
4	5	$0.2238+j0.5090$	$j0.0012$
5	6	$0.2238+j0.5090$	$j0.0012$
6	1	$0.2276+j0.2961$	$j0.0025$
1	5	$0.2603+j0.7382$	$j0.0008$

## APPENDIX – C – PARAMETERS OF IEEE-33 BUS SYSTEM

- ❖ Voltage Base – 12.66 kV
- ❖ MVA Base – 100 MVA

Table III.1: Bus load data of IEEE-33 bus system

Bus No.	P <sub>L</sub> (kW)	Q <sub>L</sub> (kVAr)	Bus No.	P <sub>L</sub> (kW)	Q <sub>L</sub> (kVAr)
2	100	60	18	90	40
3	90	40	19	90	40
4	120	80	20	90	40
5	60	30	21	90	40
6	60	20	22	90	40
7	200	100	23	90	50
8	200	100	24	420	200
9	60	20	25	420	200
10	60	20	26	60	25
11	45	30	27	60	25
12	60	35	28	60	20
13	60	35	29	120	70
14	120	80	30	200	100
15	60	10	31	150	70
16	60	20	32	210	100
17	60	20	33	60	40

Table III.2: Line data of IEEE-33 bus system

Branch Number	Sending end bus	Receiving end bus	R (Ω)	X (Ω)
1	1	2	0.0922	0.0470
2	2	3	0.4930	0.2512
3	3	4	0.3661	0.1864
4	4	5	0.3811	0.1941
5	5	6	0.8190	0.7070
6	6	7	0.1872	0.6188
7	7	8	0.7115	0.2351
8	8	9	1.0299	0.7400
9	9	10	1.0440	0.7400

Branch Number	Sending end bus	Receiving end bus	R ( $\Omega$ )	X ( $\Omega$ )
10	10	11	0.1967	0.0651
11	11	12	0.3744	0.1298
12	12	13	1.4680	1.1549
13	13	14	0.5416	0.7129
14	14	15	0.5909	0.5260
15	15	16	0.7462	0.5449
16	16	17	1.2889	1.7210
17	17	18	0.7320	0.5739
18	2	19	0.1640	0.1565
19	19	20	1.5042	1.3555
20	20	21	0.4095	0.4784
21	21	22	0.7089	0.9373
22	3	23	0.4512	0.3084
23	23	24	0.8980	0.7091
24	24	25	0.8959	0.7071
25	6	26	0.2031	0.1034
26	26	27	0.2842	0.1447
27	27	28	1.0589	0.9338
28	28	29	0.8043	0.7006
29	29	30	0.5074	0.2585
30	30	31	0.9745	0.9629
31	31	32	0.3105	0.3619
32	32	33	0.3411	0.5302
34	8	21	2.0000	2.0000
36	9	15	2.0000	2.0000
35	12	22	2.0000	2.0000
37	18	33	0.5000	0.5000
33	25	29	0.5000	0.5000